

TELEDYNE ENGINEERING SERVICES
CONTROLLED
DOCUMENT

ITES PROJ. NO. 7353
DATE 1/14/92

 **TELEDYNE
ENGINEERING SERVICES**

TECHNICAL REPORT

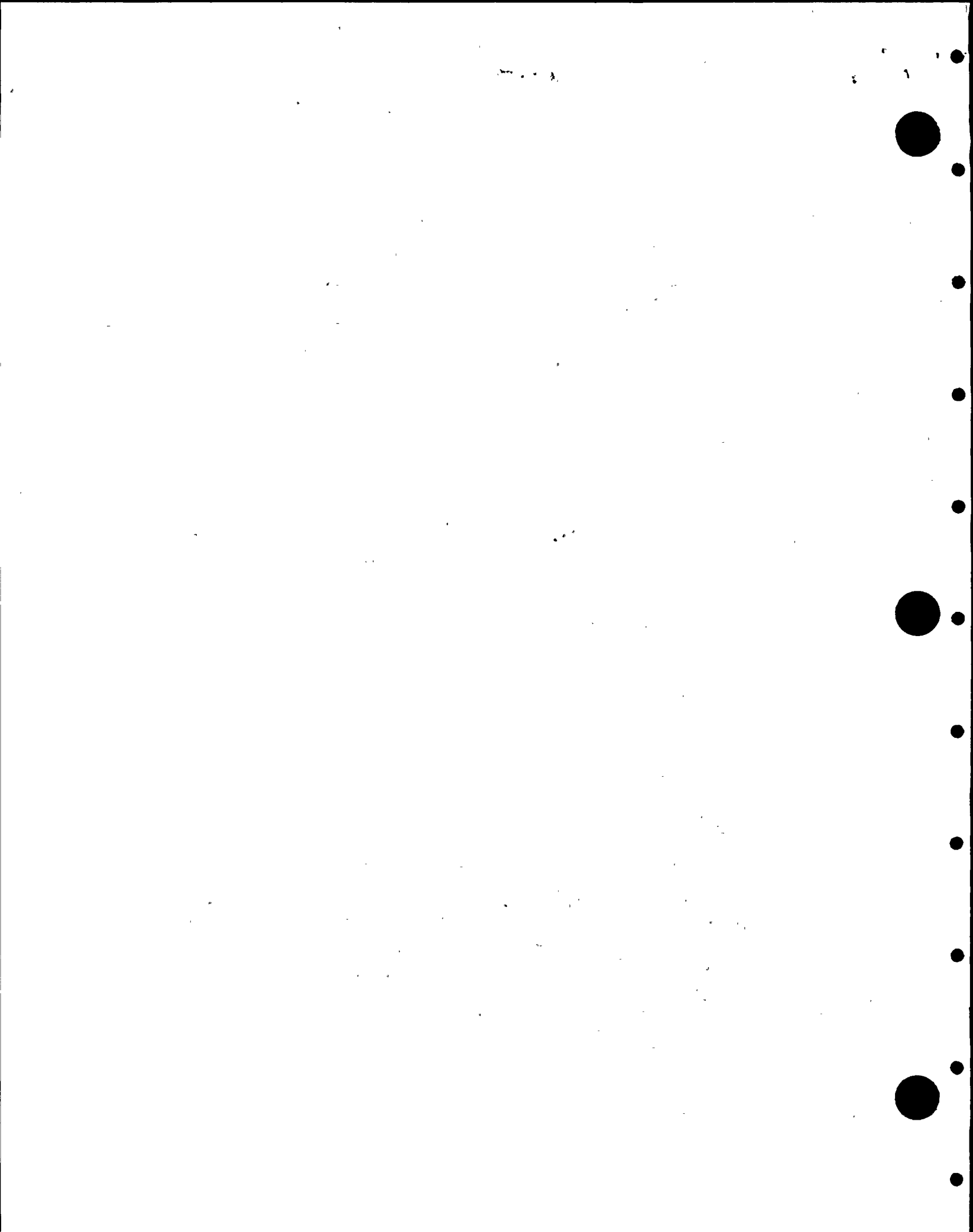
TR-7353-1

REVISION 2

**NINE MILE POINT UNIT 1
REDUCTION IN MARK I TORUS PROGRAM CONDENSATION
OSCILLATION LOAD DEFINITION
AND RESULTING EFFECT ON MINIMUM SHELL THICKNESS REQUIREMENTS**

JANUARY 14, 1992

9201220257 920117
PDR ADDCK 05000220
P PDR



NIAGARA MOHAWK POWER CORPORATION
301 PLAINFIELD ROAD
SYRACUSE, NEW YORK 13212

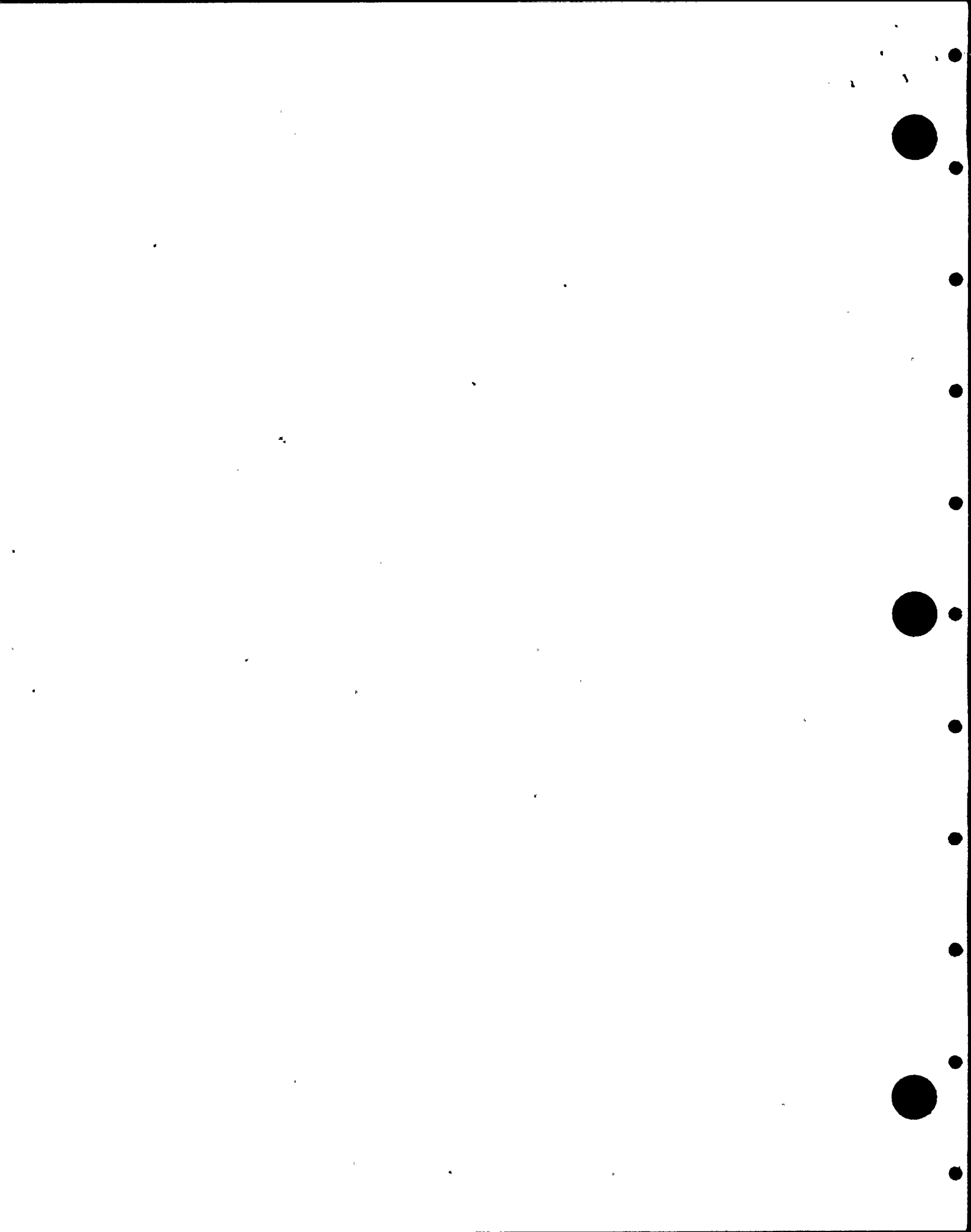
TECHNICAL REPORT TR-7353-1
REVISION 2

NINE MILE POINT UNIT 1
REDUCTION IN MARK I TORUS PROGRAM CONDENSATION
OSCILLATION LOAD DEFINITION
AND RESULTING EFFECT ON MINIMUM SHELL THICKNESS REQUIREMENTS

JANUARY 14, 1992

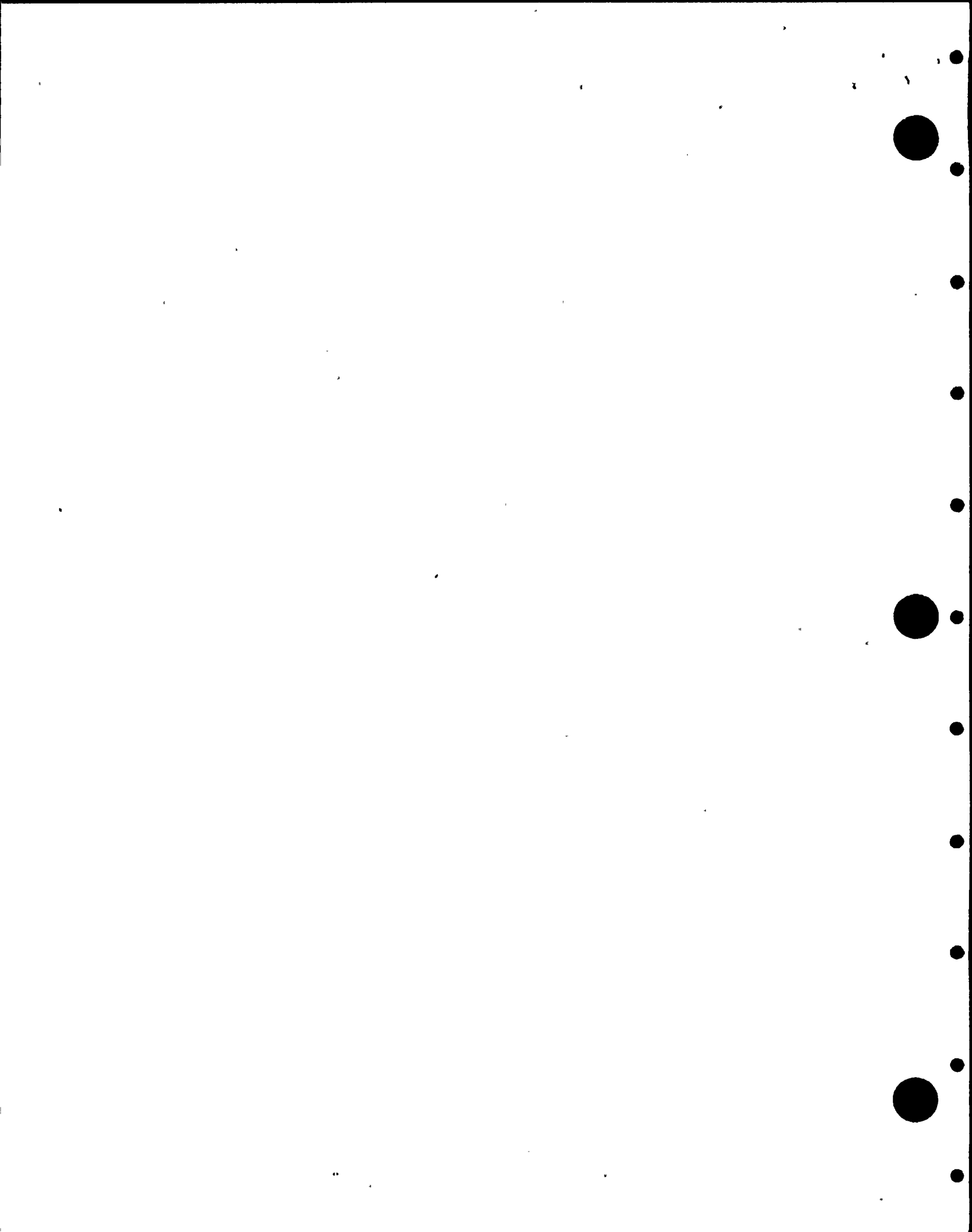
 TELEDYNE ENGINEERING SERVICES

130 SECOND AVENUE
WALTHAM, MASSACHUSETTS 02254
617-890-3350



RECORD OF REVISIONS

<u>REVISION</u>	<u>PAGE</u>	<u>DESCRIPTION</u>
1	Cover	Changed Revision 0 to Revision 1 and date from December 18, 1990 to April 22, 1991
	Title	Changed Revision 0 to Revision 1 and date from December 18, 1990 to April 22, 1991
	-ii-	Add Record of Revisions
	-iii-	Add -iii- to Table of Contents Page and "Revision 1" at top of page
	1 thru 15	Add "Revision 1" at top of page
	-13-	Based on present predictions, for the original analysis, the year the corrosion allowance will be consumed is 1994. Changed 1992 to 1994, 2005 to 2007, 2027 to 2029 and fifteen years to sixteen years.
	-15-	Changed Reference 12 from Revision 0 to Revision 1 and date from November 16, 1990 to April 22, 1991
	Appendix 1 Cover Page	Added "Revision 1" at top of page
2	Cover	Changed Revision 1 to Revision 2 and date from April 22, 1991 to January 14, 1992
	Title	Changed Revision 1 to Revision 2 and date from April 22, 1991 to January 14, 1992
	-ii-	Add Revision 2 changes to Record of Revisions
	-iii-	Add Record of Revisions (continued), Revision 2



RECORD OF REVISIONS
(Continued)

<u>REVISION</u>	<u>PAGE</u>	<u>DESCRIPTION</u>
2	-iv-	Change page no. from -iii- to -iv- and change Revision 1 to Revision 2 on Table of Contents Page
	1 thru 15	Change Revision 1 to Revision 2
	-13-	Change "* At a corrosion rate of .00126" per year" to "* At a corrosion rate of .00126" per year, applicable after 1994"
	-15-	Changed Reference 12 from Revision 1 to Revision 2 and date from April 22, 1991 to January 14, 1992
	Appendix 1 Cover Page	Change Revision 1 to Revision 2

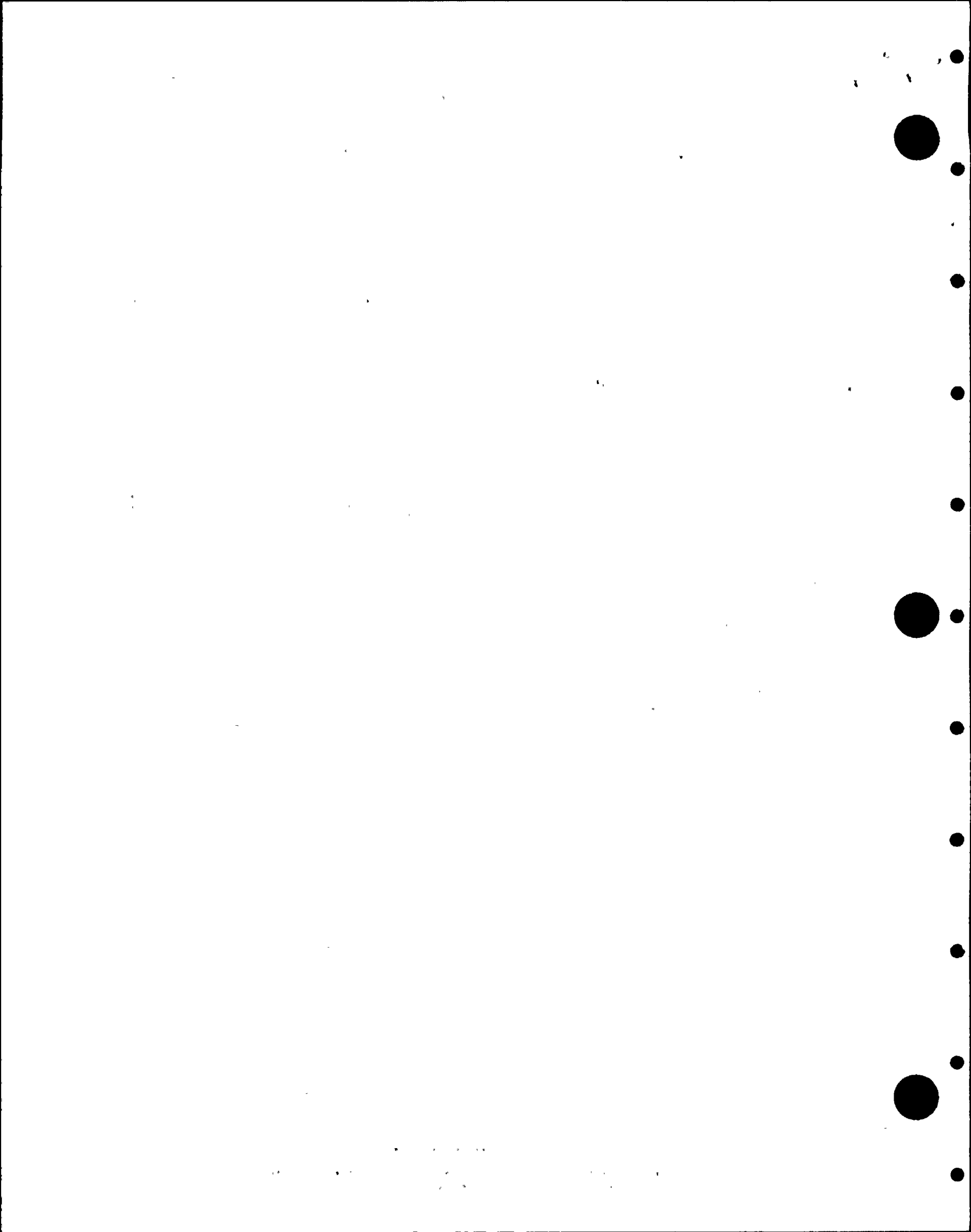
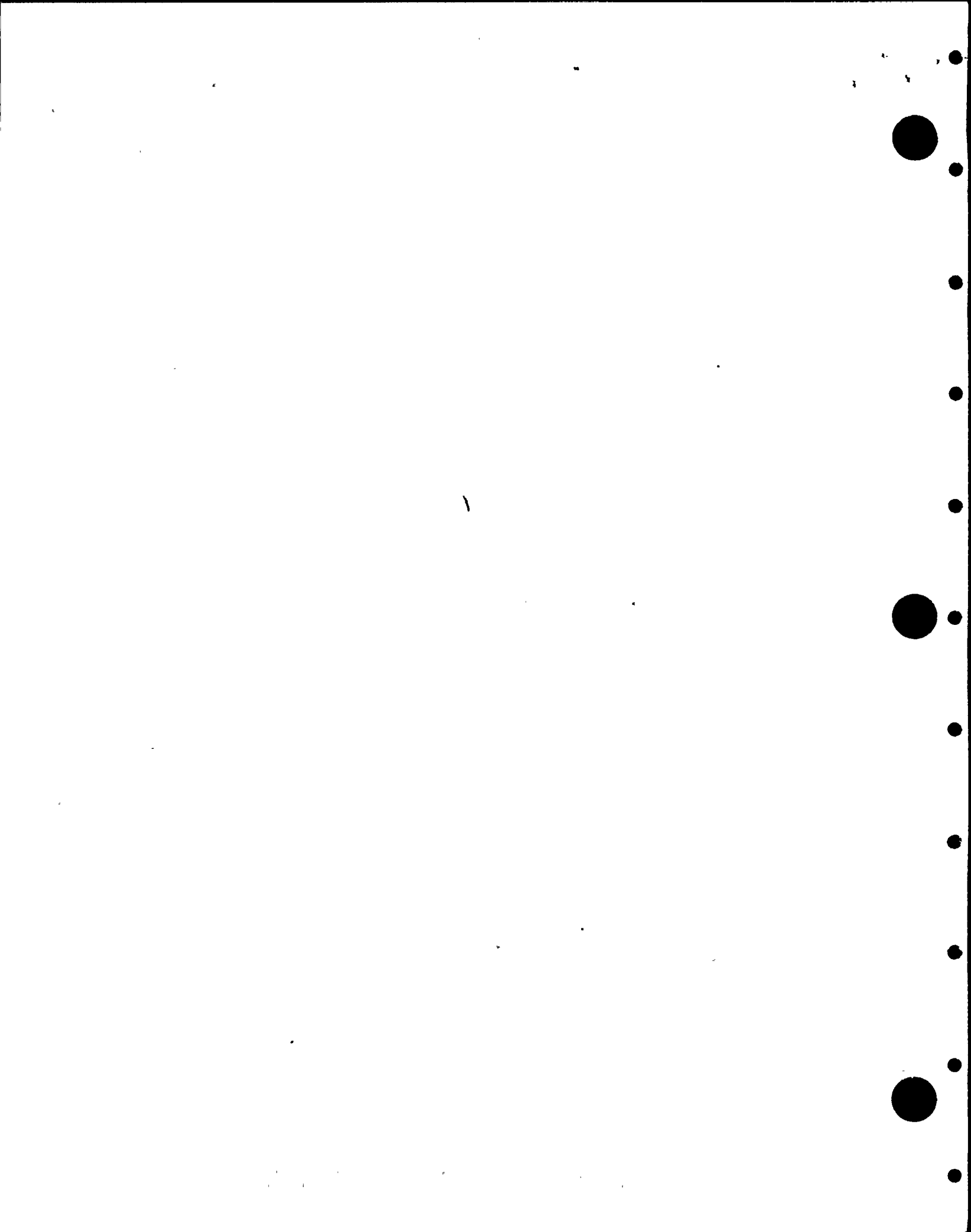


TABLE OF CONTENTS

	<u>Page</u>
1.0 INTRODUCTION	1
2.0 BACKGROUND	3
3.0 SUMMARY OF CONDENSATION OSCILLATION WORK PERFORMED FOR.. THIS EFFORT	4
4.0 COMPUTER MODEL	6
5.0 LOAD ANALYSIS	11
5.1 Deadweight and Pressure	11
5.2 Seismic	11
5.3 Condensation Oscillation	11
6.0 RESULTS	12
7.0 REFERENCES	14
8.0 APPENDIX 1	

Continuum Dynamics, Inc., Technical Note No. 90-11,
"Reduction of Torus Shell Condensation Oscillation
Hydrodynamic Loads for Nine Mile Point, Unit 1,"
Revision 0, dated November 1990



1.0 INTRODUCTION

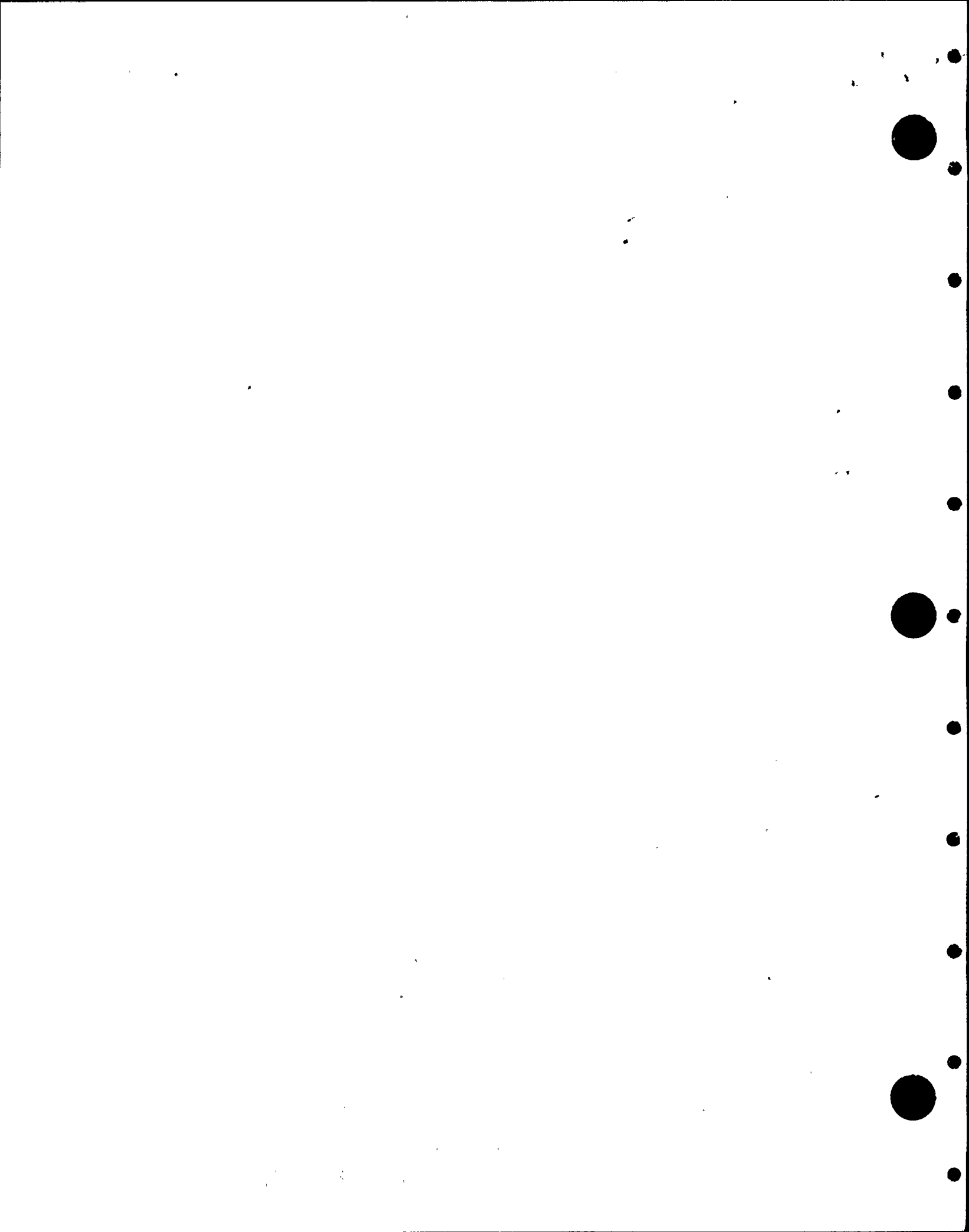
Teledyne Engineering Services (TES) has been retained by Niagara Mohawk Power Corporation (NMPC) to explore the possibility of a short term fix which will increase the present margin on the minimum required torus shell thickness at Nine Mile Point Unit 1 (NMP-1).

The purpose of the Mark I Torus Program was to evaluate the effects of hydrodynamic loads resulting from a loss of coolant accident (LOCA) and/or an SRV discharge on the torus structure. Teledyne Engineering Services Technical Report TR-5320-1, Revision 1, "Mark I Containment Program, Plant-Unique Analysis Report of the Torus Suppression Chamber for Nine Mile Point Unit 1 Nuclear Generating Station," dated September 21, 1984, summarizes the results of extensive analysis on the Nine Mile Point Unit 1 torus structure and reports safety margins against established criteria. The content of that report deals with the torus shell, external support system, vent header system and internal structures.

The loads on which the Teledyne structural analysis is based are presented primarily in G.E. Report NEDO-21888, Rev. 2, "Mark I Containment Program Load Definition Report," dated November, 1981.

The criteria used to evaluate the torus structure is the 1977 ASME Boiler and Pressure Vessel Code, Section III, Division 1, with addenda through Summer 1978 and Code Case N-197.

During the Mark I Program, TES identified a Design Basis Accident (DBA) case with the Condensation Oscillation (CO) loading condition, as the limiting event combination for the torus shell primary membrane stress intensity at mid-bay bottom dead center. Upon program completion, an independent review of the methodology and results was performed by the NRC, and its consultants, to assure conformance with NUREG-0661 Safety Evaluation Report.

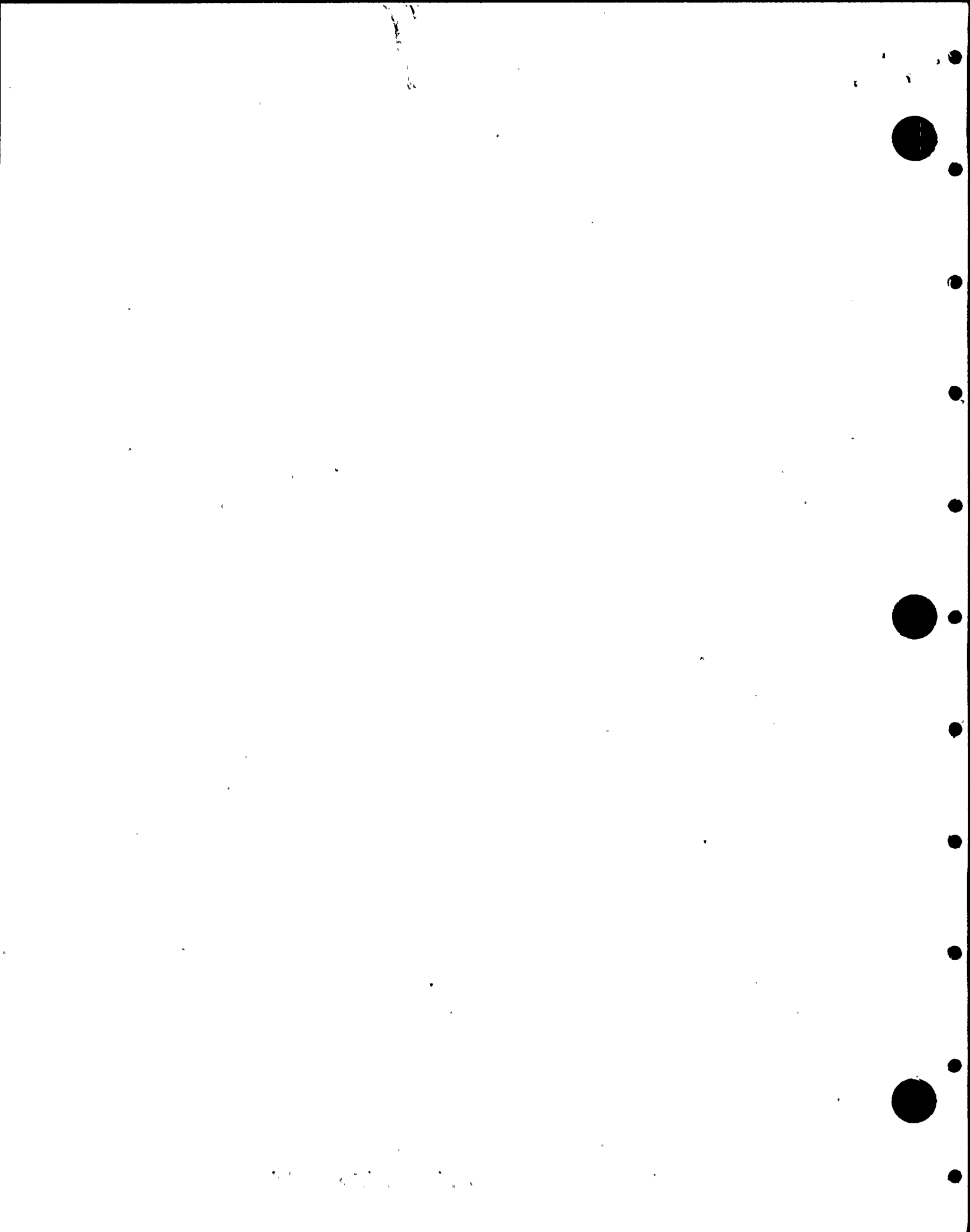


In 1979, Continuum Dynamics, Inc. was asked by the Mark I owners group, through G.E., to assess the conservatism in the Condensation Oscillation torus loads measured during the FSTF blowdown tests. This effort confirmed generally accepted conservatism in the tests with regard to test initial condition thermodynamics, and identified a significant conservatism which was not identified during test design. This conservatism was introduced by the very geometry of the test facility, one-sixteenth sector which is equivalently a 22-1/2° segment of the Mark I Pressure Suppression Pool Torus. The test facility, although full-scale in cross section, attempted to simulate at full-scale the condensation phenomenon in one bay only. End caps were required to contain the pool water and the airspace above the pool in the bay. The analysis, which analyzes the hydrodynamic consequences of these end caps, was presented to the Mark I owners in 1980. To expedite completion of this issue, the Mark I owners decided not to pursue reducing this conservatism at that time. This work is revisited for this effort and developed specifically for Nine Mile Point Unit 1.

The joint Teledyne and Continuum Dynamics effort presented herein consists of an analytical reduction in the Mark I Torus Program Condensation Oscillation Load Definition. The analysis shows that the eight downcomer bays have bay averaged CO loads which are conservative by at least 19% at frequencies other than 5-6 Hz and for four downcomer bays, the bay averaged CO loads are conservative by at least 38% at frequencies other than 5-6 Hz. The load conservatisms in the 5-6 Hz frequency band are 6% and 28% for the eight and four downcomer bays, respectively.

Removal of these conservatisms results in a smaller minimum shell thickness requirement.

The methods of structural analysis and the structural models used are identical to those used in the original Mark I Torus Program.



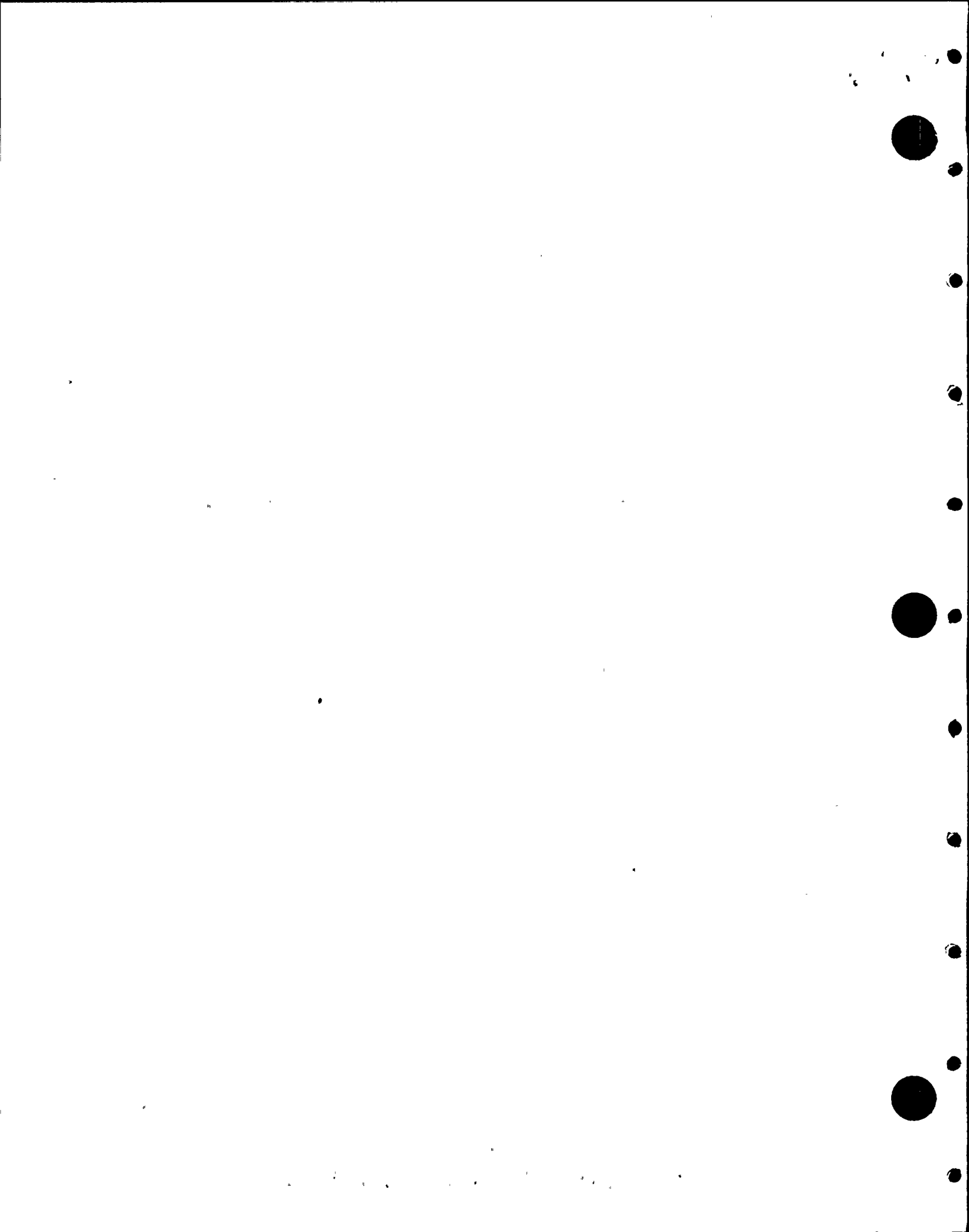
2.0 BACKGROUND

The Mark I Program (GE) determined the magnitude of the Condensation Oscillation (CO) loading⁽³⁾ based on the test results from the Full Scale Test Facility (FSTF). As a result of the FSTF geometric boundary condition configuration, the facility was one bay with end caps to contain the fluid, a conservative prediction of the CO shell pressure loading was obtained. Conservatism in the CO load definition on the order of 15 to 30 percent was recognized during the Program but the Mark I Owners' Group determined at that time that it would not be cost effective to fund the analysis and documentation effort necessary to achieve further reduction in the CO load definition. Most of the Mark I plants had adequate margin on Code⁽⁶⁾ stress allowables for the CO frequency domain event combination loading and therefore, did not require any further refinement to the load definition.

However, the NMP-1 torus has a thin shell (0.46 in.) compared with most of Mark I plants, and as a result, the postulated event combination which includes DBA pressure and CO (event combination 20) controls the margin on torus shell thickness. TES and NMPC recognized this problem as being critical early in the Mark I program, and we jointly took the necessary steps to mitigate loads from this event combination. First, TES refined the Torus Analysis for DBA pressure and CO including modeling techniques and the post processing of results. Then, TES and NMPC initiated a series of thin shell meetings at GE for NMP-1 and Oyster Creek. These meetings identified areas of conservatism in the load definition to be further explored by GE.

The reduction in NMP-1 DBA pressure resulting from these meetings was essential to the successful compliance of NMP-1 to the Mark I Program Structural Acceptance Criteria⁽¹¹⁾ for the CO event combination. The DBA pressure, rather than the CO loading conservatisms, were addressed based on cost and time considerations.

This report deals with the refinement of the CO load definition specifically for Nine Mile Point Unit 1.



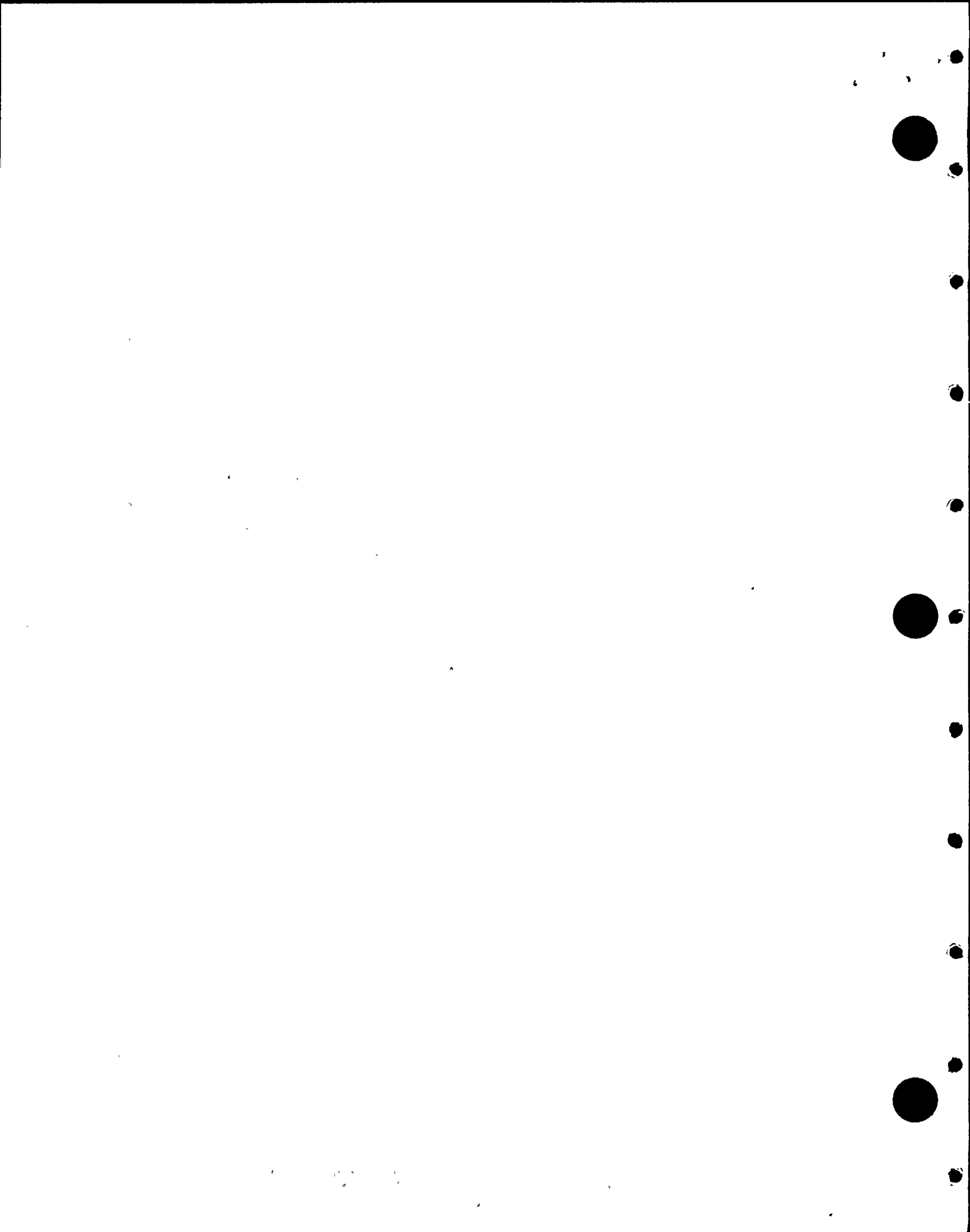
3.0 SUMMARY OF CONDENSATION OSCILLATION WORK PERFORMED FOR THIS EFFORT

Pressures measured in the FSTF facility are measured as if all other bays are exactly in phase or are coherent with the bay modeled by FSTF. In addition, the rigid end caps in the FSTF facility imply that adjoining bays also have the same number of downcomers. In Nine Mile Point, adjoining bays only have one half of the number of downcomers. These differences have been exploited in the condensation oscillation load reduction effort performed herein.

Continuum Dynamics, Inc. (CDI), under contract to TES, has performed the hydrodynamic loading portion of the following described work. CDI was a consultant to the Mark I Owners' Group in the area of hydrodynamic loading phenomenon.

An approximate acoustic model of the Nine Mile Point containment, as if configured for testing by the FSTF facility, has been developed. This acoustic model computes the torus bottom center pressure anticipated in Nine Mile Point with the vent sources configured in an 8-4-8-4 downcomer per bay configuration and utilizes the information that there is a lack of coherence among the condensation pressures at the downcomer exits for most of the frequency range. This analysis has assumed, for practical reasons, that the torus can be unwound for analysis and has provided a table of bottom pressure load reduction factors as a function of frequency.

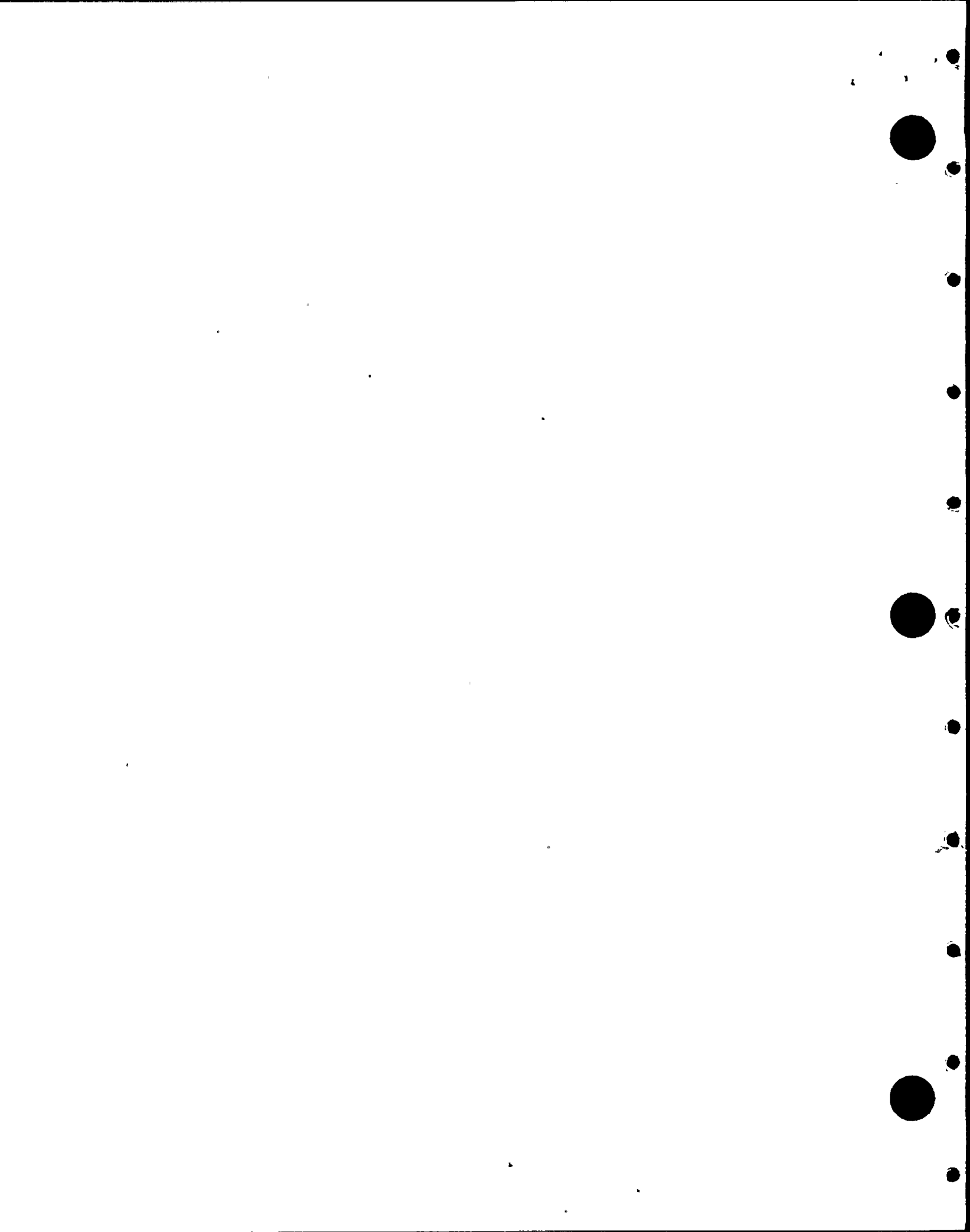
An analysis has also been performed, and is presented in the Continuum Dynamics Report, that addresses the influence that actual Torus curvature has on the analytically assumed "unwrapped" configuration. It was determined that the additional load reduction from a curvature correction would be small and no credit has been taken for this conservatism.



In addition, although it is shown that the load reduction factors are larger for smaller water acoustic speeds, no attempt has been made to take credit for this conservatism either.

The analysis has been done for both the bays containing eight (8) downcomers and the vent bays containing four (4) downcomers.

TES has determined the differential pressure transmissibility between the Load Definition Report, Reference 3, and newly derived CO definitions from Reference 9. We have adjusted the component stresses at the critical torus shell location by hand. The critical location is that which had been determined to control the margin on minimum required torus shell thickness in the Reference 10 report. Implicit in the adjustment of stresses by hand is the fact that the existing 1/40th torus finite element model fundamental physical results have been used for both the vent bay reduced loading and the non-vent bay reduced loading, separately.



4.0 COMPUTER MODEL

Analysis of the torus suppression chamber was accomplished using the STARDYNE computer model shown in Figures 1 through 4. The shell model shown was used to calculate the effects of all loads on shell stress.

The detailed finite element model simulates one-half of the non-vent bay. It is bounded by the ring girder on one end and the mid-bay point on the other. This model was constructed with the assumption that the small offset that exists between the ring girder and mitre joint will not affect results; accordingly, the offset is not included in the model.

Modeling of the water mass was accomplished using a 3-D virtual mass simulation as an integral part of the structural analysis.

This model includes 525 structural nodes, 615 plate elements, 2193 static degrees of freedom and 364 dynamic degrees of freedom. Symmetric boundary conditions were used at both ends of the model.

This is the same model that was used in the original Torus Analysis and reviewed and accepted by the NRC.

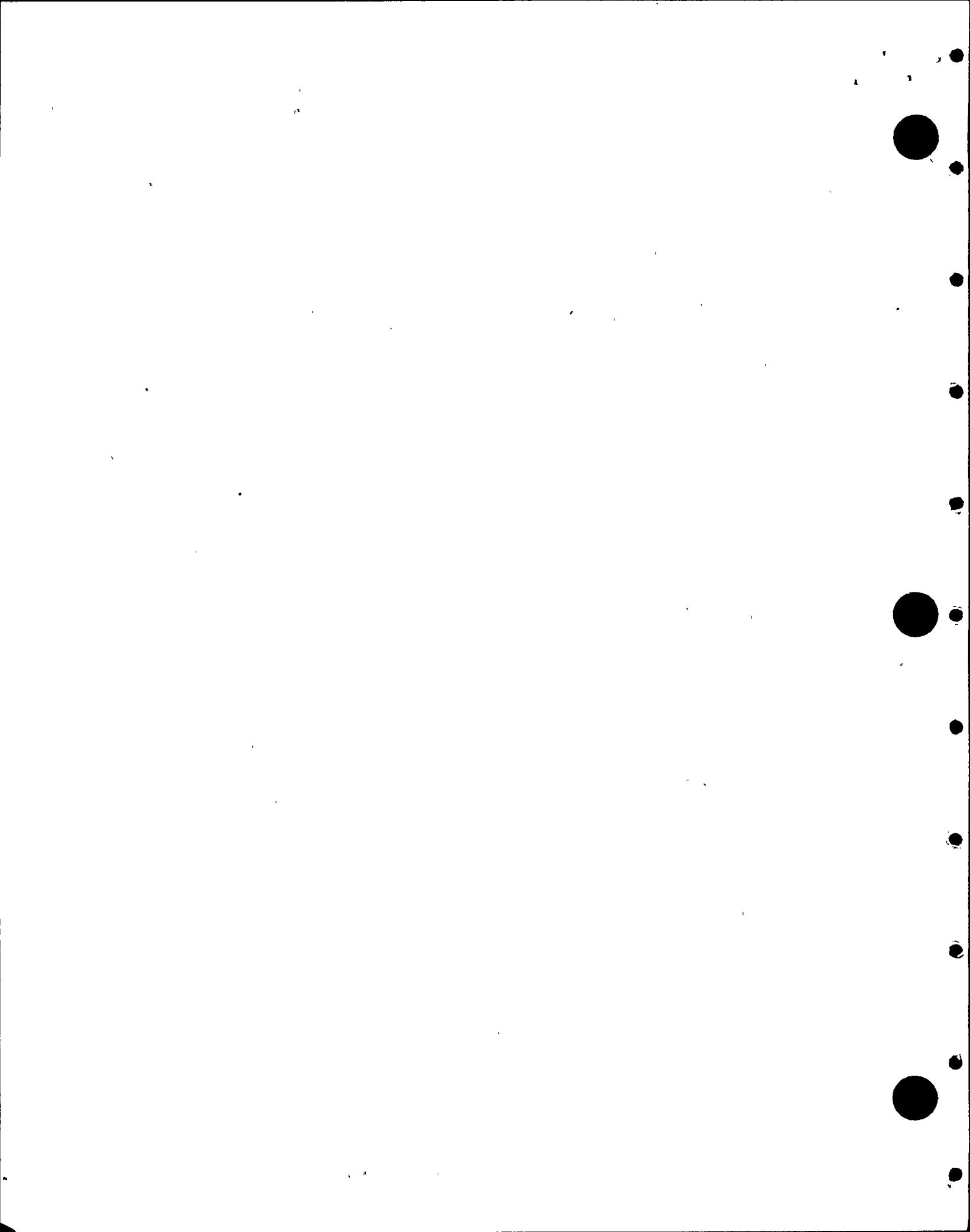
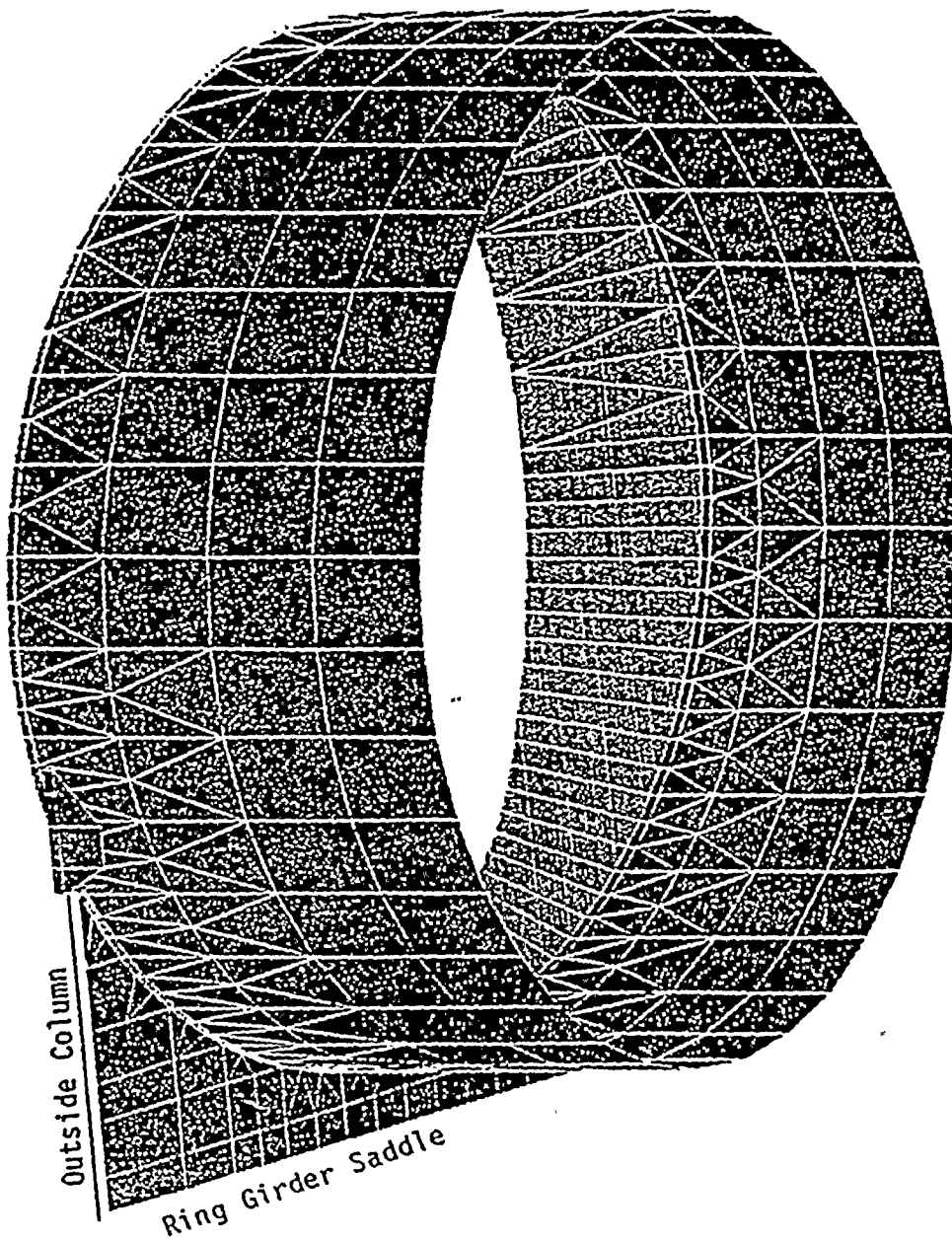


Figure 1

Detailed 1/40th Shell Model



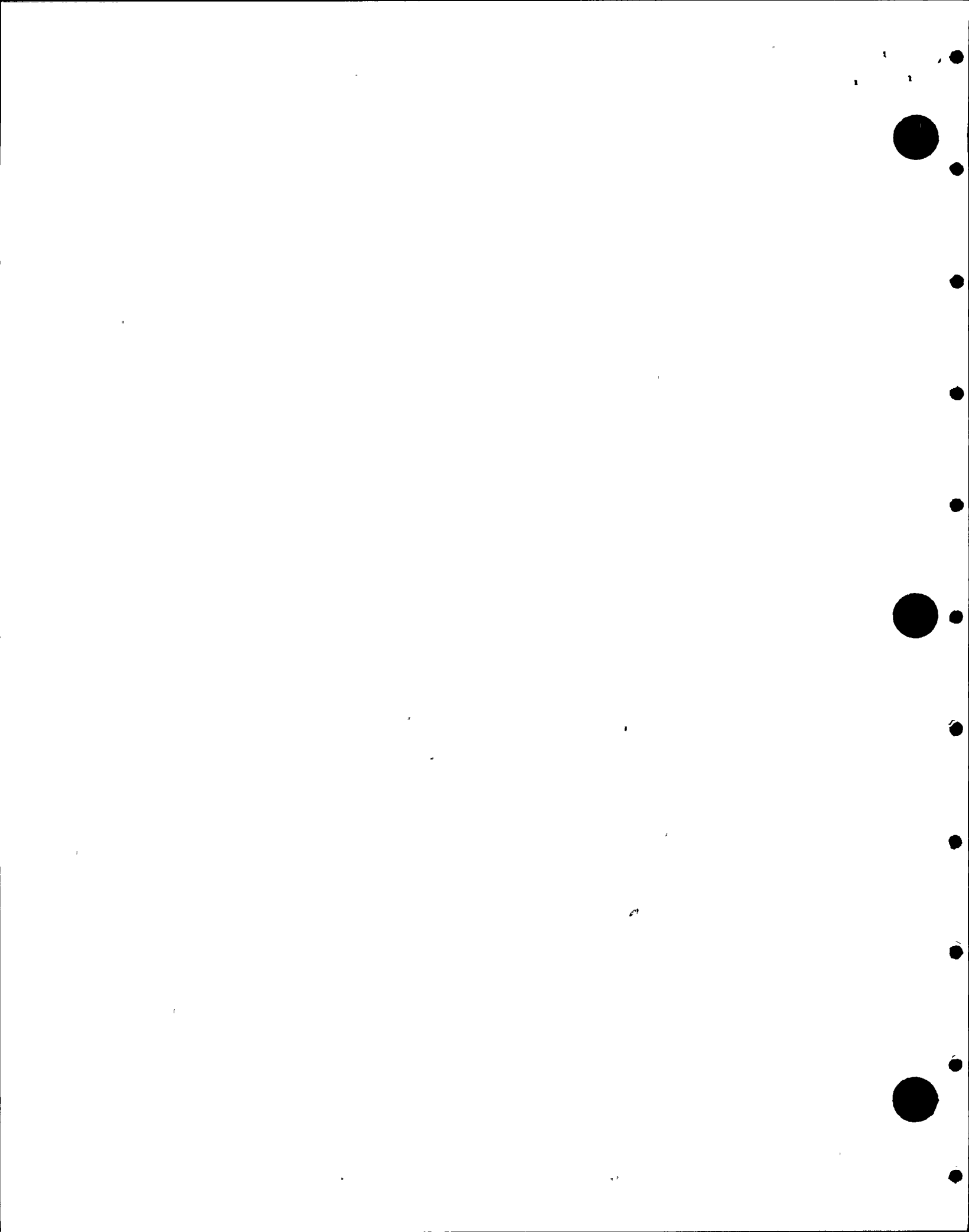
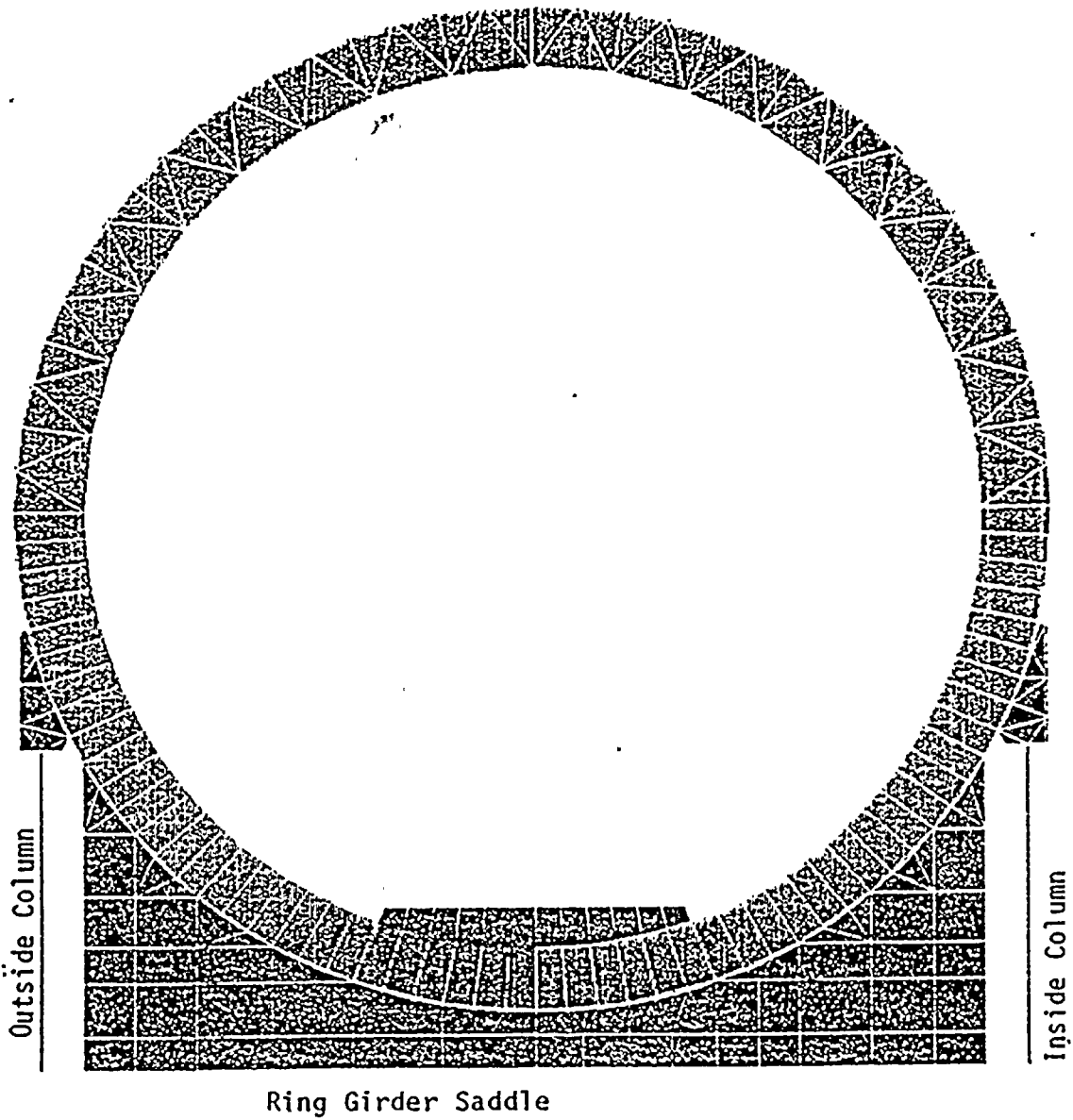


Figure 2

Torus 1/40th Shell Model



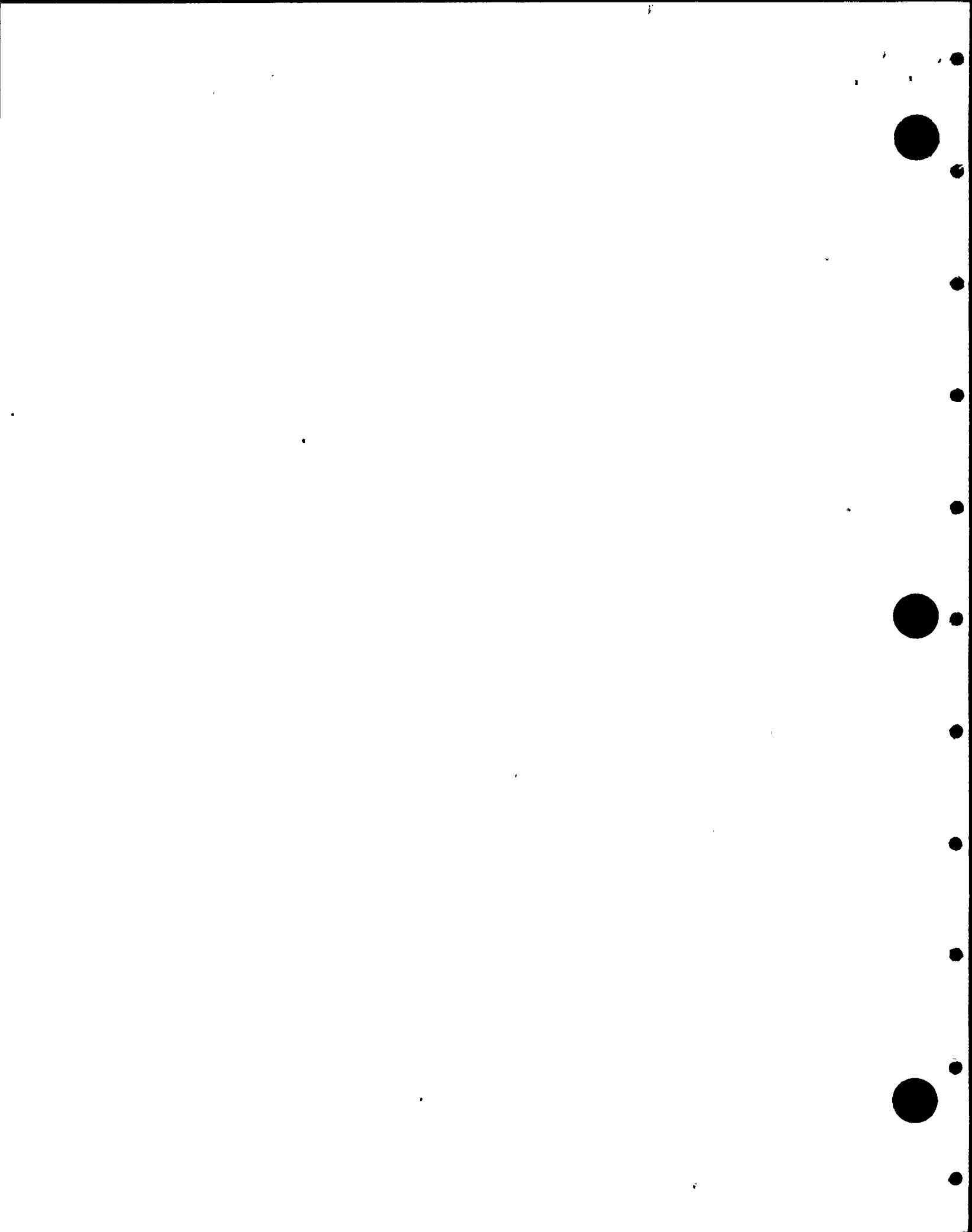
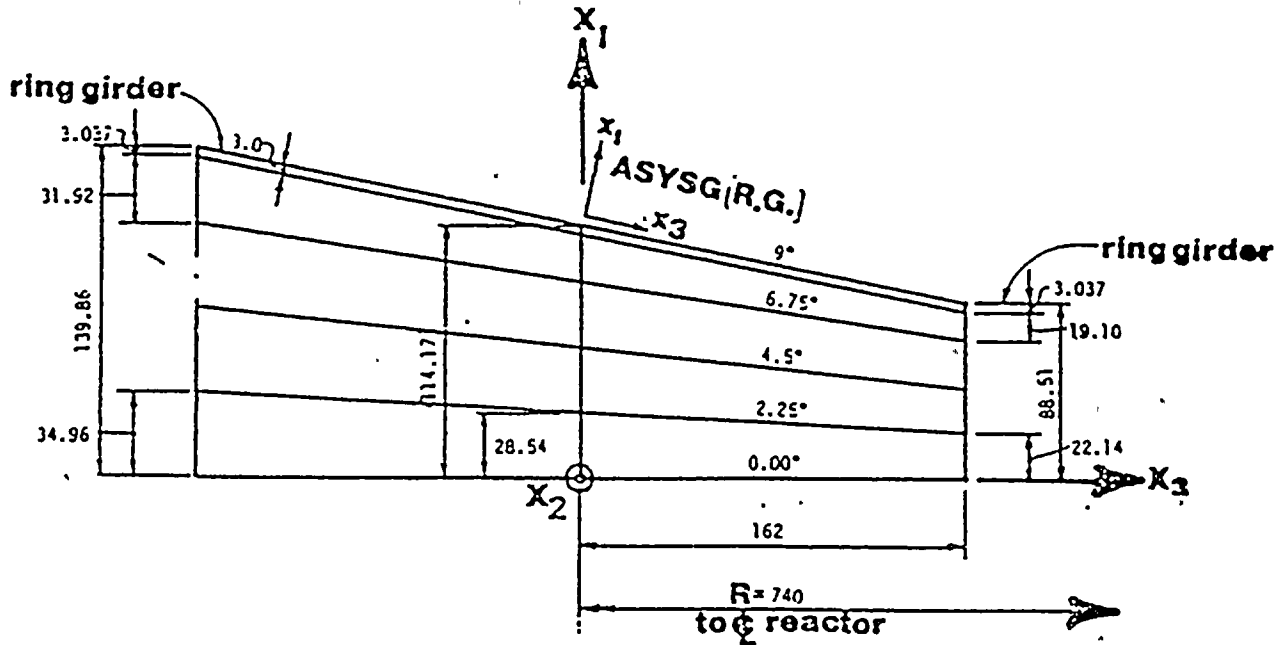


Figure 3

Detailed Shell Model

1/40th
TORUS MODEL



NINE MILE NUCLEAR PLANT UNIT 1

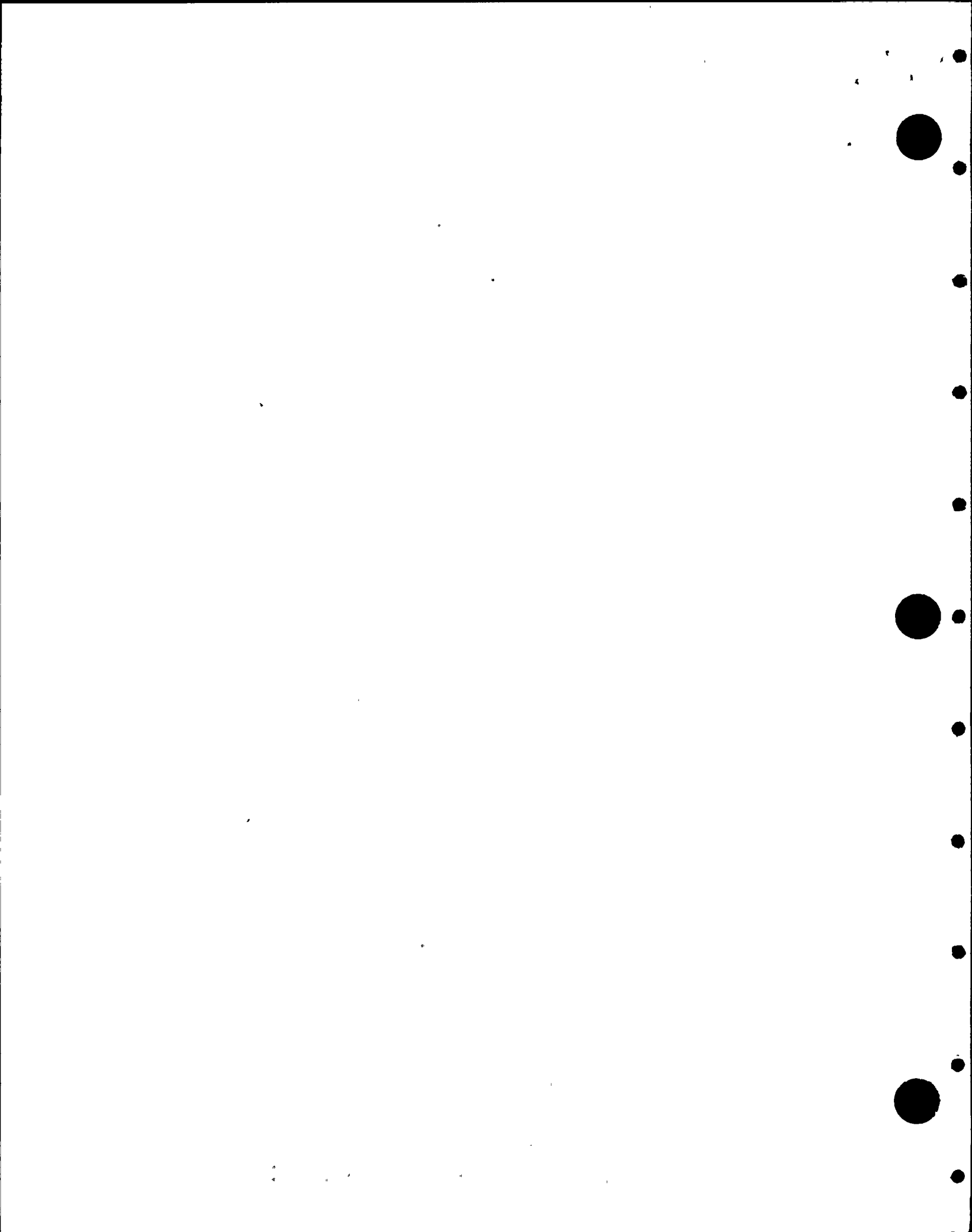
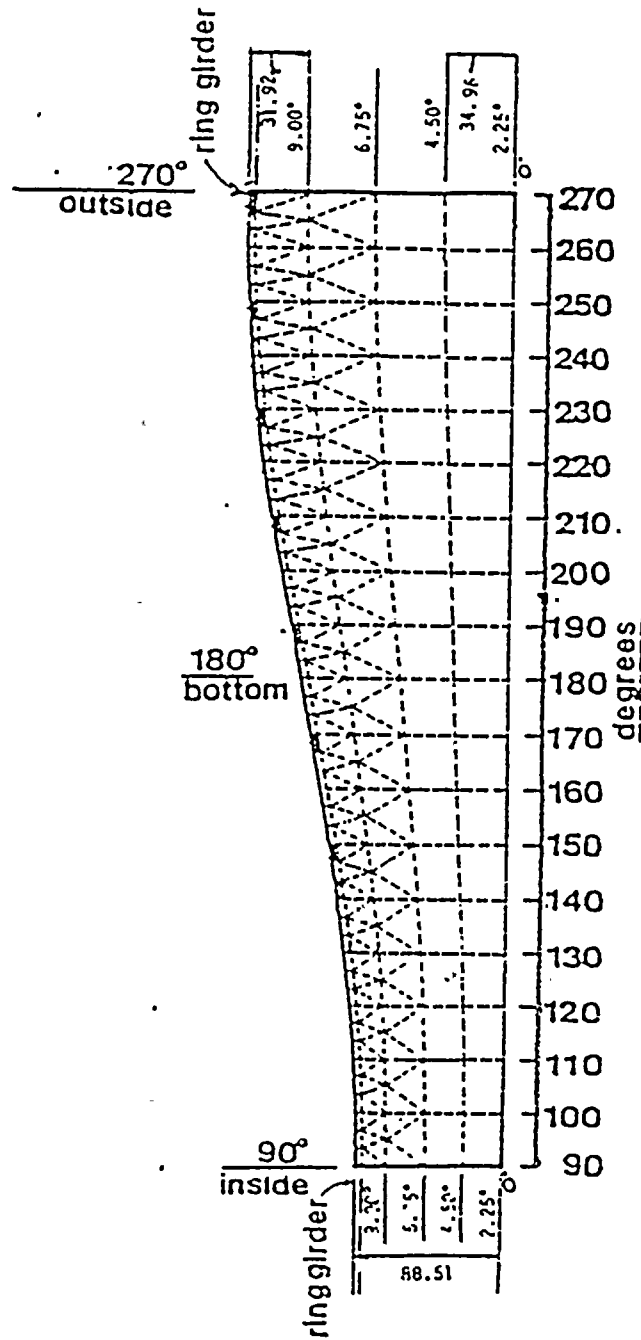
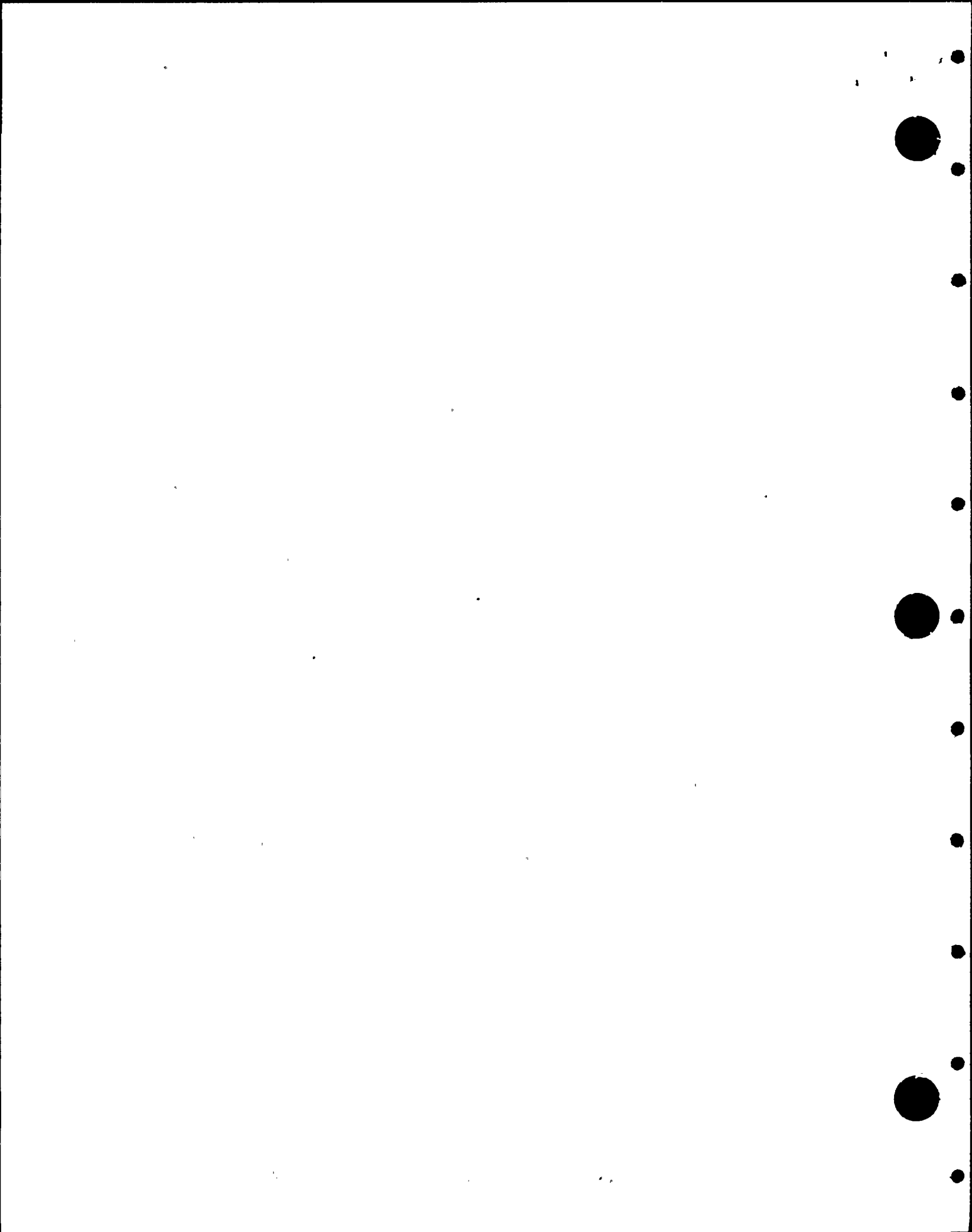


Figure 4

Torus 1/40th Shell Model Lower Half





5.0 LOAD ANALYSIS

5.1 Deadweight and Pressure

Deadweight and internal pressure analyses were done using the computer model shown in Figure 1. The water weight considered was that which corresponds to a downcomer submergence of 4.25'. The DBA pressure used was 26 psig.

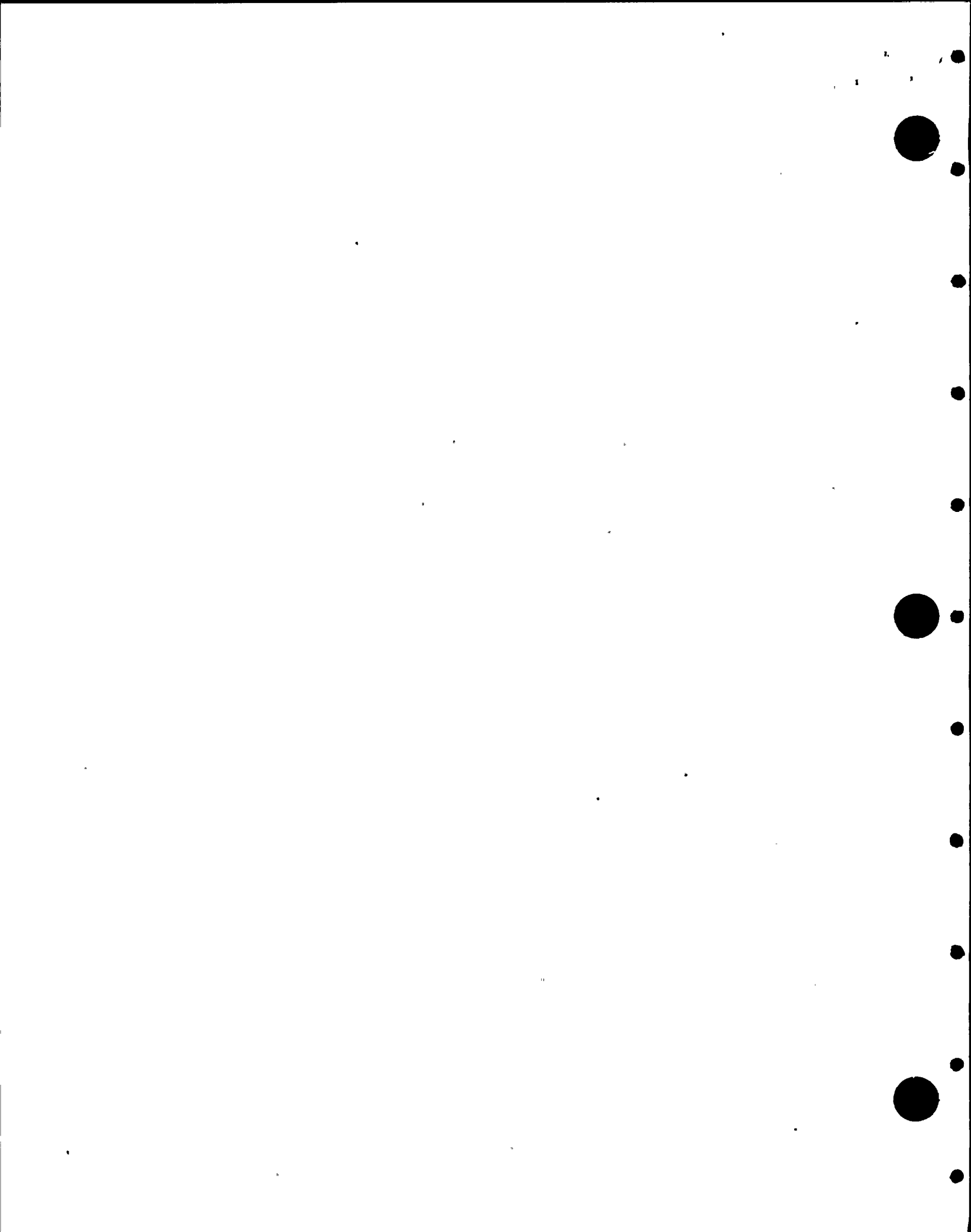
5.2 Seismic

Seismic analysis for shell stress was done by applying static G loads to the model in Figure 1.

5.3 Condensation Oscillation

The condensation oscillation shell load is specified as a spectrum of pressures in 1 Hz bands (Reference 3). The analysis for this load was performed by considering the effects of unit loads at each load frequency (harmonic analysis) and then scaling and combining the individual frequency effects to determine total stress at the critical element. The three variations in the CO spectrum (Reference 3) were evaluated by rescaling the results of the unit load analysis. 100% of water mass was used for all CO analysis. The reduction factors presented in Table 1 of Reference 9 were applied to the individual harmonic pressures.

The combination of individual harmonic stresses into total element stress was done by considering frequency contributions at 31 Hz and below. The actual combination was done by adding the absolute value of the four highest harmonic contributors to the SRSS combination of the others for shell stress. This combination method and use of the 31 Hz cutoff are the result of extensive numerical evaluation of full scale test data, which is reported and discussed in References 4 and 7.



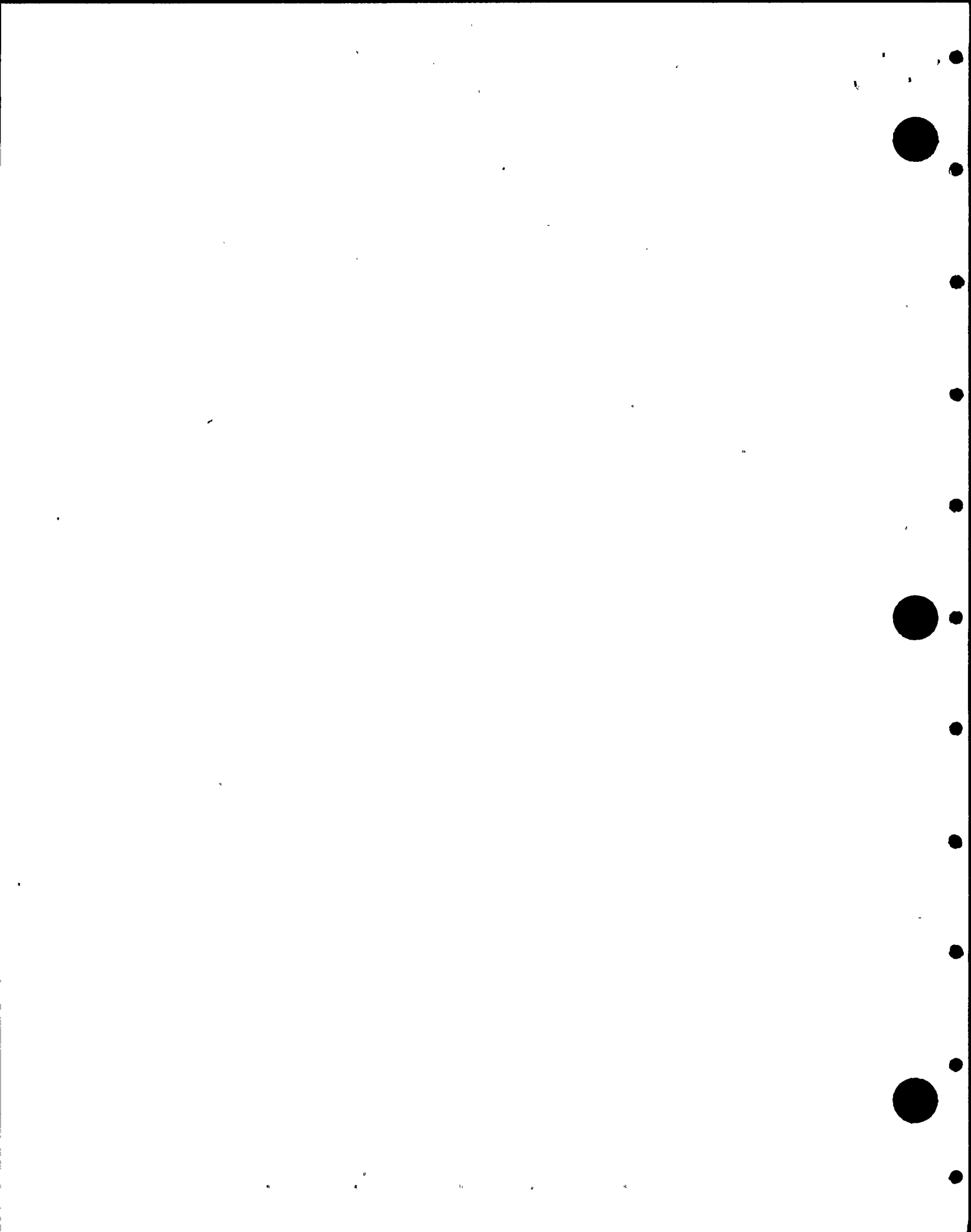
6.0 RESULTS

The controlling Mark I Containment Program event combination for shell stress was Event Combination 20 which involves Condensation Oscillation (CO) loading as a major contributor to the primary membrane stress intensity and resulted in a free shell total membrane stress of 16,025 psi which provides for a corrosion allowance of $(1 - (16025/16500)) \cdot 46 = .013$ inches. This membrane stress occurs at the bottom of the mid-bay of the Torus, which is element 19 of the finite element model, and represents the largest, and therefore, controlling membrane stress.

Element 19 has been re-evaluated by hand using the same procedures for condensation oscillation as well as deadweight, seismic and internal pressure, as were used in the original torus analysis. The only difference is the incorporation of the CO load reduction factors for the bays containing eight (8) downcomers and the bays containing four (4) downcomers. This re-evaluation is contained in TES Calculation Package 7353-1, Revision 0, Reference 12.

These CO load reduction factors are given in Reference 9, Table 1 entitled "Condensation Oscillation Rigid Wall Pressure Amplitude Reduction Factors for Nine Mile Point." The average values from these tables have been used since bay averaging was used to process FSTF data and this averaging introduces no additional approximation than what has already been utilized.

Three evaluations of element 19 have been done for this effort (Reference 12). The first evaluation reproduced the original analysis. The second evaluation provided the stresses for the bays containing eight downcomers and the third evaluation provided the stresses for the bays containing four downcomers. Condensation Oscillation stresses were evaluated at the component level for each frequency and component stresses at each frequency were then combined with the other frequencies. The resulting component stresses were then combined with deadweight, seismic and pressure stresses and then the maximum principal stress was evaluated. This eliminated conservatism which would be introduced by combining principal stresses.



CONTROLLING SHELL STRESSES - NINE MILE POINT UNIT 1

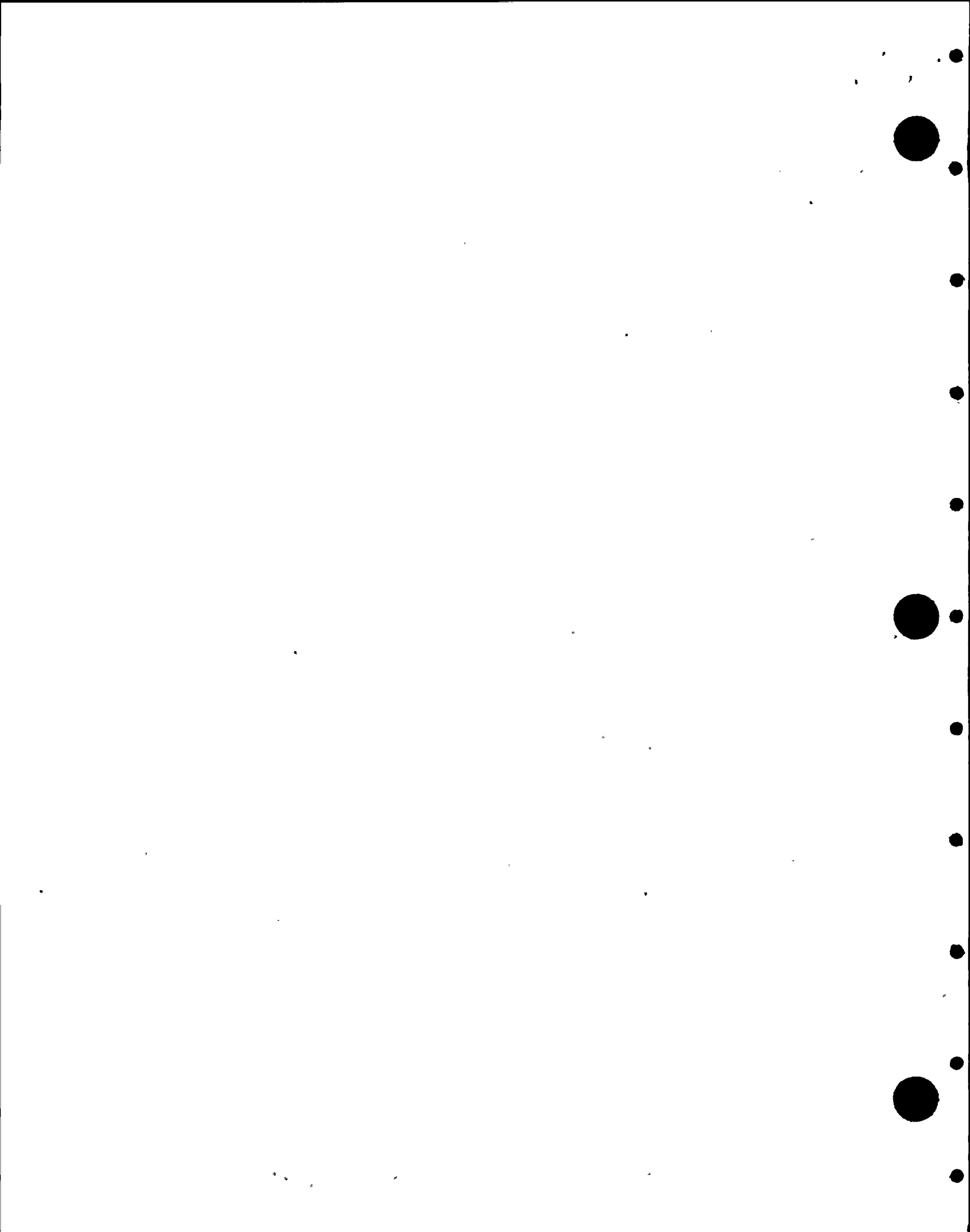
<u>Condition</u>	<u>Type of Stress</u>	<u>Location</u>	<u>Actual Stress, psi</u>	<u>Allowable Stress, psi</u>
Original Analysis	Membrane	Free Shell Element 19	16,025	16,500
Original Analysis	Membrane & Bending	Free Shell Element 19	16,618	24,750
Reduced C.O. 8 D.C. Bay	Membrane	Free Shell Element 19	15,452	16,500
Reduced C.O. 8 D.C. Bay	Membrane & Bending	Free Shell Element 19	16,044	24,750
Reduced C.O. 4 D.C. Bay	Membrane	Free Shell Element 19	14,460	16,500
Reduced C.O. 4 D.C. Bay	Membrane & Bending	Free Shell Element 19	15,040	24,750

CORROSION ALLOWANCE

<u>Condition</u>	<u>Corrosion Allowance, In.</u>	<u>Year Corrosion Allowance Will Be Consumed*</u>
Original Analysis	.0132	1994
Reduced C.O. 8 D.C. Bay	.0292	$\frac{.0292 - .0132}{.00126} + 1994 = 2007$
Reduced C.O. 4 D.C. Bay	.0569	$\frac{.0569 - .0132}{.00126} + 1994 = 2029$

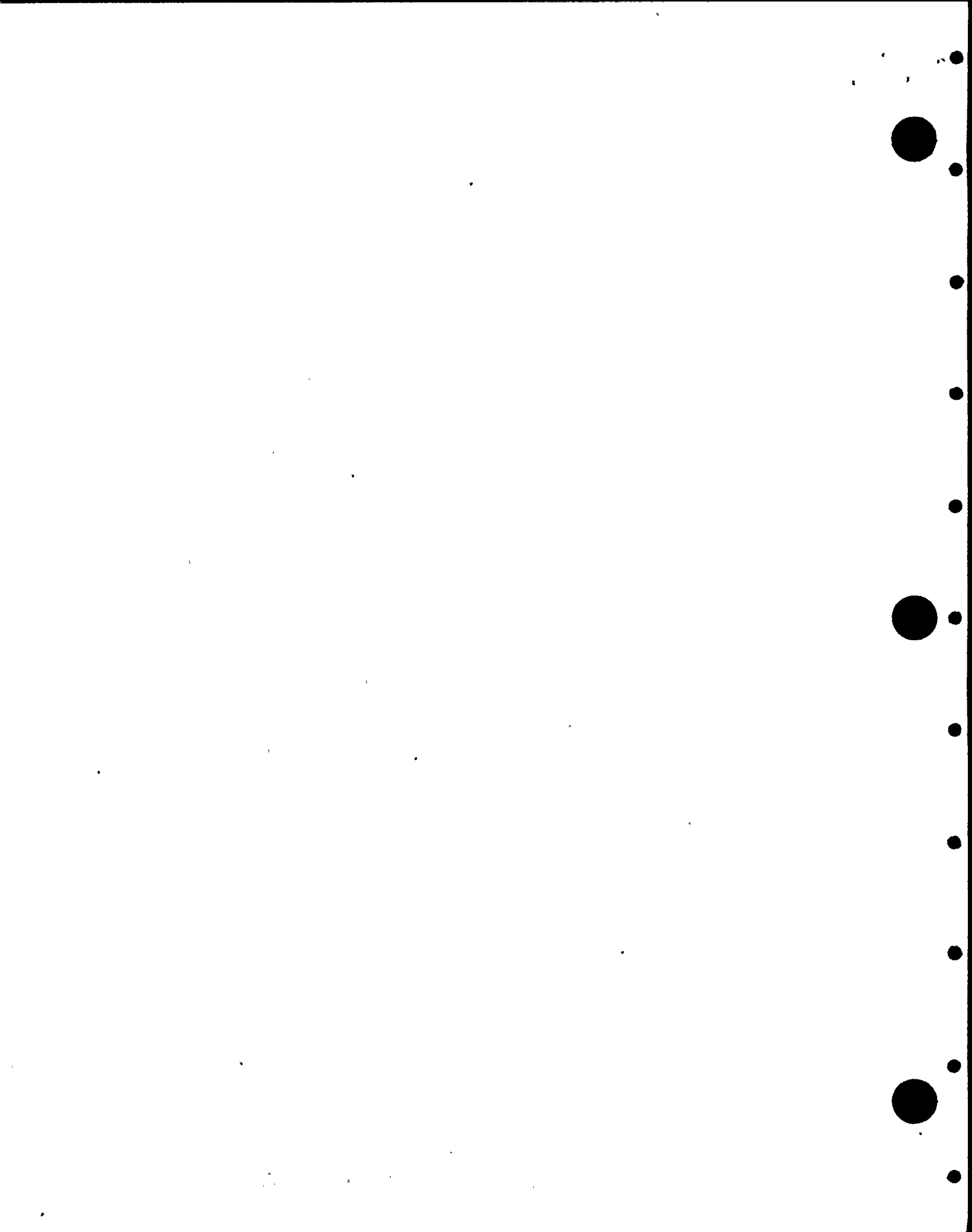
* At a corrosion rate of .00126" per year, applicable after 1994

Based on the foregoing, and an anticipated operating life to the year 2024, it appears that half the bays, i.e., those with four downcomers, will not need any attention; and that the eight downcomer bays will need attention within the next sixteen years.



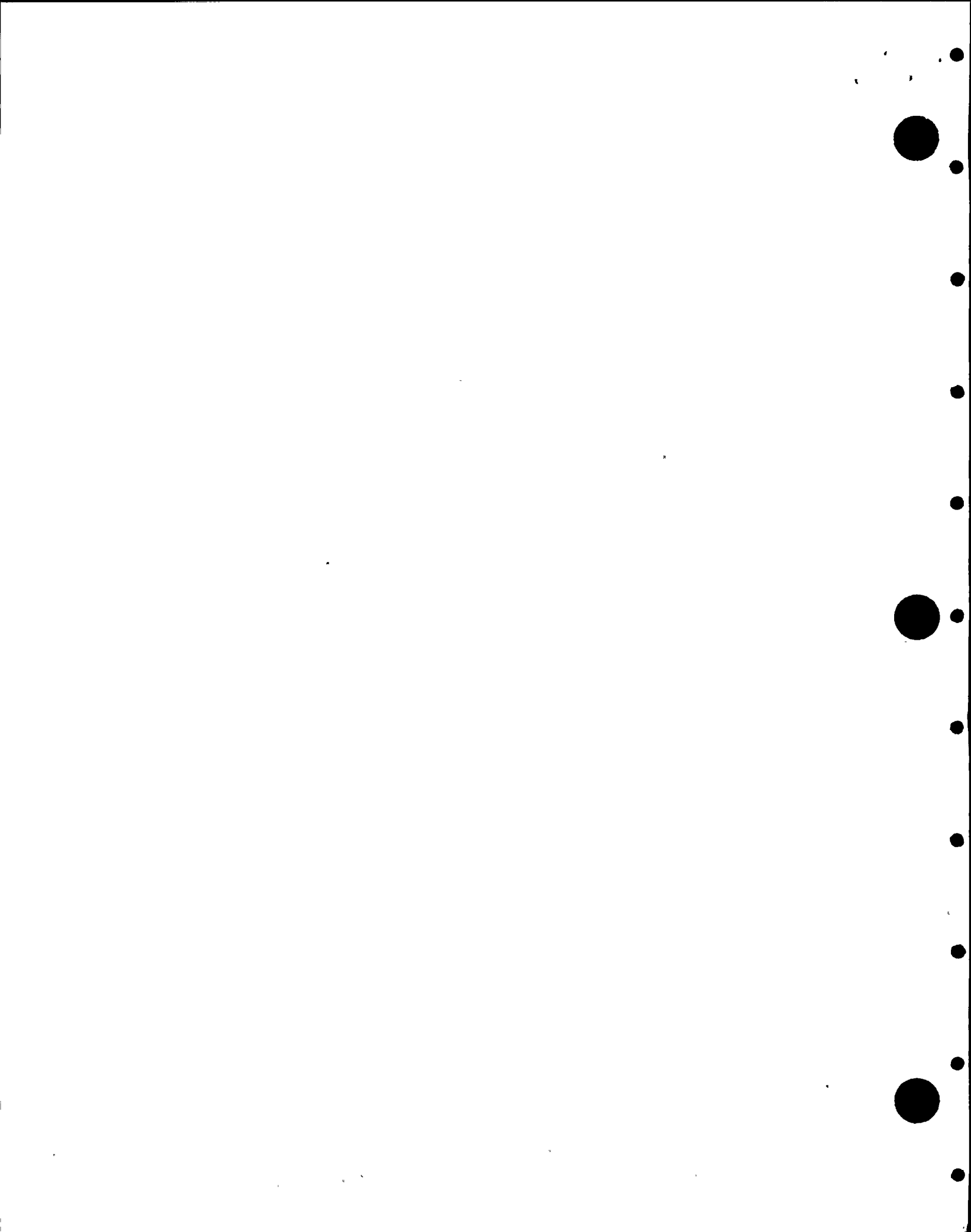
7.0 REFERENCES

1. PR-7461, Revision 1, "Reduction in Mark I Torus Program Condensation Oscillation Load Definition," dated February 13, 1990.
2. TES Report TR-5320-1, Rev. 1, "Mark I Containment Program, Plant-Unique Analysis Report of the Torus Suppression Chamber for Nine Mile Point Unit 1 Nuclear Generating Station," dated September 21, 1984.
3. G.E. Report NEDO-21888, Rev. 2, "Mark I Containment Program Load Definition Report," dated November 1981.
4. G.E. Report NEDE-24840, "Mark I Containment Program - Evaluation of Harmonic Phasing for Mark I Torus Shell Condensation Oscillation Loads," dated October 1980.
5. G.E. Report NEDO-24574, Rev. 1, "Mark I Containment Program - Plant-Unique Load Definition - Nine Mile Point 1 Nuclear Generating Plant," dated July 1981.
6. ASME B&PV Code, Section III, Division 1 through Summer 1977.
7. Structural Mechanics Association Report SMA-12101.04-R002D, "Response Factors Appropriate for Use with CO Harmonic Response Combination Design Rules," dated March 1982.
8. G.E. Supplementary Support Effort (SSE) Response Number 310, dated February 8, 1982.

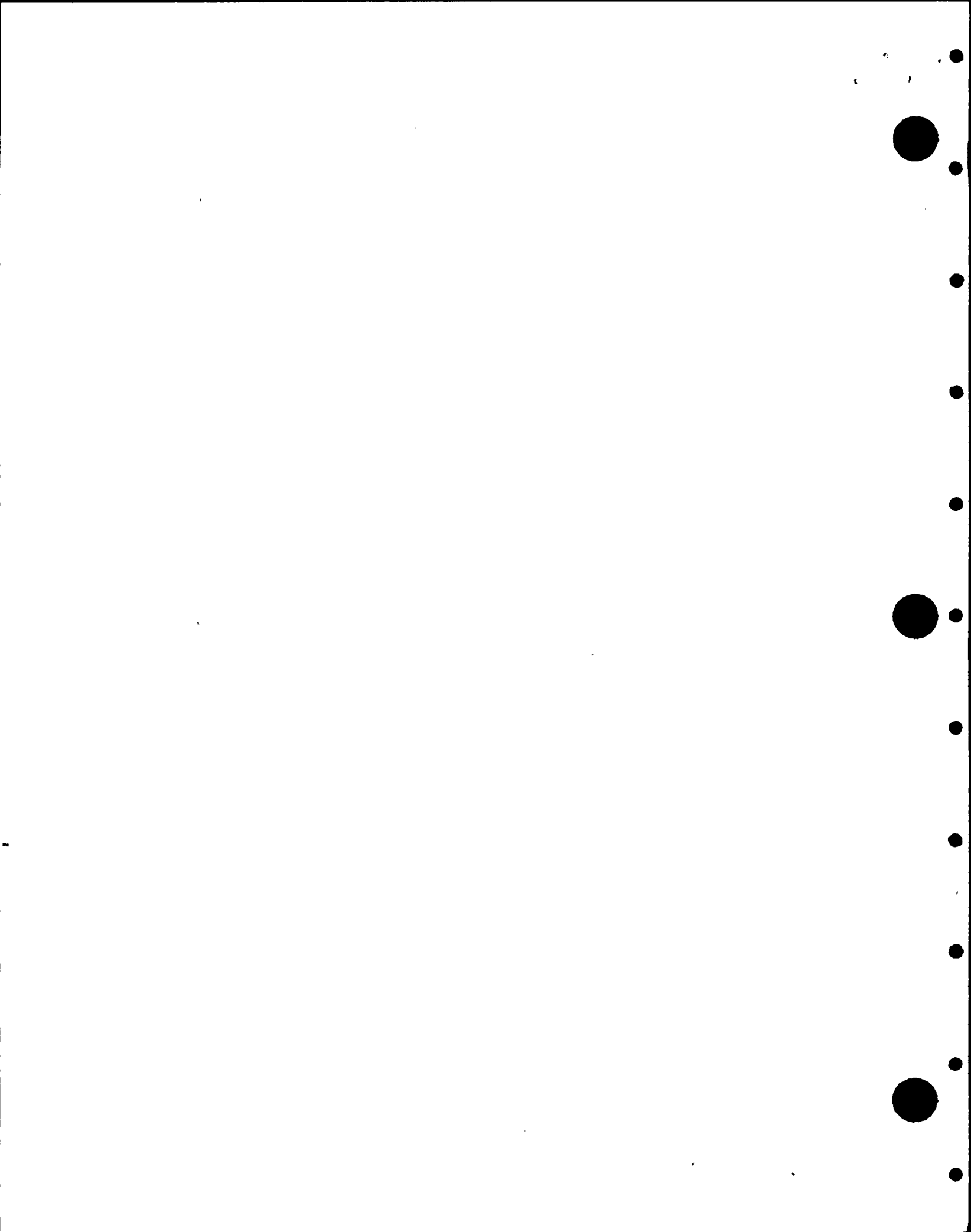


7.0 REFERENCES (Continued)

9. Continuum Dynamics Technical Note No. 90-11, "Reduction of Torus Shell Condensation Oscillation Hydrodynamic Loads for Nine Mile Point Unit 1," dated November 1990.
10. TES Technical Report TR-6801-2, "Mark I Torus Shell and Vent System Thickness Requirements," Nine Mile Point Unit 1 Nuclear Station, January 29, 1988, Rev. 1.
11. Mark I Containment Program, Structural Acceptance Criteria, Plant Unique Analysis Application Guide, NEDO-24583-1, October 1978.
12. TES Calculation Package 7353-1, Revision 2, "Nine Mile Point Unit 1, Reduction in Mark I Torus Program Condensation Oscillation Load Definition and Resulting Effect on Minimum Shell Thickness Requirements," dated January 14, 1992.



8.0 APPENDIX 1



REDUCTION OF TORUS SHELL
CONDENSATION OSCILLATION
HYDRODYNAMIC LOADS FOR
NINE MILE POINT
UNIT 1

Revision 0

Prepared by

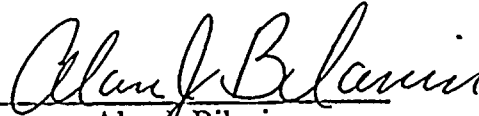
Continuum Dynamics, Inc.
P.O. Box 3073
Princeton, New Jersey 08543

TELEDYNE ENGINEERING SERVICES
CONTROLLED
DOCUMENT

TES PROJ. NO. 7353
DATE 11-20-90

Prepared Under Purchase Number G2194 for

Teledyne Engineering Services
130 Second Avenue
Waltham, Massachusetts 02254


Alan J. Bilanin

November 1990

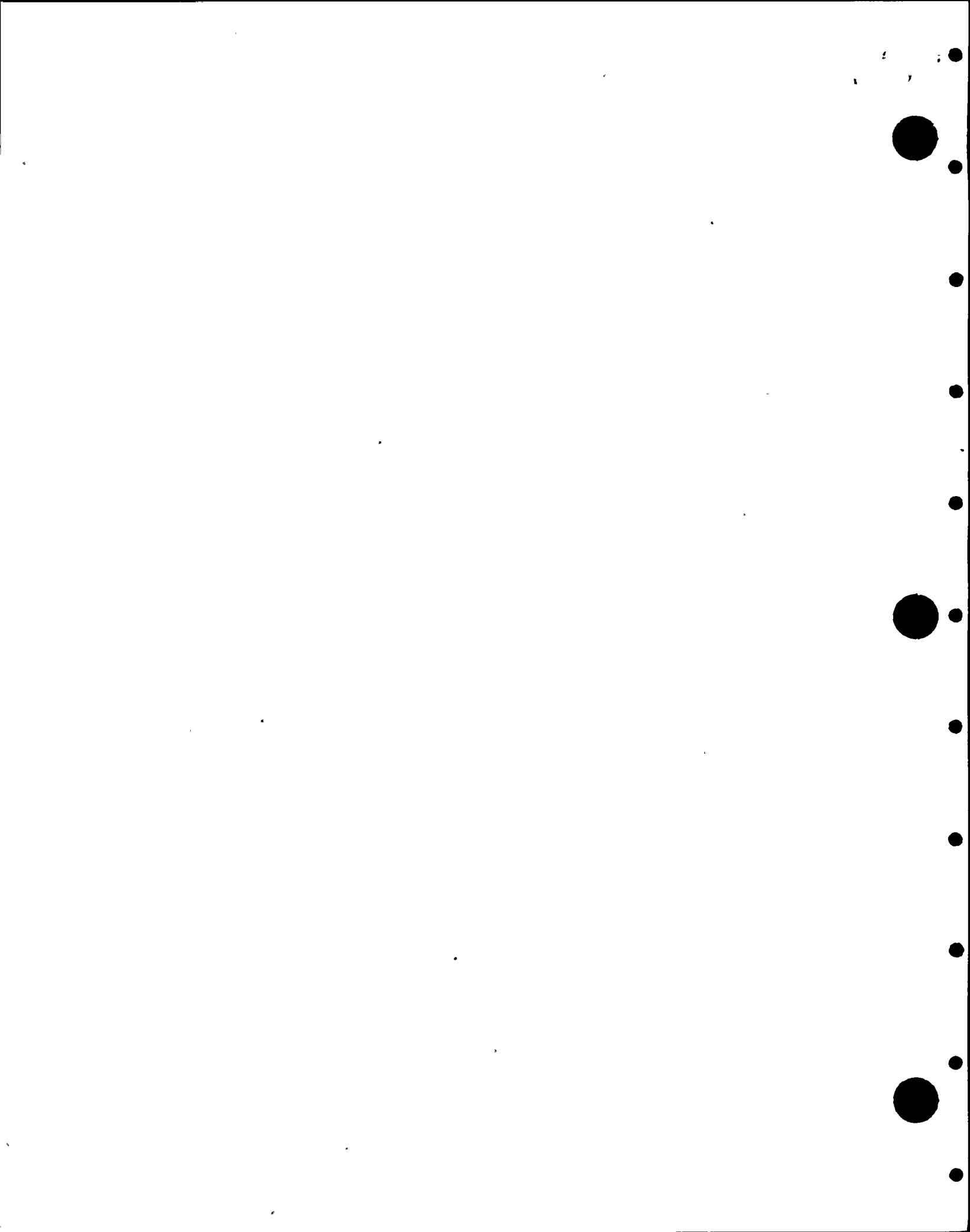
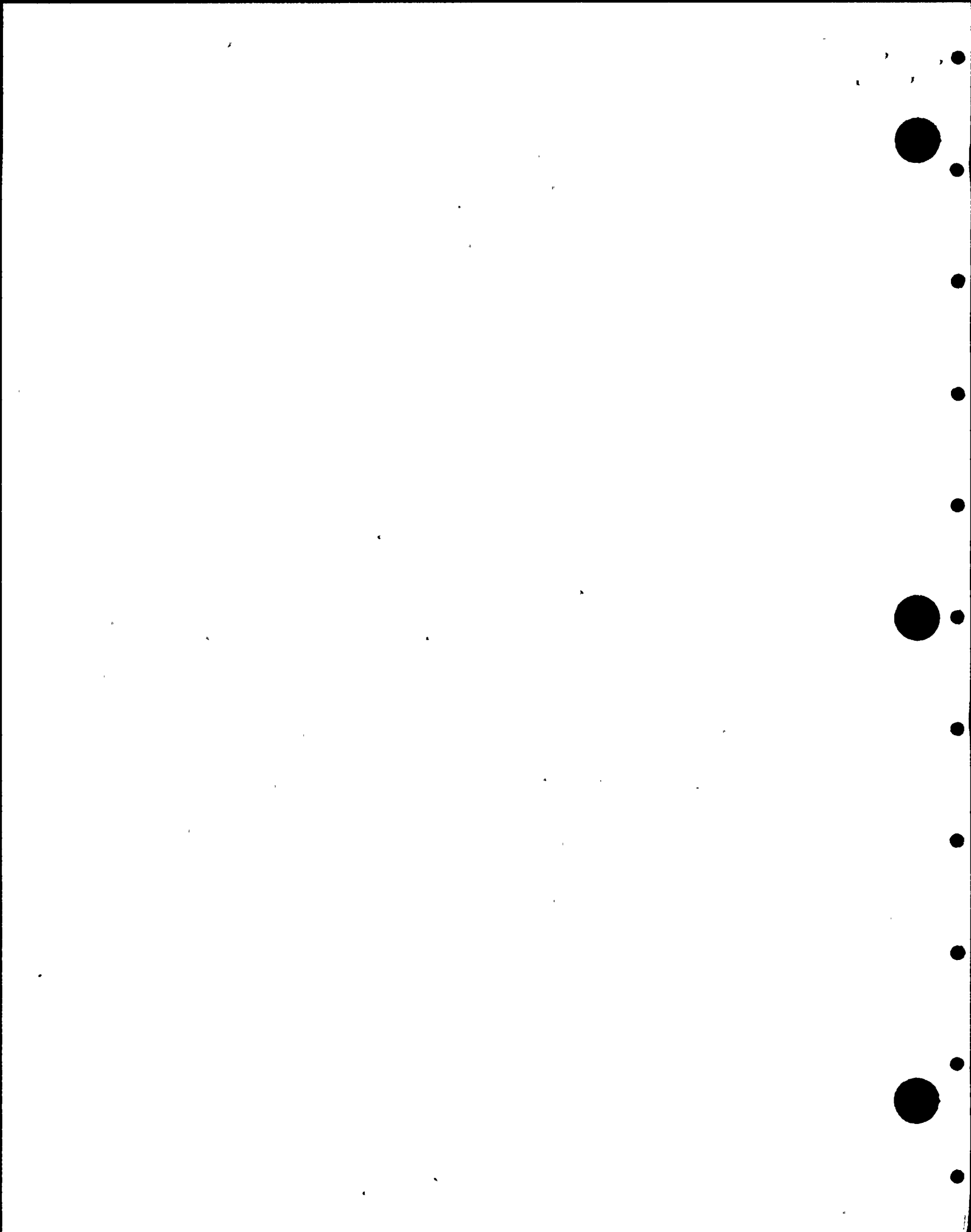


TABLE OF CONTENTS

<u>Section</u>	<u>Page</u>
EXECUTIVE SUMMARY	ii
INTRODUCTION	1
CONDENSATION OSCILLATION DOWNCOMER PRESSURE	2
NINE MILE POINT DOWNCOMER GEOMETRY	6
ANALYSIS	8
RESULTS	13
REFERENCES	18
APPENDIX - ANALYSIS OF TORUS CURVATURE EFFECTS	19



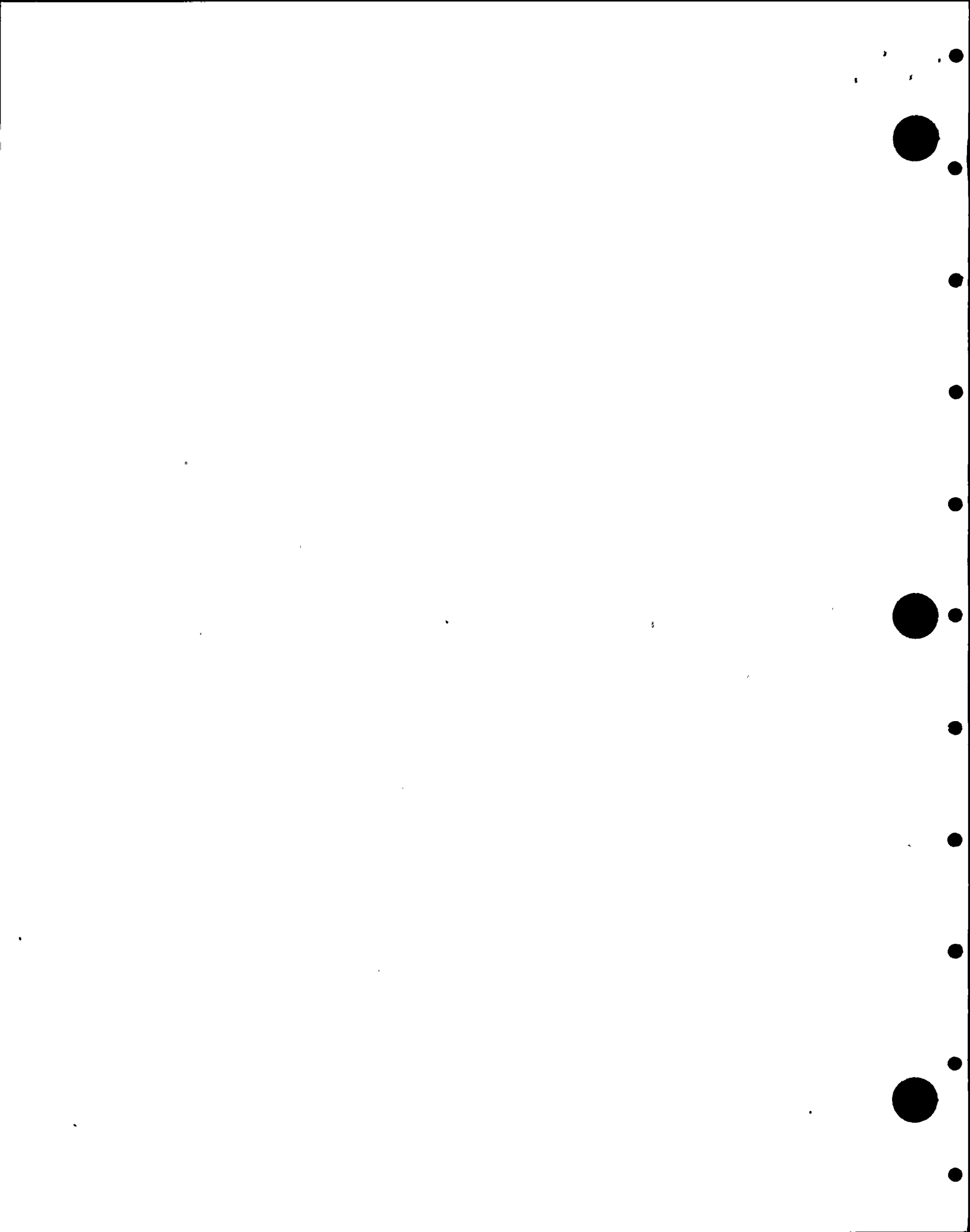
EXECUTIVE SUMMARY

An analysis is reported which investigates the conservatism of the hydrodynamic torus condensation oscillation load definition derived from data taken in the Mark I Full-Scale Test Facility (FSTF). It is shown that during condensation oscillation (CO), the condensation events at the downcomer exits are, as a function of frequency, random in phase for most harmonic components. As a consequence of this observation, and the geometrical constraints built into the FSTF, measured CO loads applied to Nine Mile Point are conservative for two reasons.

- o Alternate downcomer bays in Nine Mile Point have four-eight-four-eight, etc., downcomers per bay. The FSTF facility, by construct, assumes that all bays have eight downcomers per bay.
- o The FSTF modeled a 22 1/2° sector of a prototypical Mark I suppression pool. The water was contained in the sector by two very rigid end caps which would not exist in a full suppression pool. These end caps hydrodynamically act as mirrors. This results in a measured load, as if all bays in a full torus had condensation phenomenon identical in phase and amplitude, to the instrumented bay.

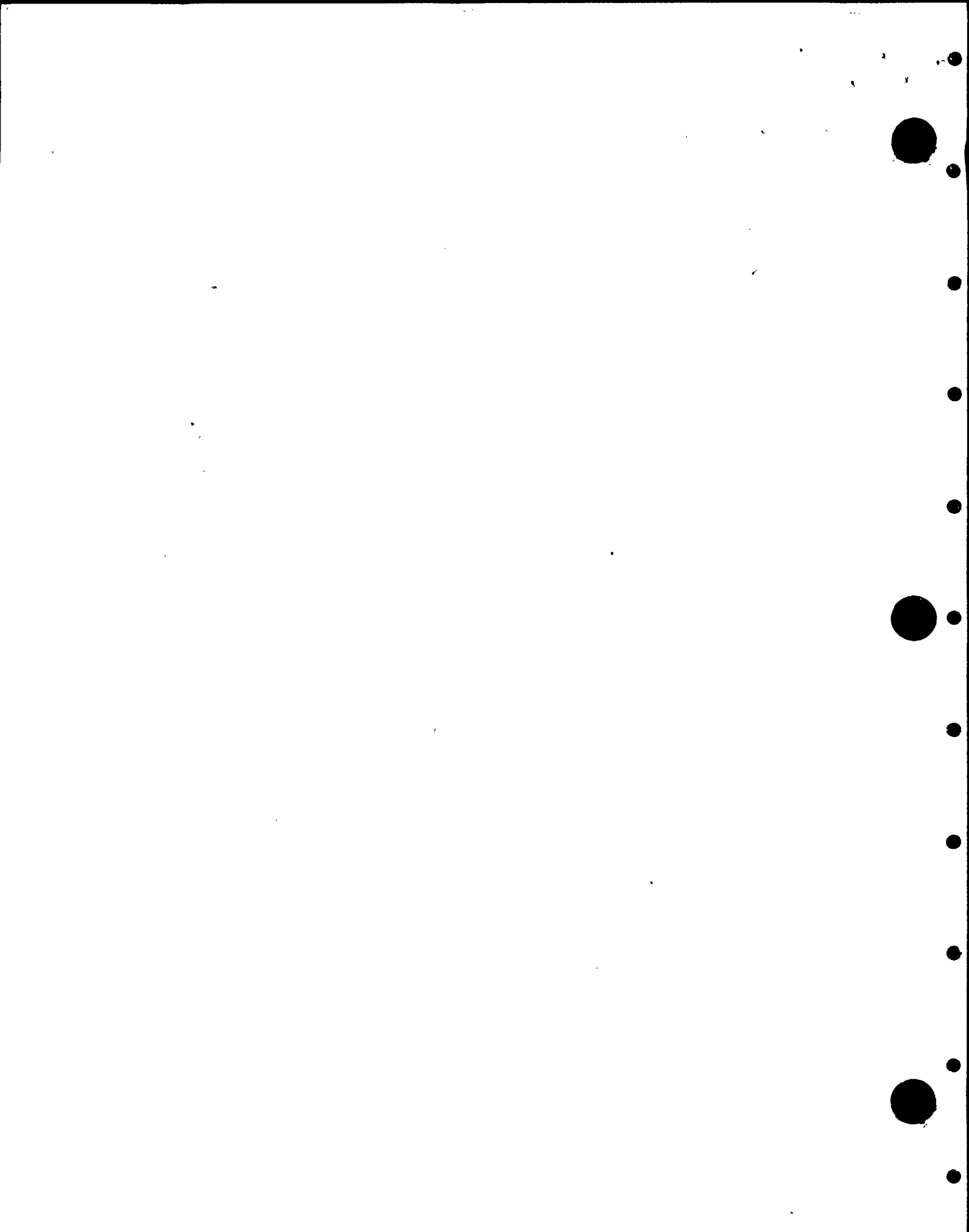
The analysis contained herein shows that for Nine Mile Point:

- o Eight downcomer bays have bay averaged CO loads which are conservative by at least 19% at frequencies other than 5-6 Hz.
- o Four downcomer bays have bay averaged CO loads which are conservative by at least 38% at frequencies other than 5-6 Hz.



INTRODUCTION

In 1979, Continuum Dynamics, Inc. was asked by the Mark I owners group, through G.E., to assess the conservatism in the Condensation Oscillation torus loads measured during the FSTF blowdown tests. This effort confirmed generally accepted conservatism in the tests with regard to test initial condition thermodynamics, and identified a significant conservatism which was not identified during test design. This conservatism was introduced by the very geometry of the test facility, a one-sixteenth sector which is equivalently a $22\ 1/2^\circ$ segment of the Mark I Pressure Suppression Pool Torus. The sector or segment is referred to as a bay in subsequent discussion. The test facility, although full-scale in cross section, attempted to simulate at full-scale the condensation phenomenon in one bay only. End caps were required (which do not exist in actual suppression pool tori) to contain the pool water and the airspace above the pool in the bay. The analysis, which analyzes the hydrodynamic consequences of these end caps, was presented to the Mark I owners in 1980 and is documented as Reference 1. Since the documentation may not have received wide distribution, key portions of the analysis which are needed to support the current work are repeated here. An attempt is made here to assemble one document which supports reduction of the condensation oscillation load definition (Ref. 2) for Nine Mile Point.



CONDENSATION OSCILLATION DOWNCOMER PRESSURE

The FSTF facility contained one bay with eight downcomers which were fed steam from a prototypical main vent. The details of the facility and the instrumentation utilized is documented in Reference 3. During condensation oscillation, steam exiting the downcomers established a pulsating steam-water interface at the downcomer exit. This pulsation, resulting from unsteady steam condensation, produces pressure pulses which are transmitted through the pool water to the torus walls. Curiously, the loads which would be transmitted to the torus walls of a prototypical suppression pool torus depend on the correlation of the unsteady condensation at the exit of each downcomer.

Fortunately, in FSTF, the correlation between unsteady condensation at each downcomer exit is easy to assess as a consequence of pressure transducers located three feet above each of the eight downcomers. During condensation oscillation the steam-water interface is positioned as schematically illustrated in Figure 1 relative to the downcomer exit transducers. The unsteady pressure signals measured by these transducers is then, for the most part, a measure of the unsteadiness in condensation at the steam-water interface near which the transducer is mounted.

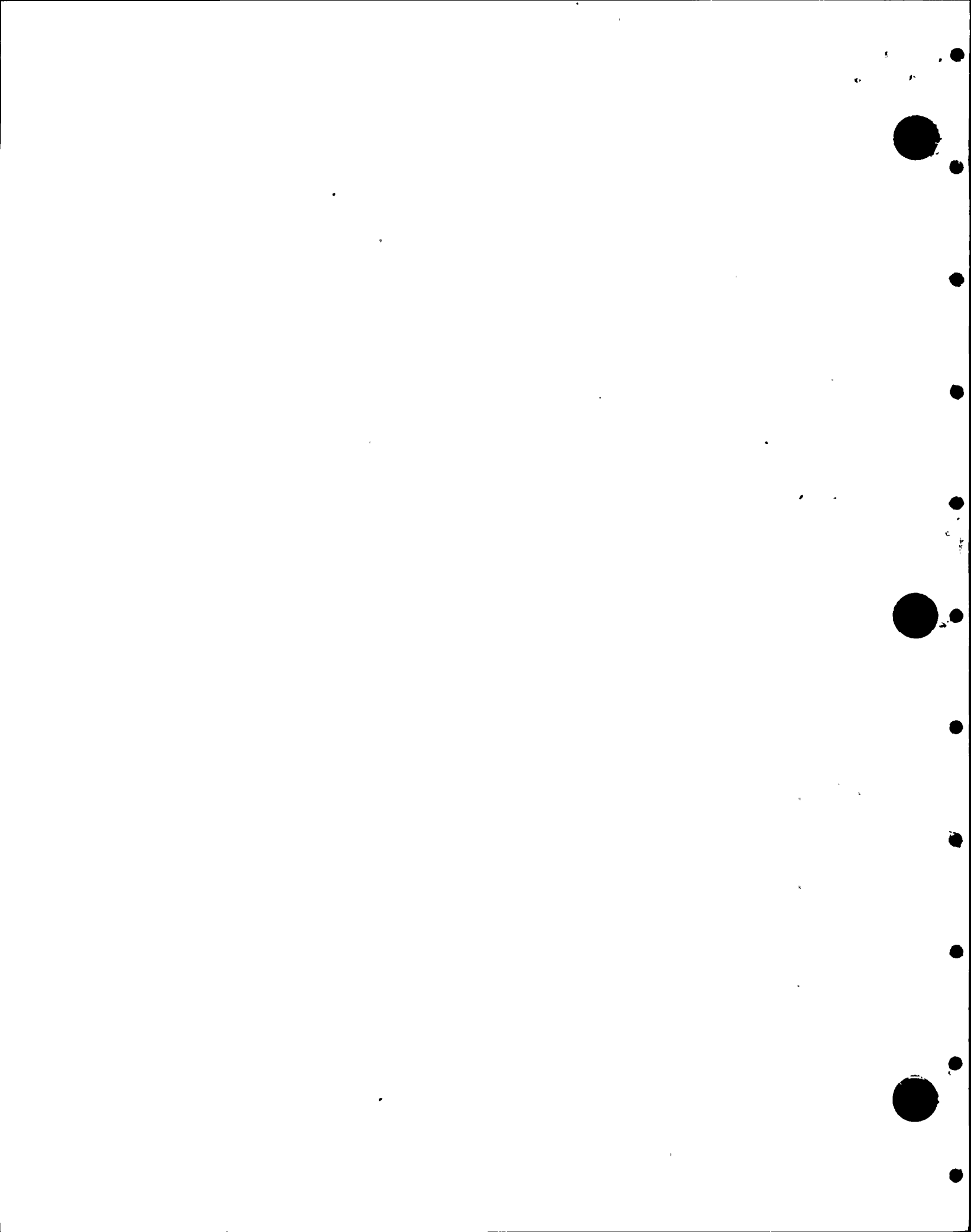
The mean square pressure between transducers in two downcomers with pressures $p_i(t)$ and $p_j(t)$ is given by

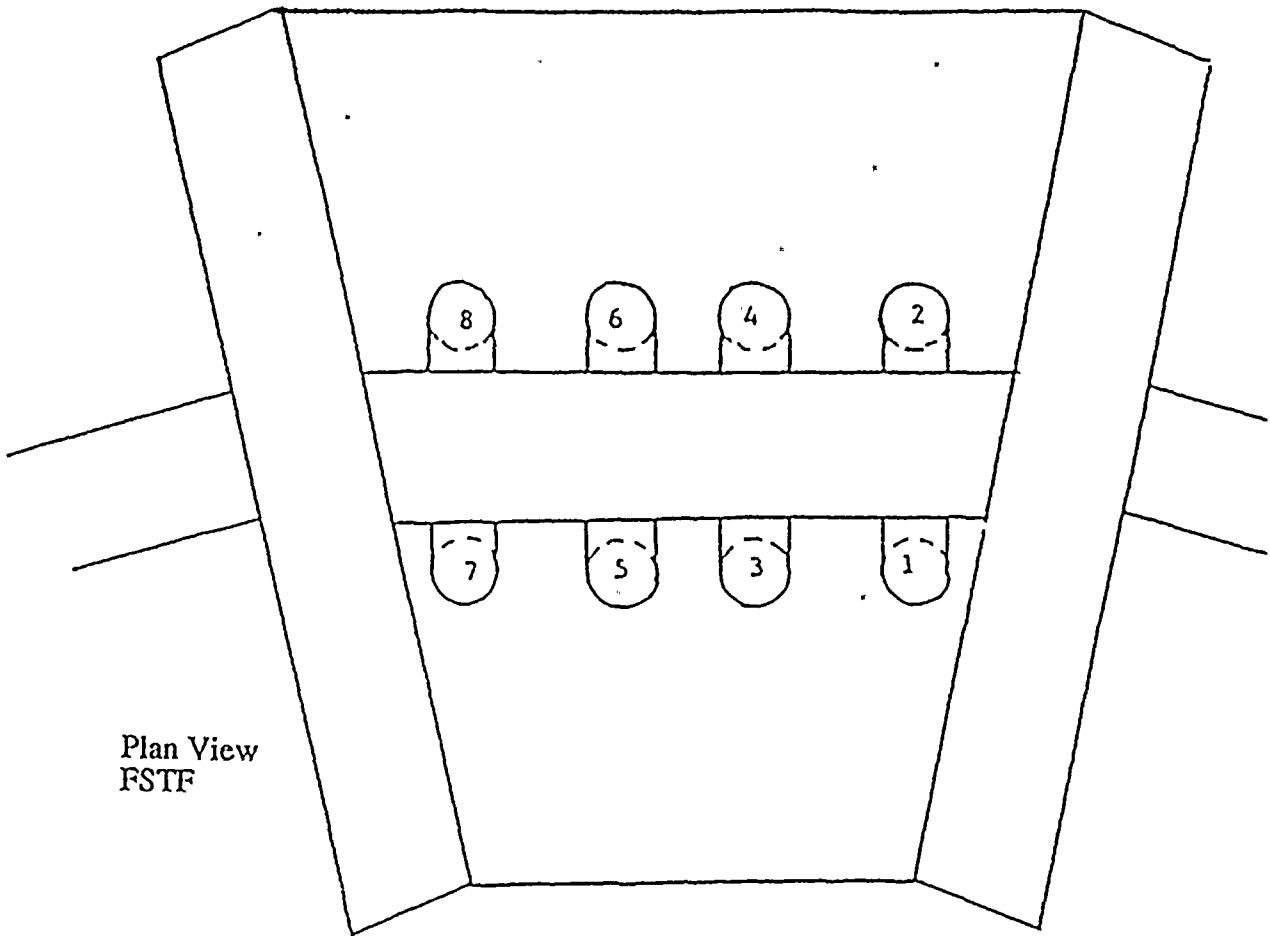
$$\overline{(p_i + p_j)^2}^* = \overline{p_i^2}^* + \overline{p_j^2}^* + 2 \overline{p_i p_j}^* \quad (1)$$

where the overbar star notation denotes time average. The signals p_i and p_j are random and coherent if $\overline{p_i p_j}^* = 0$ when $i \neq j$. The correlation coefficient

$$\rho_{ij} = \frac{\overline{p_i p_j}^*}{\sqrt{\overline{p_i^2}^*} \sqrt{\overline{p_j^2}^*}} = 0 \quad (2)$$

then is necessarily equal to zero.





Plan View
FSTF

VENT
1
2
3
4
5
6
7
8

TRANSDUCER
P5123
P5243
P5323
P5443
P5523
P5643
P5723
P5843

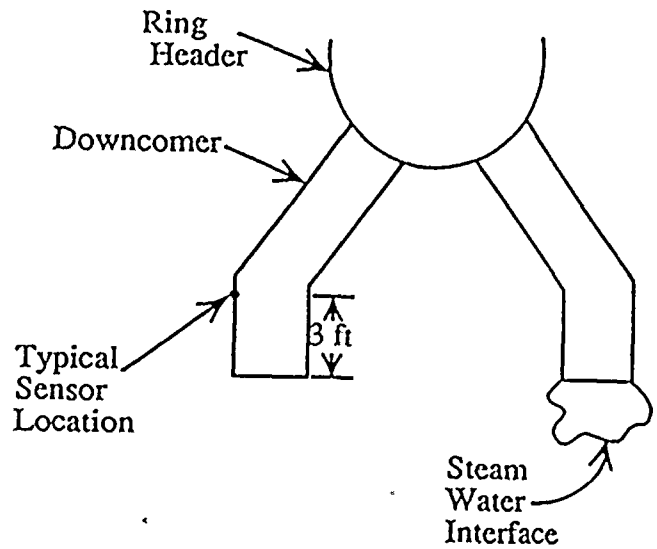
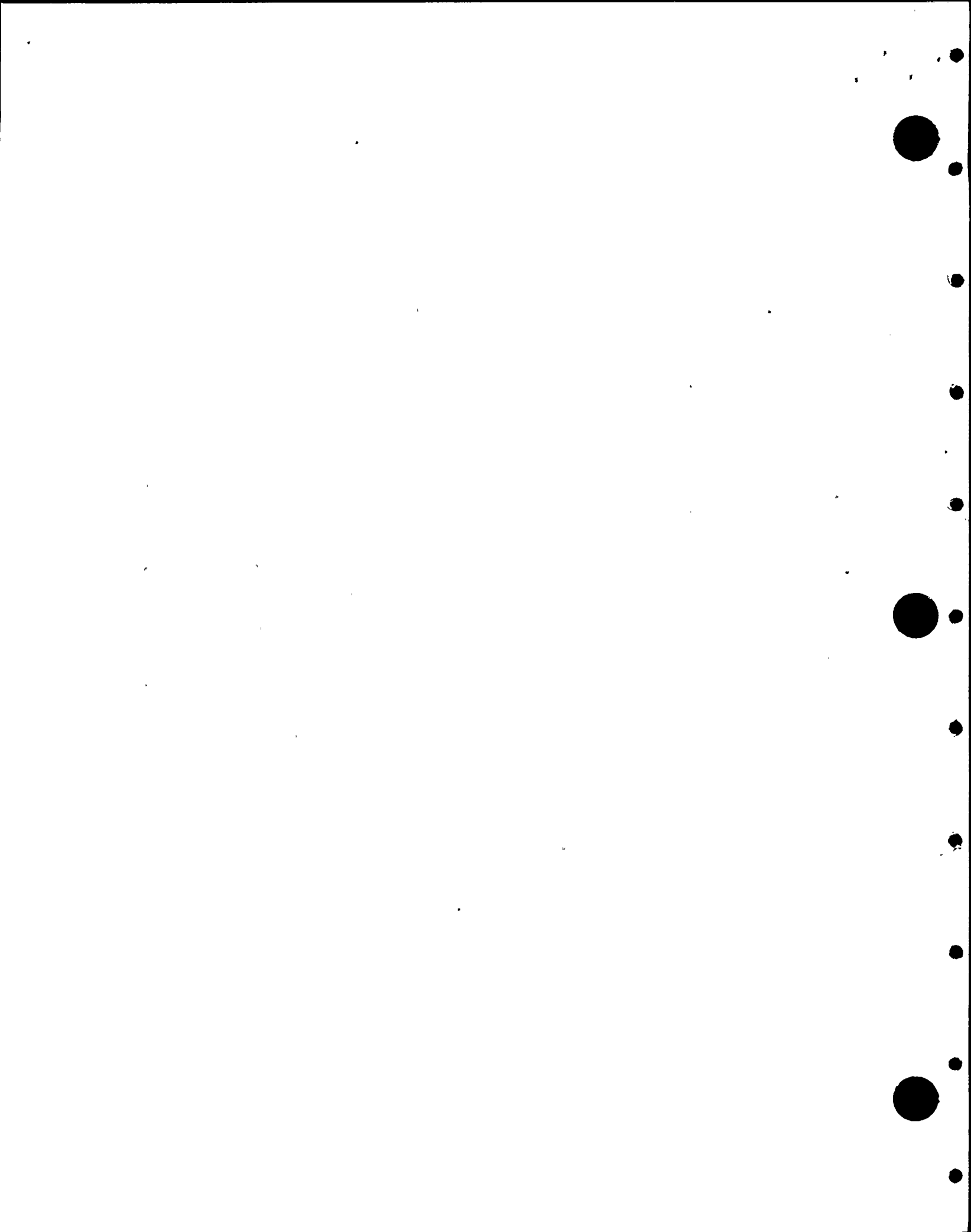
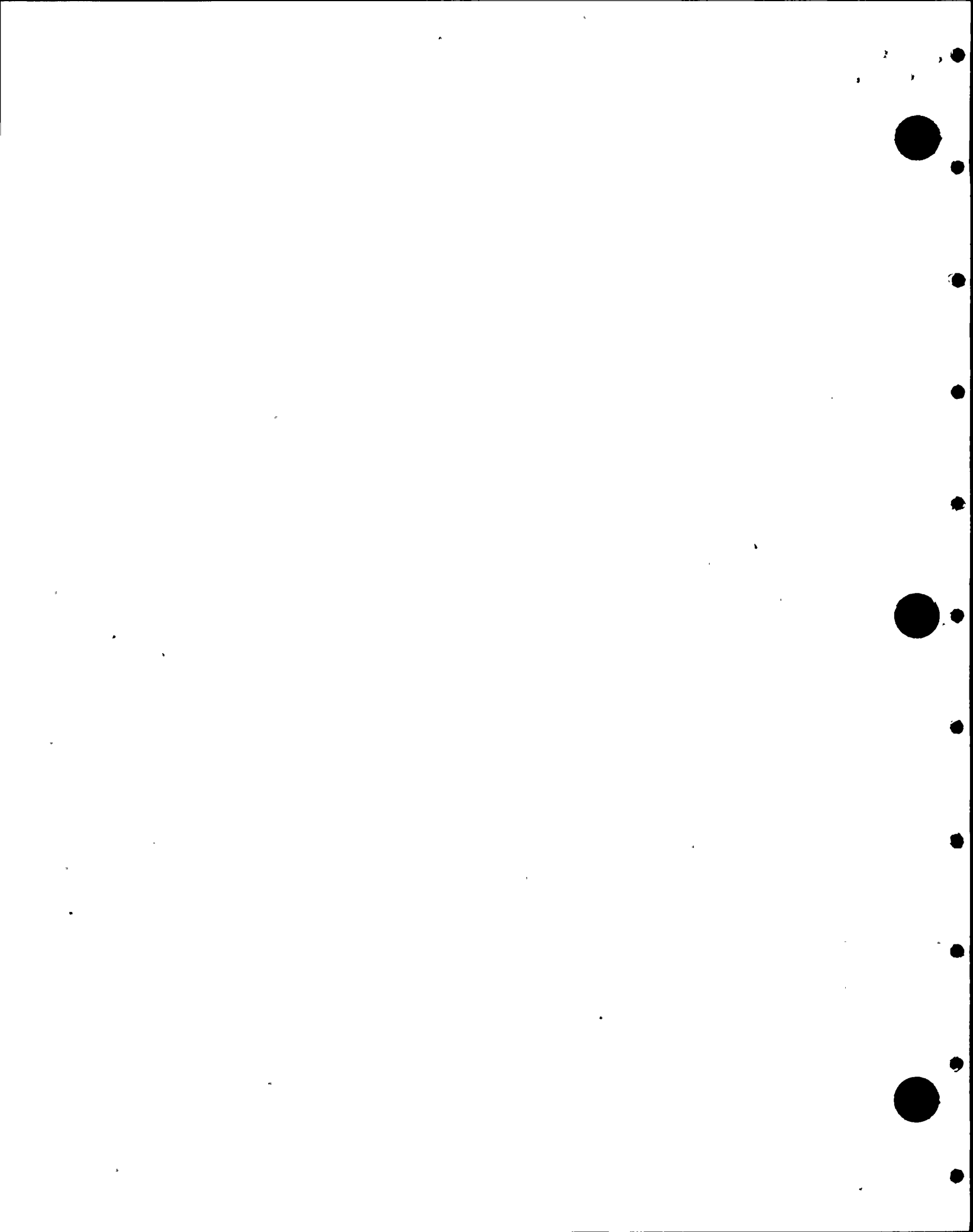


Figure 1. Downcomer exit pressure transducers in FSTF.



During Run M8 in the FSTF test series, upon which the load definition is based, strong condensation oscillation loads were observed on the torus shell for the time period 20-35 seconds after test initiation. The data from vent exit pressure transducers 3-5 was Fourier decomposed and then used to construct the mean square pressure signal $\overline{(p_i + p_j)^2}$ and components $\overline{p_i^2} + \overline{p_j^2}$ and $2\overline{p_i p_j}$ for 15 of the downcomer pair combinations. These components were calculated as a function of bandwidth with the band starting at zero frequency. Typical results are shown in Figure 2 between downcomers 5 and 6 in the bandwidth range 0-50 Hz. The result is that the pressure signals measured at the downcomer exits are correlated only between 5 and 6 Hz. Note that vents 5 and 6 are very close physically to each other and little if any cross talk (cross correlation) is observed at other than at 5-6 Hz. Analysis of other downcomer pair combinations during condensation oscillation also show correlation only at the 5-6 Hz. frequency. In fact, the correlation coefficient in the frequency range 5-6 Hz. is approximately 0.5.

The following analysis allows the conclusion to be drawn, that it is reasonable to expect, that during condensation oscillation in a full torus, condensation phenomenon at downcomer exits are for the most part (except 5-6 Hz.) random and incoherent. Therefore, tests run in the FSTF facility must necessarily measure higher loads, because of the reflection built into the end caps required by the facility. These end caps do not permit incoherent pressures from adjoining bays to sum up to a lower load. This result is now quantified with regard to measured loads in FSTF and evaluated for Nine Mile Point.



CORRELATION OF PRESSURE SOURCES:

$$\overline{(p_5+p_6)^2}^* = \overline{p_5^2}^* + \overline{p_6^2}^* + 2\overline{p_5 p_6}^*$$

$$\overline{p_5^2}(\omega) = \left[\int_0^\omega \hat{p}_5(\omega) e^{i\omega t} \right]^2^*$$

Transform

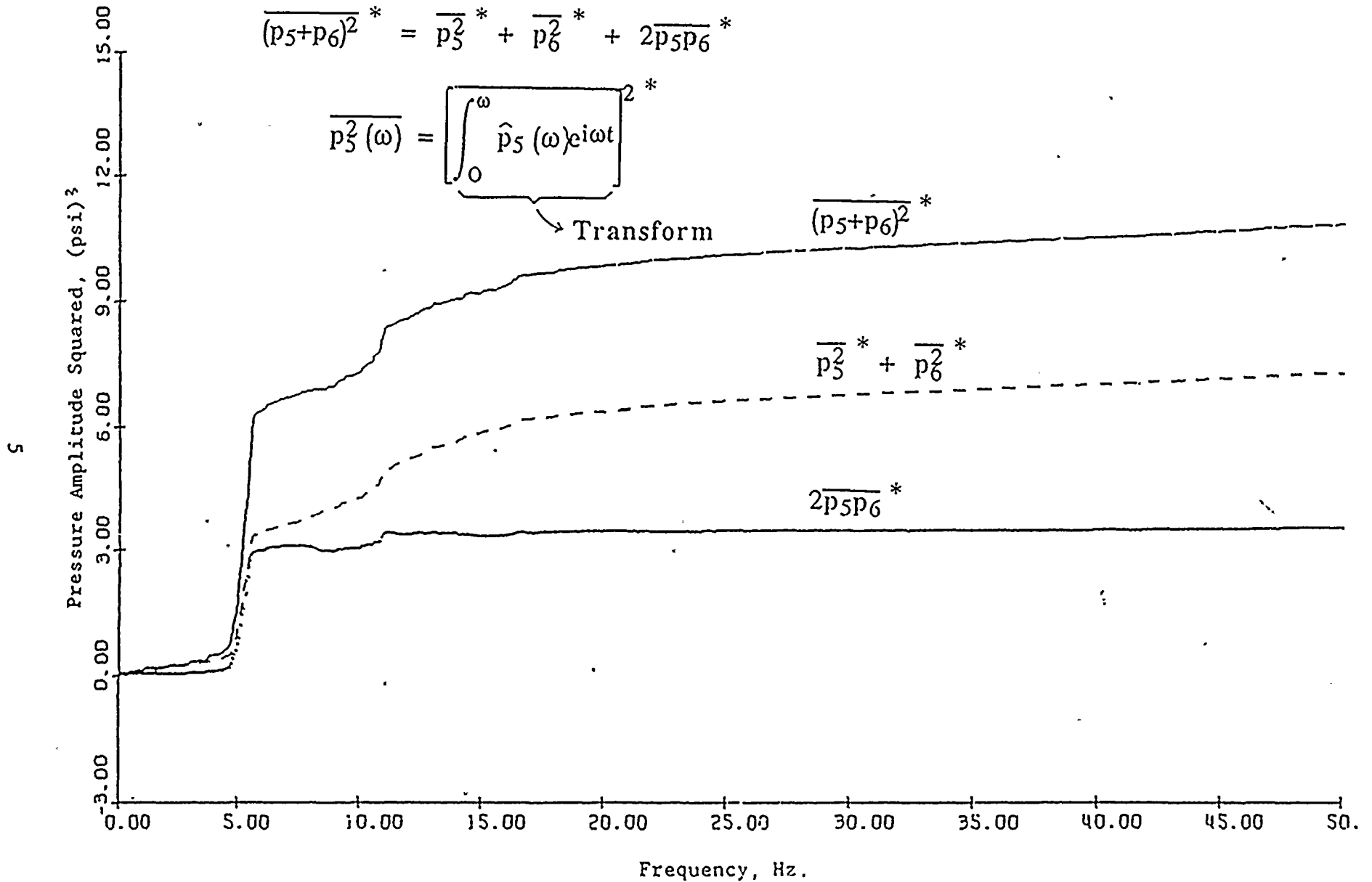
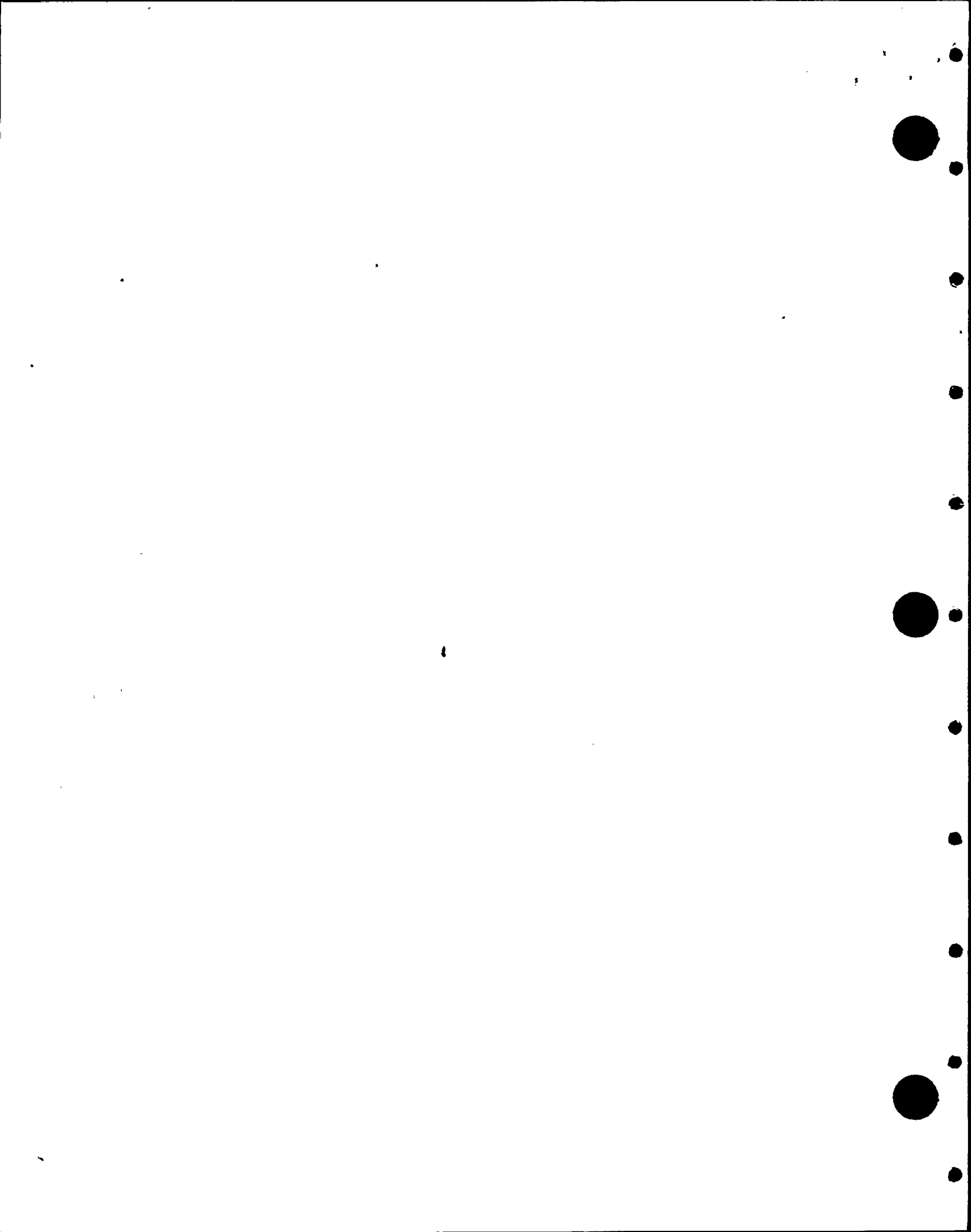
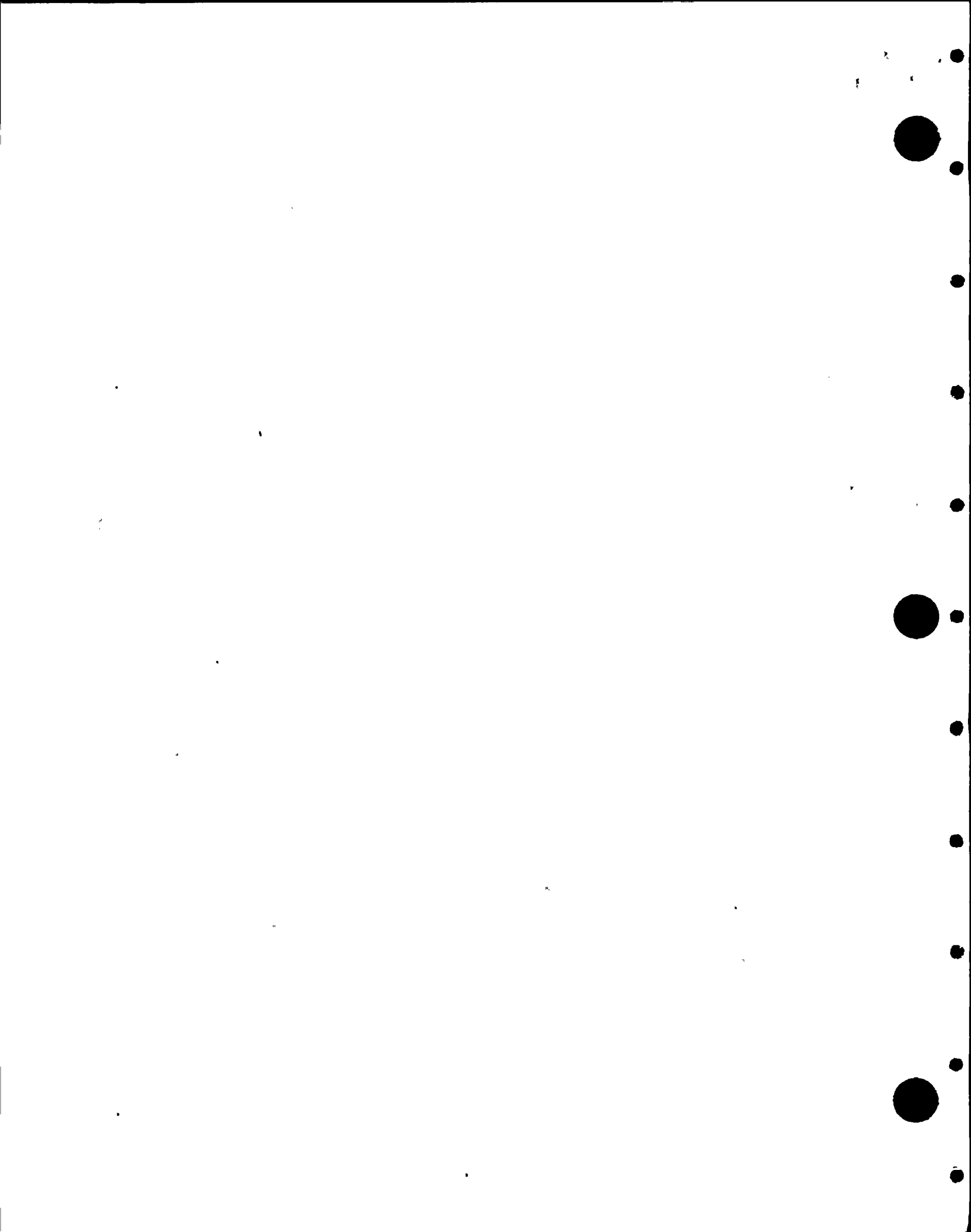


Figure 2. Mean Square pressure signals between downcomers 5 and 6, FSTF Run M8, 20 - 35 seconds during condensation oscillation as a function of frequency (measured from zero frequency.).



NINE MILE POINT DOWNCOMER GEOMETRY

On Figure 3 is shown the plan view of the Nine Mile Point suppression pool torus with bays alternating between four and eight downcomers, respectively. It is clear from this geometry that the bottom dead center pressure loads in a four downcomer bay will differ considerably from that in an eight downcomer bay. In the analysis to follow, analytic models are developed to account for the alternating distribution of downcomers in bays as well as the toroidal geometry. It will be seen that significant load reductions are shown to exist in the current bottom center load definition resulting from incoherence between sources and alternating number of downcomers between bays. Little or no relief can be identified with torus curvature which in the Appendix is shown to modify the distribution of pressure along the bottom of the torus only slightly.



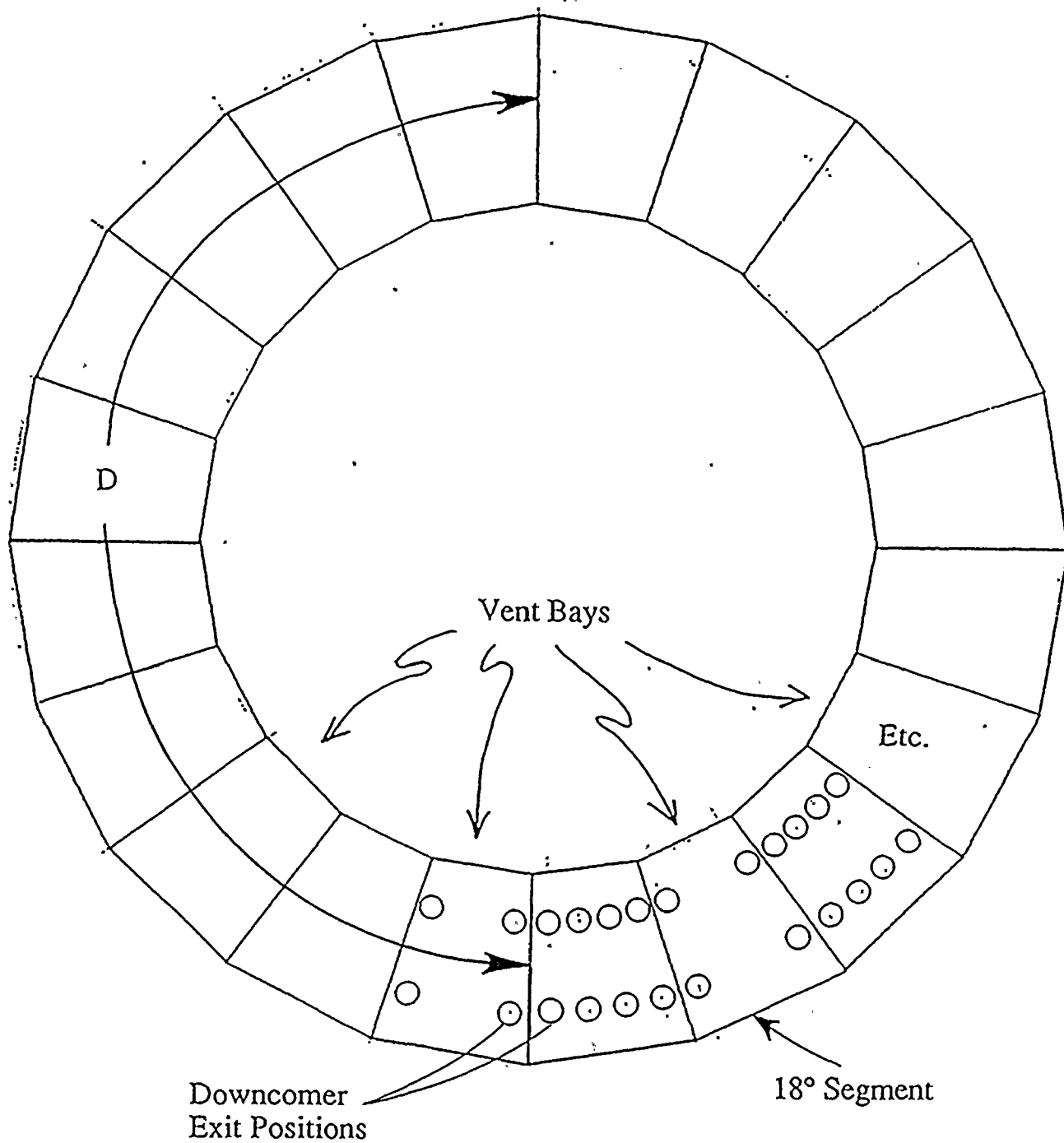
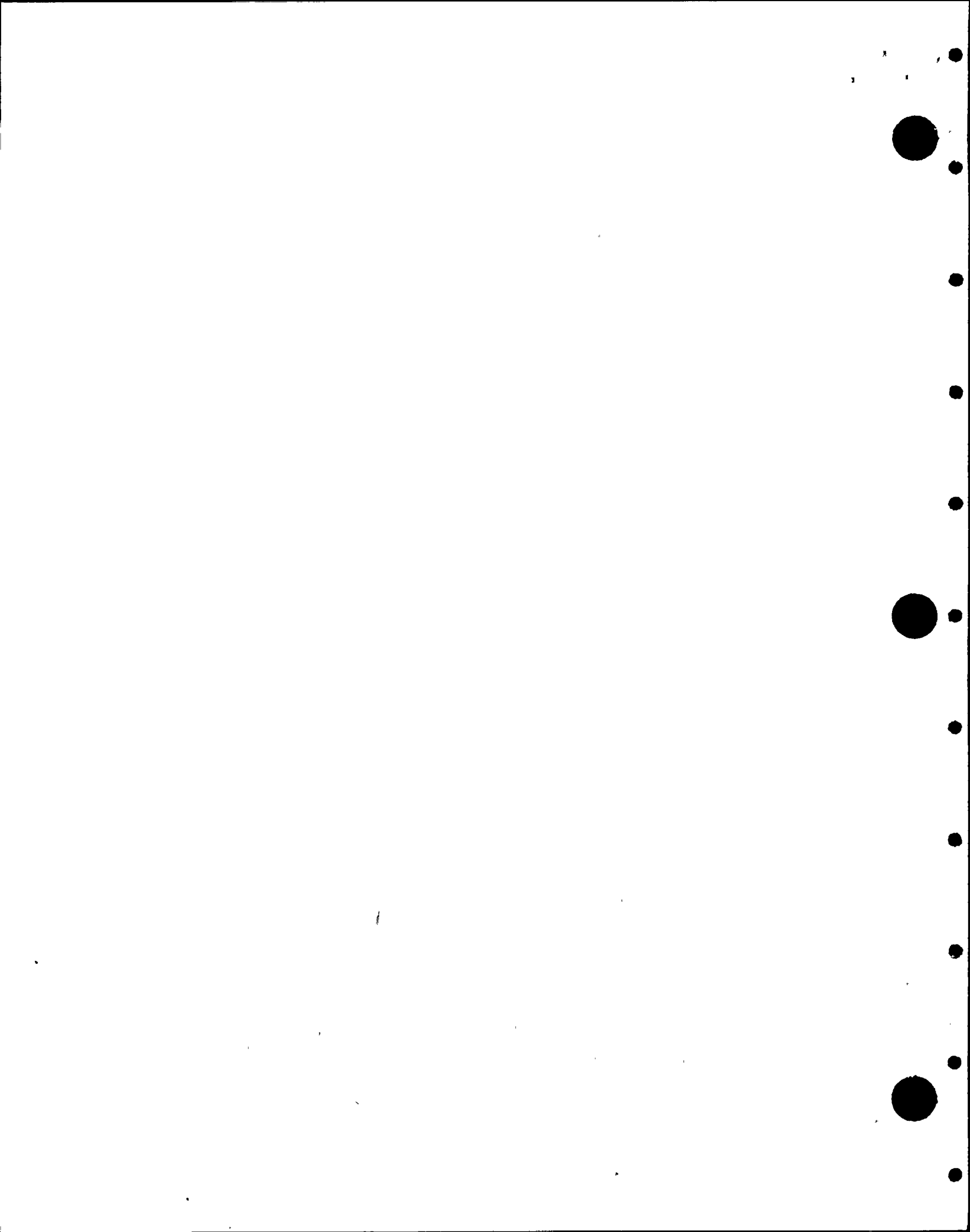


Figure 3. Plan view of Nine Mile Point suppression pool showing 8-4-8-4 downcomer/bay geometry. (Not to Scale)



ANALYSIS

The analysis of a full torus proceeds by unwinding the torus as shown in Figure 4. The torus has radius a and a source is located at $r = r_v$, $\theta = \theta_v$, and $z = 0$. At $z = D$ (half circumference) the pressure must satisfy a reflection boundary condition to account for waves traveling to the right and left of the torus. The pressure p satisfies the wave equation

$$\frac{\partial^2 p}{\partial r^2} + \frac{1}{r} \frac{\partial p}{\partial r} + \frac{1}{r^2} \frac{\partial^2 p}{\partial \theta^2} + \frac{\partial^2 p}{\partial z^2} - \frac{1}{c^2} \frac{\partial^2 p}{\partial t^2} = 0 \quad (3)$$

where c is the acoustic speed in the pool. The solution to the wave equation must satisfy the following boundary conditions

$$\begin{aligned} p(r, 0, z, t) &= p(r, \pi, z, t) = 0 & 0 \leq r \leq a, 0 \leq z \leq D \\ \frac{\partial p}{\partial r}(a, \theta, z, t) &= 0 & 0 \leq \theta \leq \pi, 0 \leq z \leq D \\ \frac{\partial p}{\partial z}(r, \theta, D, t) &= 0 & 0 \leq r \leq a, 0 \leq \theta \leq \pi \end{aligned} \quad (4)$$

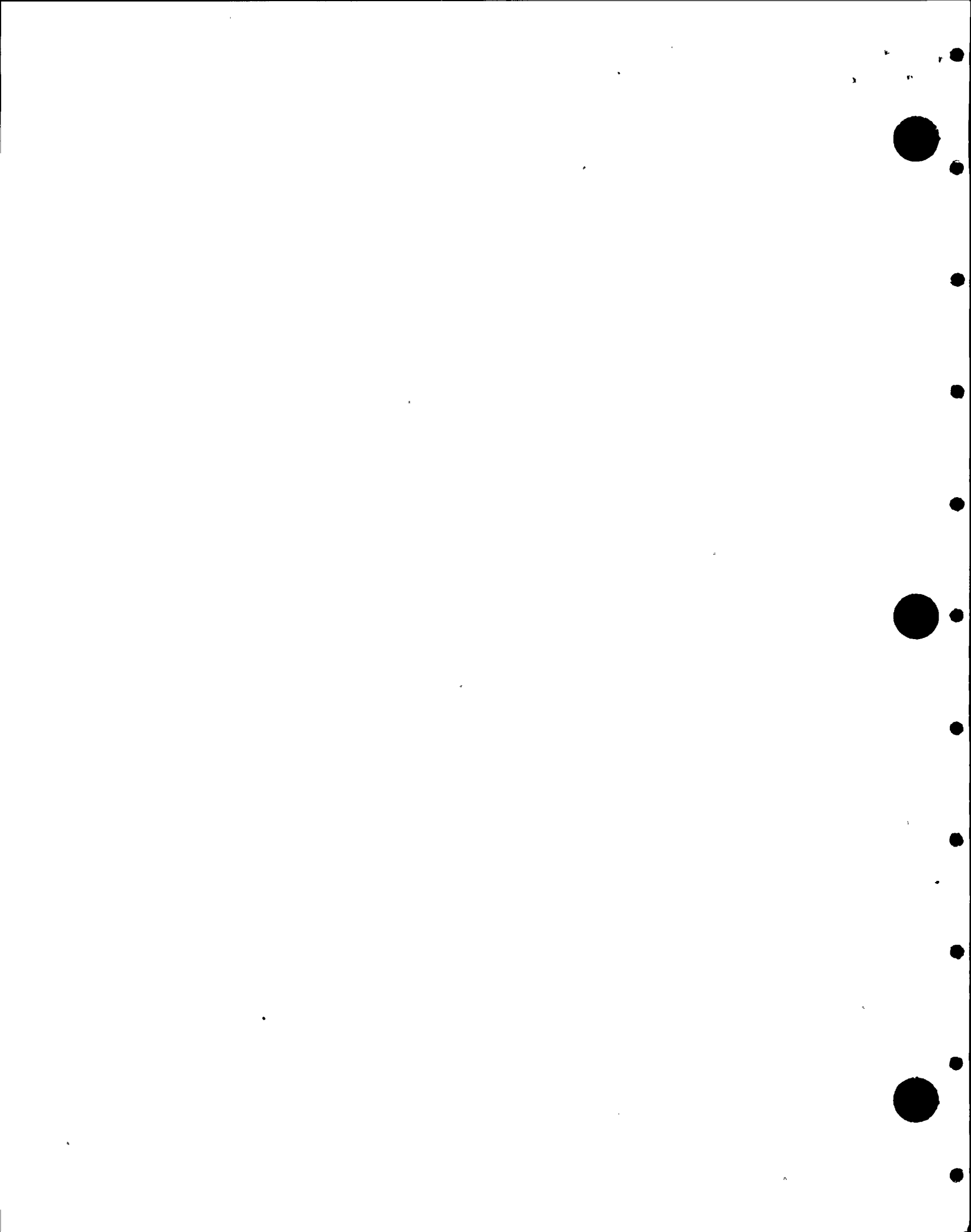
For harmonic time dependence of the form $e^{i\omega t}$ it has been shown (Ref.1) that the root mean square pressure \bar{p} on the torus wall satisfies (note overbar denotes r.m.s.)

$$\bar{p}(a, \theta, z) = \frac{2p\omega\bar{Q}}{\pi a^2} \sum_{n=1}^{\infty} \sum_{j=1}^{\infty} \hat{c}_{nj} \sin n\theta \cosh[\alpha_{nj}(D-z)] \quad (5)$$

where

$$\hat{c}_{nj} = \frac{\sin n\theta_v}{\alpha_{nj} \sinh[\alpha_{nj} D]} \frac{J_n(m_n^j \frac{r_v}{a})}{J_n(m_n^j)} \left[\frac{(m_n^j)^2}{(m_n^j)^2 - n^2} \right]$$

$$\alpha_{nj} = \frac{1}{a} \sqrt{(m_n^j)^2 - \left(\frac{\omega a}{c}\right)^2}$$



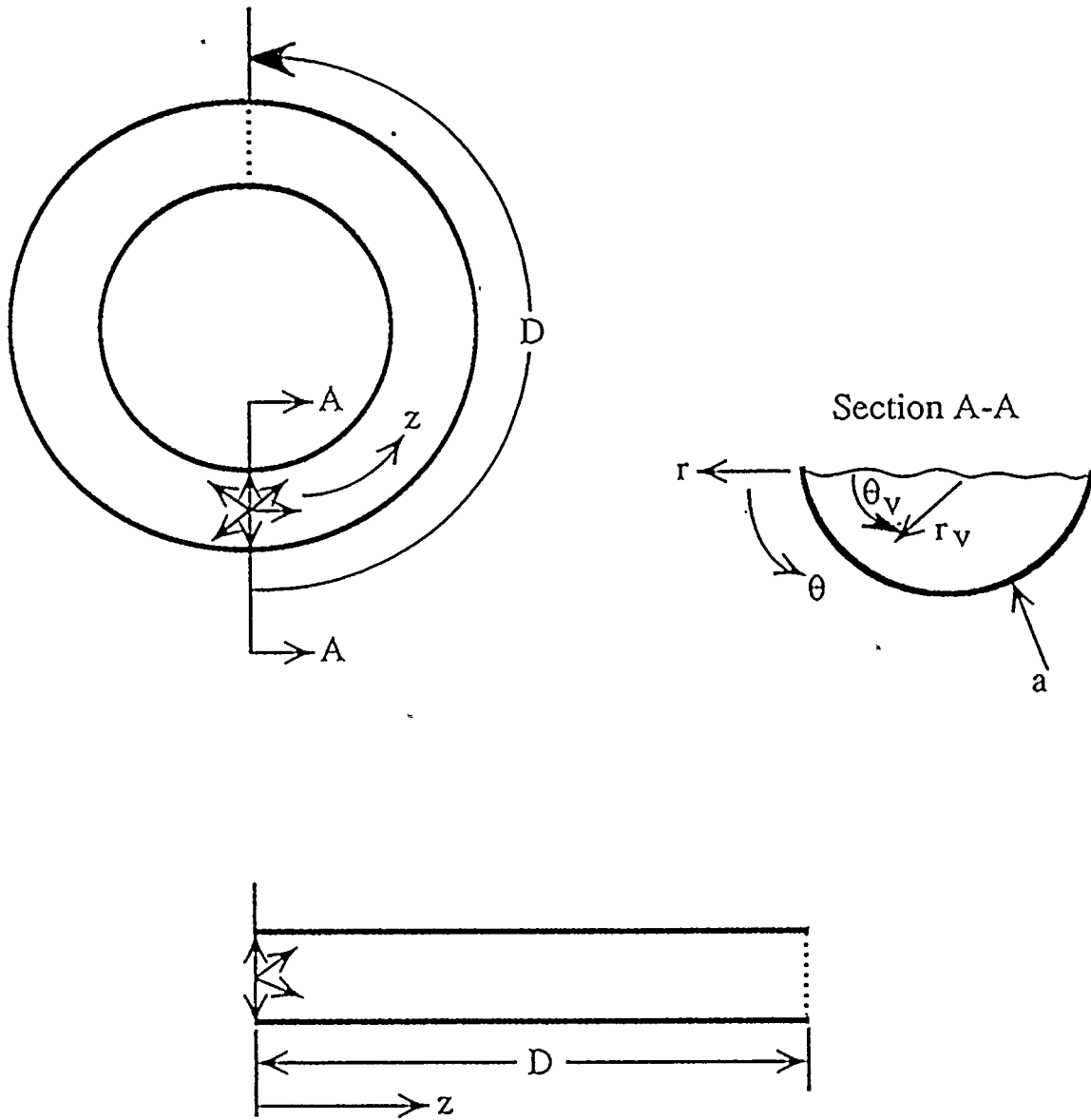
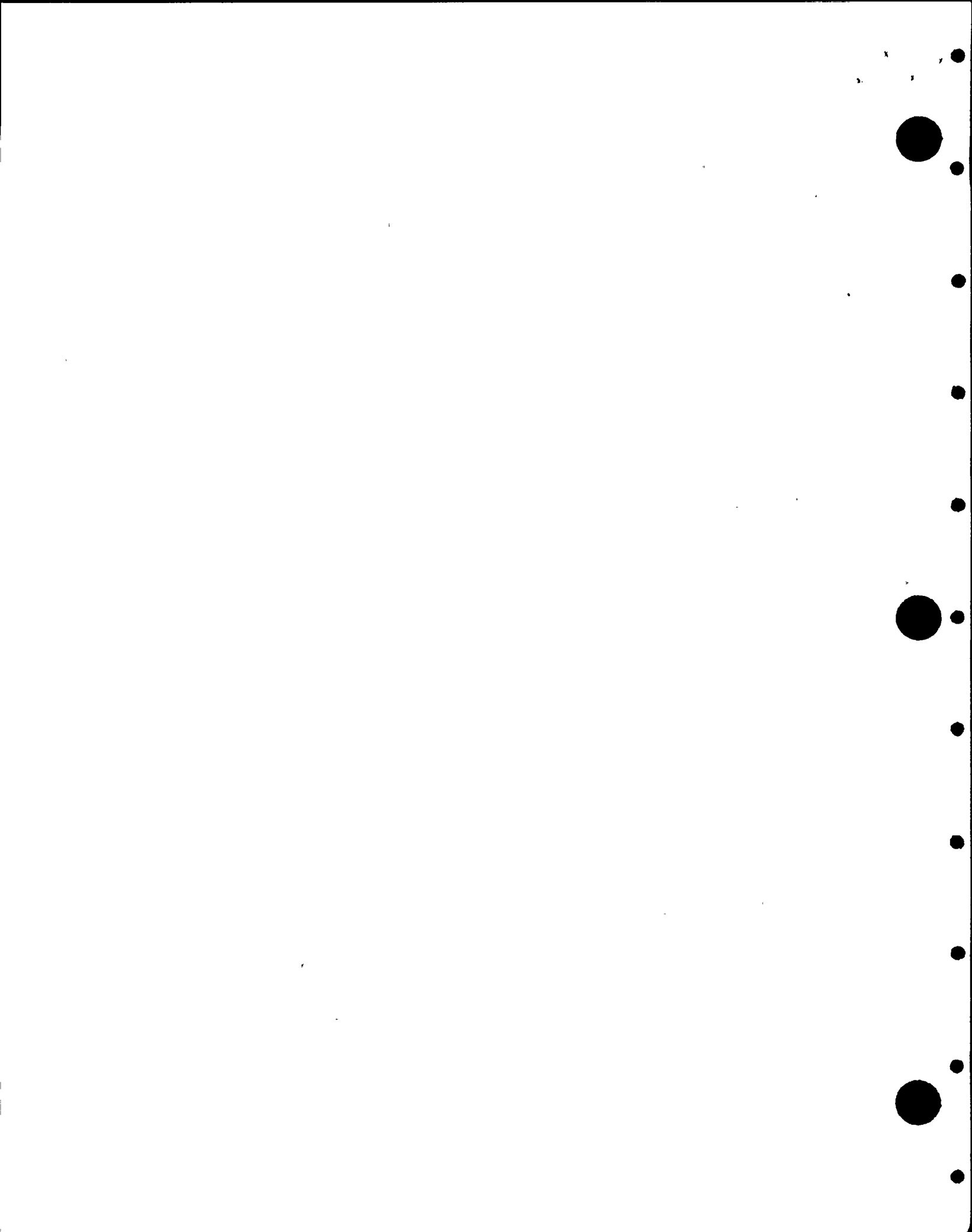


Figure 4. Coordinate system for analysis of Mark I Torus. A source is located at $r = r_v$, $\theta = \theta_v$, $z = 0$.



$$m_n^j = j^{\text{th}} \text{ stationary value of the Bessel function } J_n \quad (6)$$

The analysis to this point is exactly that which was given in Reference 1. Since we are interested in computing the variation of the load by going from eight vent to four vent says the area averaged vertical component of the rms pressure is not computed as before but is averaged over θ only by

$$\bar{p}_{av} = \frac{1}{2a} \int_0^\pi \bar{p} \sin\theta \, a d\theta \quad (7)$$

yielding the important result (as before) that only the $n=1$ term in the pressure will result in a net vertical load on the torus shell. Therefore,

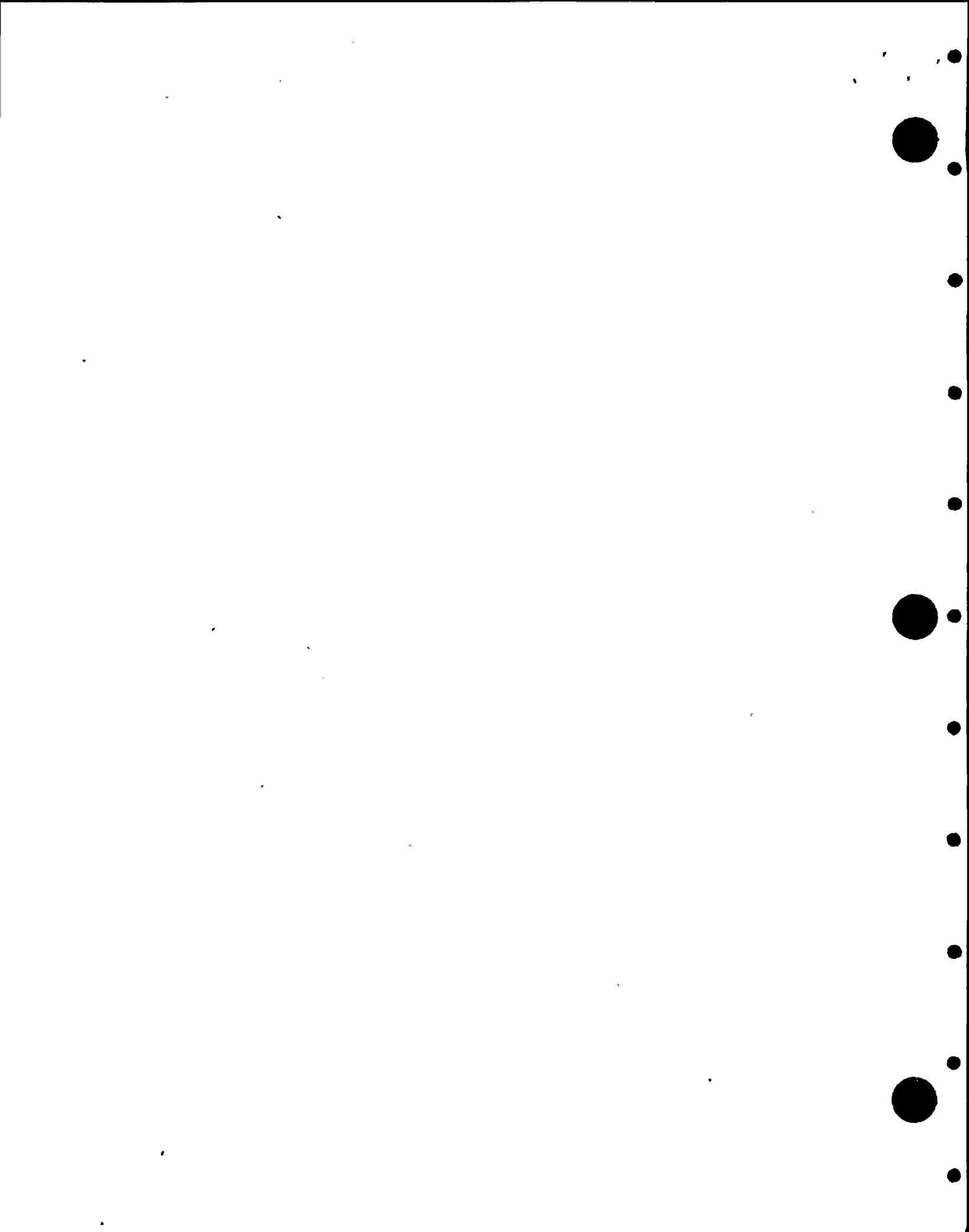
$$\bar{p}_{av}(z) = \frac{\rho\omega\bar{Q}}{2a^2} \sum_{j=1}^{\infty} \hat{c}_{1j} \cosh[\alpha_{1j}(D-z)], \quad 0 \leq z \leq D \quad (8)$$

Now in the FSTF facility, if the sources are assumed correlated it has been shown (Ref. 1) that the source strength is related to the experimentally measured pressure by

$$\bar{Q}_c = \frac{\bar{p}_{av} \ell_v a^2}{2\rho\omega} \left[\sum_{j=1}^{\infty} K_{j1} \cosh\left[\alpha_{1j} \frac{\ell_v}{4}\right] \right]^{-1} \quad (9)$$

where

$$K_{j1} = \frac{\sin\theta_v \sinh\left[\alpha_{1j} \frac{\ell_v}{4}\right] J_1\left(m_1^j \frac{\ell_v}{a}\right) \left[\frac{(m_1^j)^2}{(m_1^j)^2 - 1} \right]}{\alpha_1^2 \sinh\left[\alpha_{1j} \frac{\ell_v}{2}\right] J_1(m_1^j)} \quad (10)$$



The subscript c denotes the source strength for the correlated case and λ_v is the distance between downcomers in FSTF.

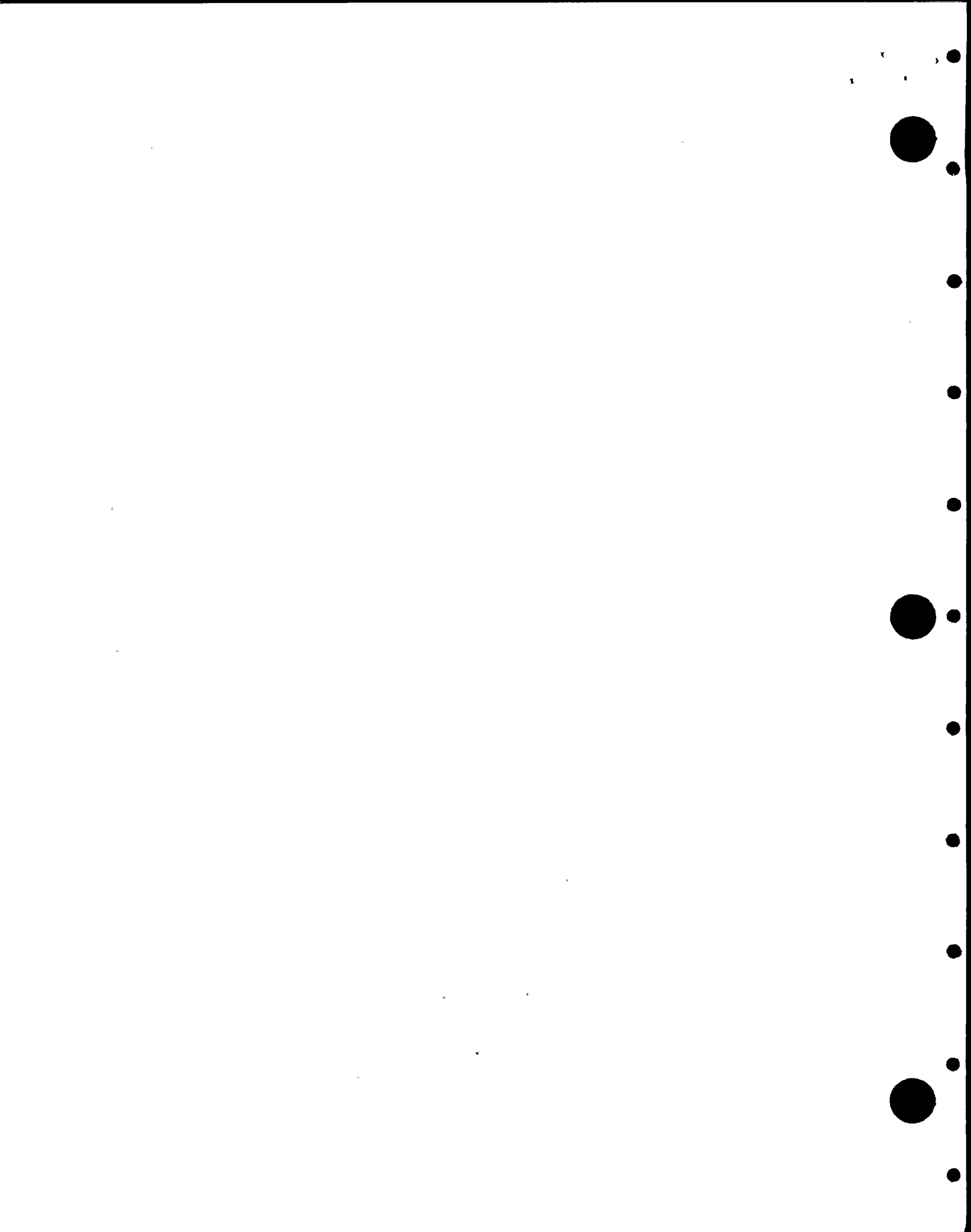
However, when the vents are uncorrelated the sources have been shown (Ref. 1) to be related to the correlated source strength by

$$\bar{Q}_u = \sqrt{8} \bar{Q}_c \quad (11)$$

The above pressure solution summed over the appropriate downcomer locations permit the direct computation of condensation oscillation load reduction factors. As a check the non-correlated load reduction factors for FSTF are reproduced here by

1. Determining \bar{Q}_c for $\bar{p}_{av} = 1$ and $\lambda_v = 4.88$ ft. ;
2. Determining $\bar{Q}_u = \sqrt{8} \bar{Q}_c$
3. Summing \bar{p}_{av} over 8 downcomers/FSTF bay over 16 bays as the square root of the sum of the squares.
4. Plotting the result as Figure 5 (since the average pressure for the correlated case was taken to be unity this summation is the load reduction factor).

The results are shown in Figure 5 (Ref.1). This is the reduction of harmonic amplitude which would be measured in FSTF had the facility included all 16 segments (except at 5-6 Hz.). It is seen from the plotted result that the harmonic load reduction factors are both a function of frequency and pool water acoustic speed. By assuming a high acoustic speed (5000 ft./sec.) conservative load reduction factors are anticipated. These results when squared can be compared to Figure 9 of Reference 1 and, since derived by an independent summation method, provide a check on the current analysis.



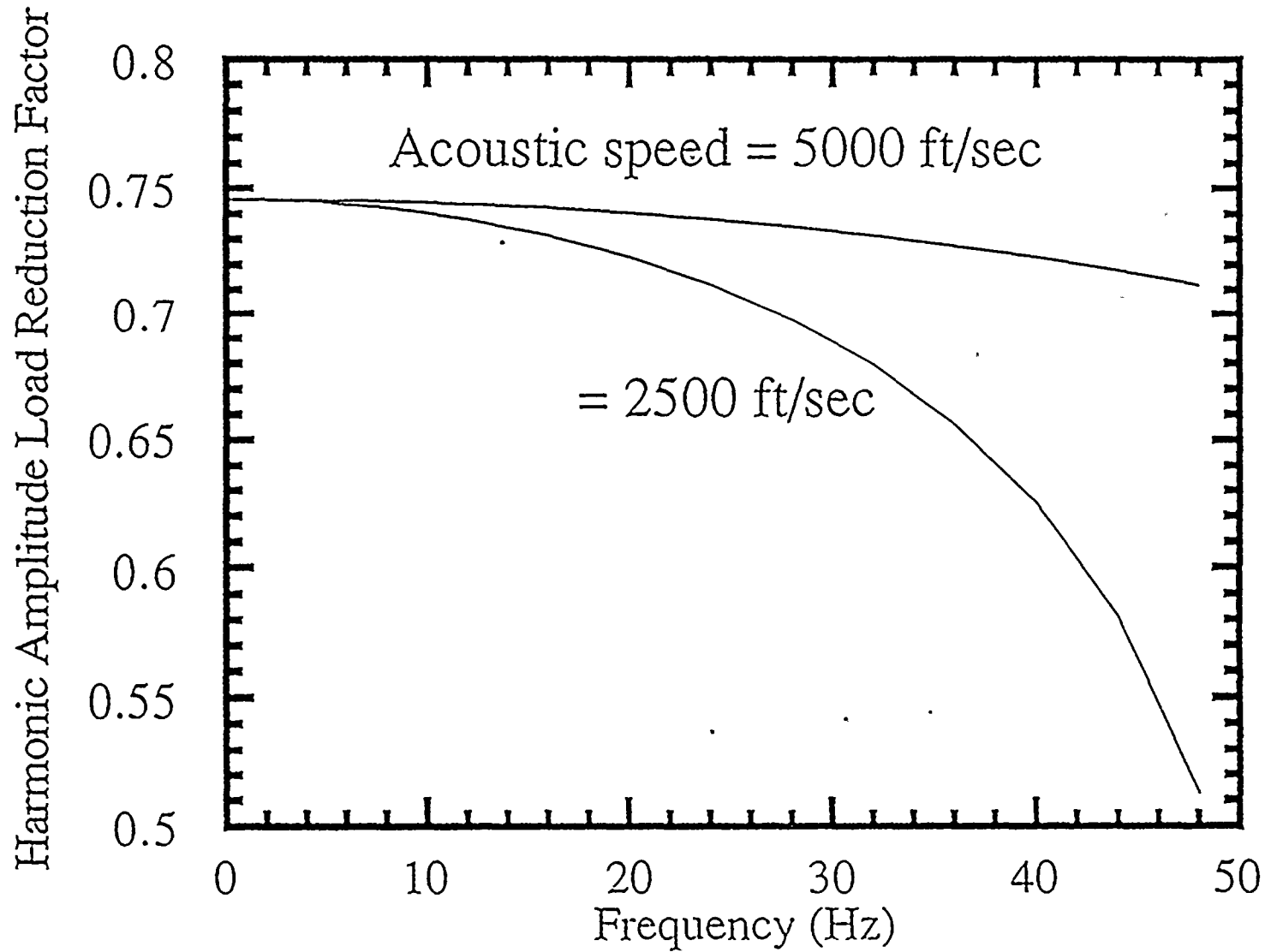
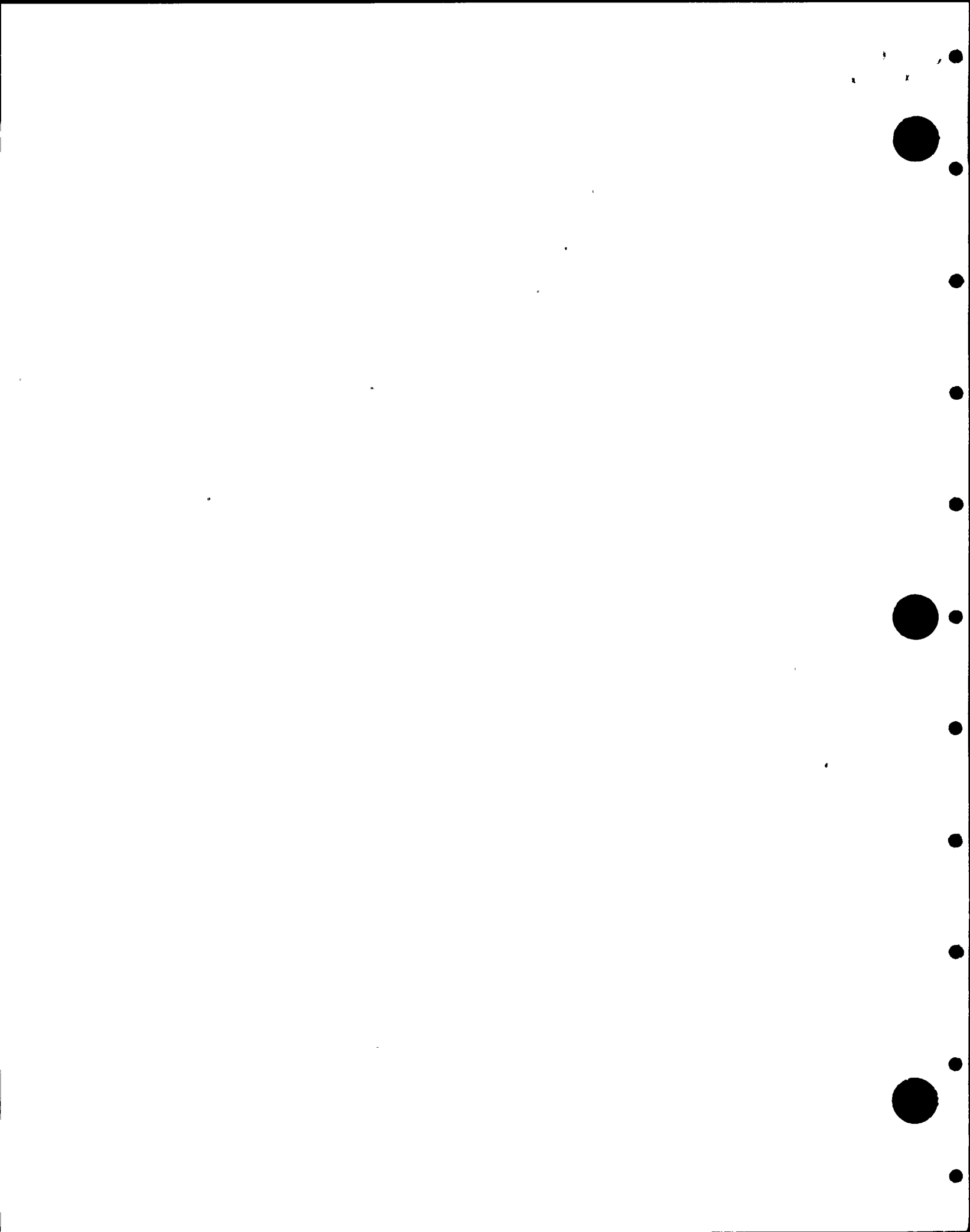


Figure 5. Harmonic amplitude load reduction factor (uncorrelated sources) for FSTF.



RESULTS - NINE MILE POINT

Referring to Figure 3, load reduction factors for Nine Mile Point are computed by:

For Correlated Sources

1. Evaluating the source strength \bar{Q}_c for $\bar{p}_{av} = 1$ for FSTF physical dimensions.
2. Summing the pressure for each frequency and location of each downcomer in Nine Mile Point according to:

$$\text{Load Reduction Factor} = \sum_{d=0}^{120} \bar{p}_{av}(z, \omega)$$

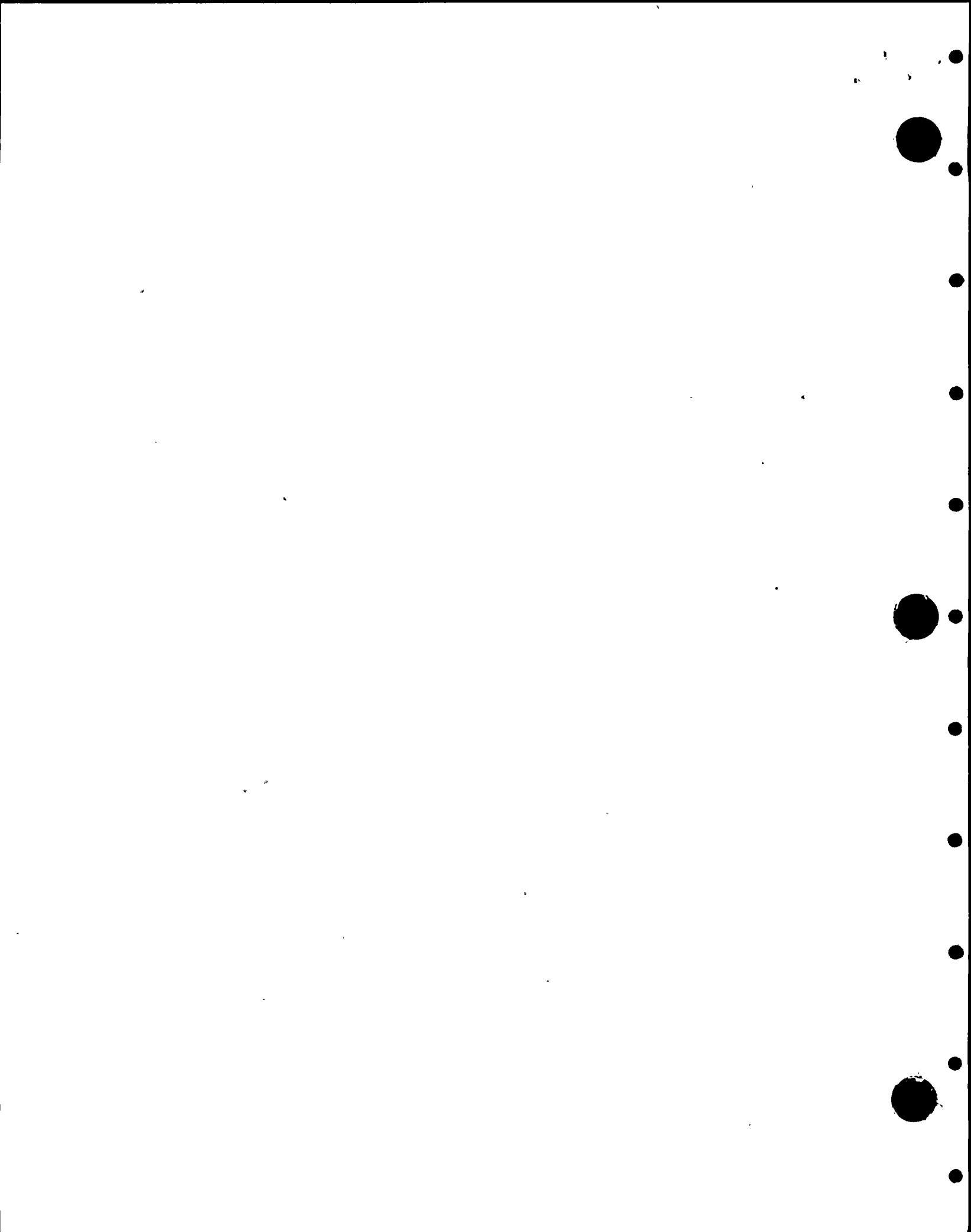
(Note that downcomer spacing and torus dimensions are as per Nine Mile Point)

For Uncorrelated Sources

1. Evaluating the uncorrelated source strength $\bar{Q}_u = \sqrt{8} \bar{Q}_c$ for $\bar{p}_{av} = 1$ in FSTF.
2. Summing the pressure for each frequency and location of each downcomer in Nine Mile Point according to

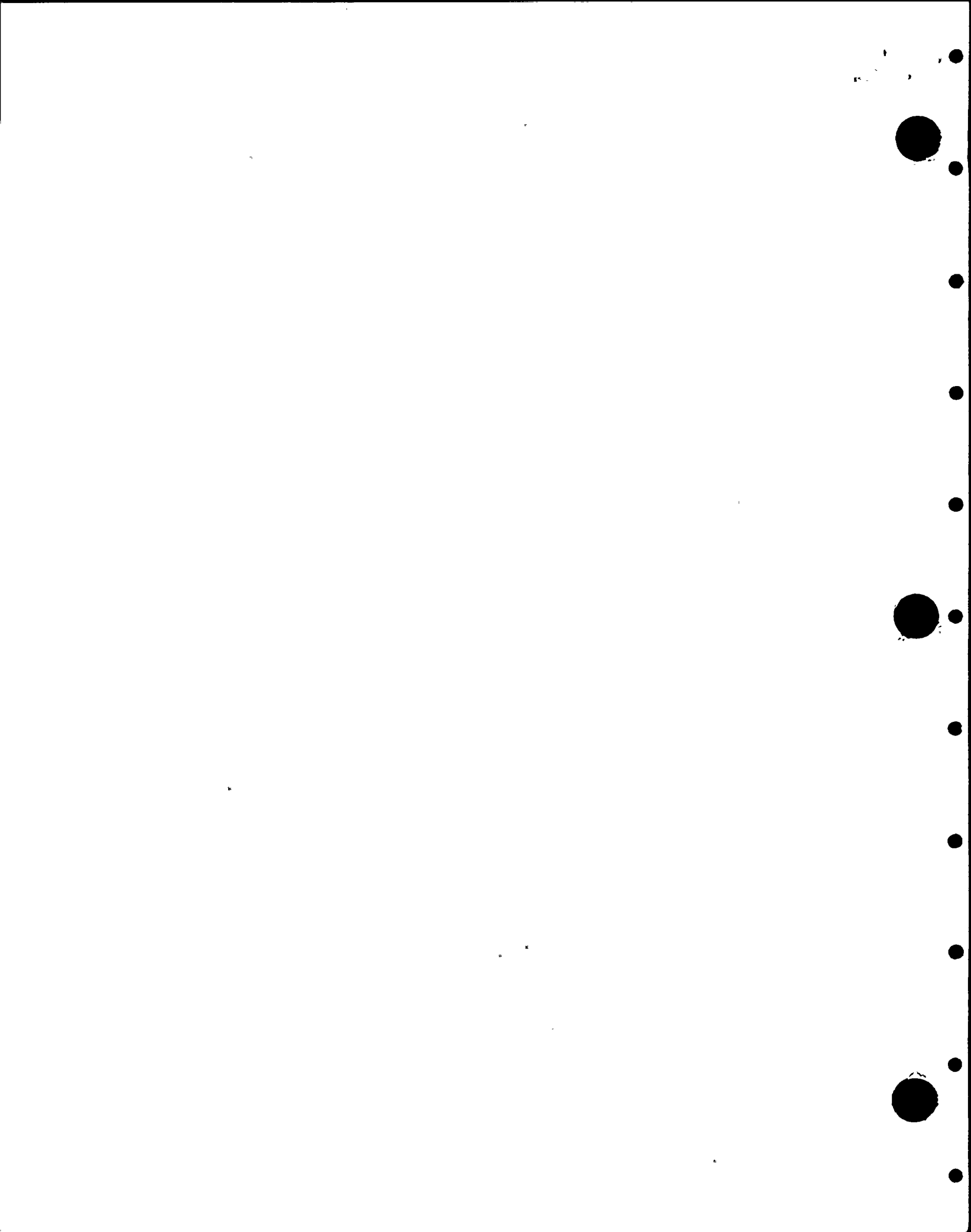
$$\text{Load Reduction Factor} = \left(\sum_{d=0}^{120} \bar{p}_{av}^2(z, \omega) \right)^{1/2}$$

The results of the above calculations are plotted in Figure 6 for an acoustic speed of 5000 ft./sec. at frequencies of 5-6 Hz. and 30-31 Hz. for illustration. Note that the local reduction factor is now a function of position along the bay and is a minimum in the center of the four downcomer bay as was expected. Also, note the anticipated result that there exists significant load reduction in the bay averaged eight downcomer bays and four downcomer bays, even when the sources are correlated.



The results above may be utilized in a conservative manner by specifying load reduction factors which are a maximum in the eight downcomer and four downcomer bays, respectively. Referring to Figure 6, the eight downcomer bay conservative load reduction factor is evaluated at station four and the four downcomer conservative load reduction factor is always evaluated at station eight, which is very conservative.

Conservative load reduction factors for Nine Mile Point are given in Table 1 entitled: "Condensation Oscillation Rigid Wall Pressure Amplitude Reduction Factors for Nine Mile Point." Note that only in the 5-6 Hz. frequency range is the reduction factor given for correlated sources as discussed above. Recall that no credit (load reduction) is taken for reduced acoustic speed which is surely the case during condensation oscillation. These load reduction factors are to be applied directly to the Condensation Oscillation Baseline Rigid Wall Pressure Amplitudes in Torus Shell Bottom Dead Center as given in Table 4.4.1-2 in the Mark 1 Load Definition Report NEDO-21888. After these tables are reduced by the load reduction factor the structural analysis should be undertaken as per the Load Definition Report except that the factor used to adjust the Nine Mile Point Downcomer/Pool area from FSTF is not to be used since this adjustment is included in the plant unique analysis. Also note that columns entitled "Reduction Factor, Average Value" (columns three and five) have been tabulated and may be used in place of the "Maximum" values (columns two and four) since bay averaging was used to process FSTF data and this averaging introduces no additional approximations.



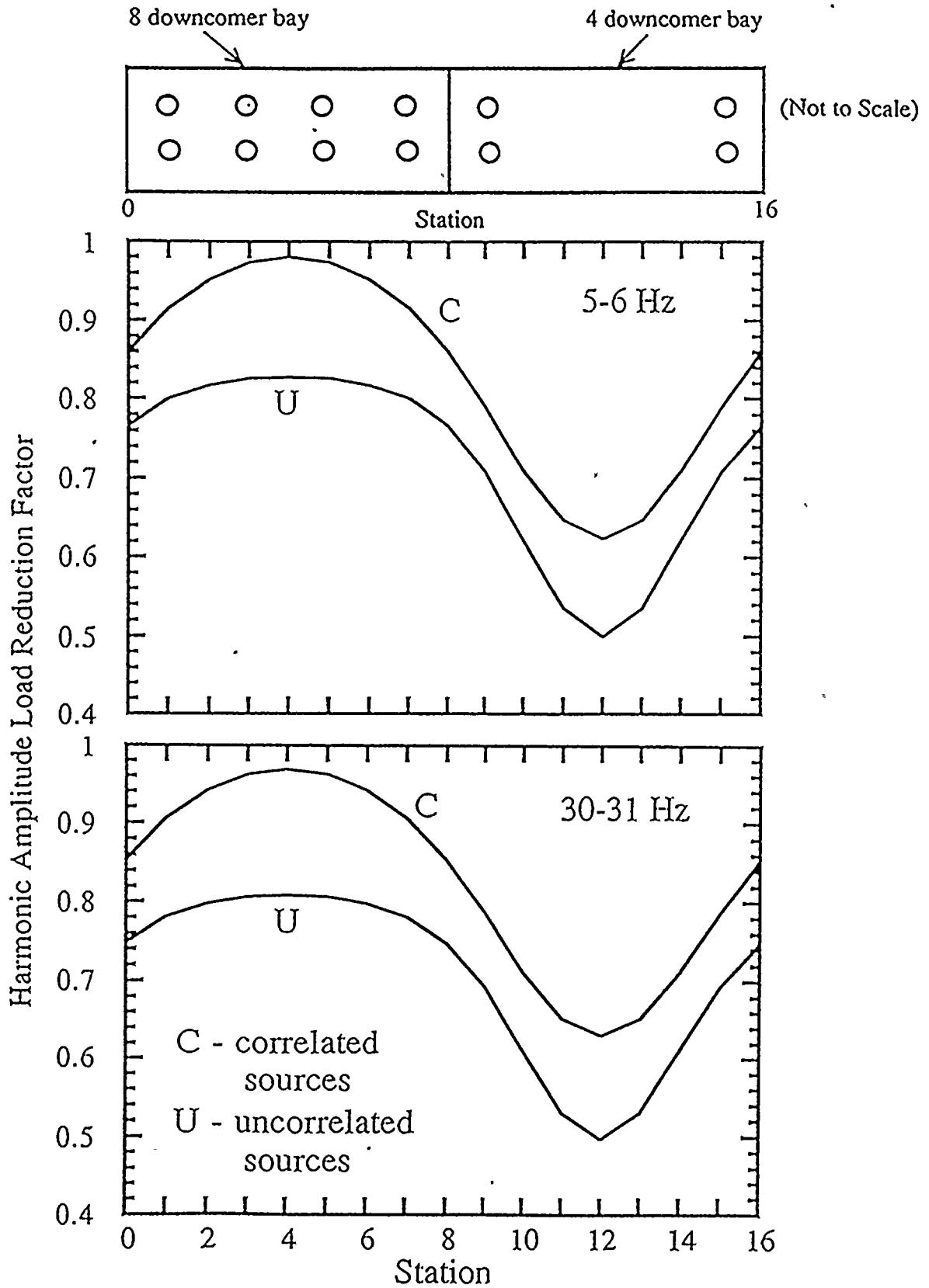


Figure 6. Harmonic amplitude load reduction factor as a function of frequency. Acoustic speed = 5000 ft/sec for Nine Mile Point.

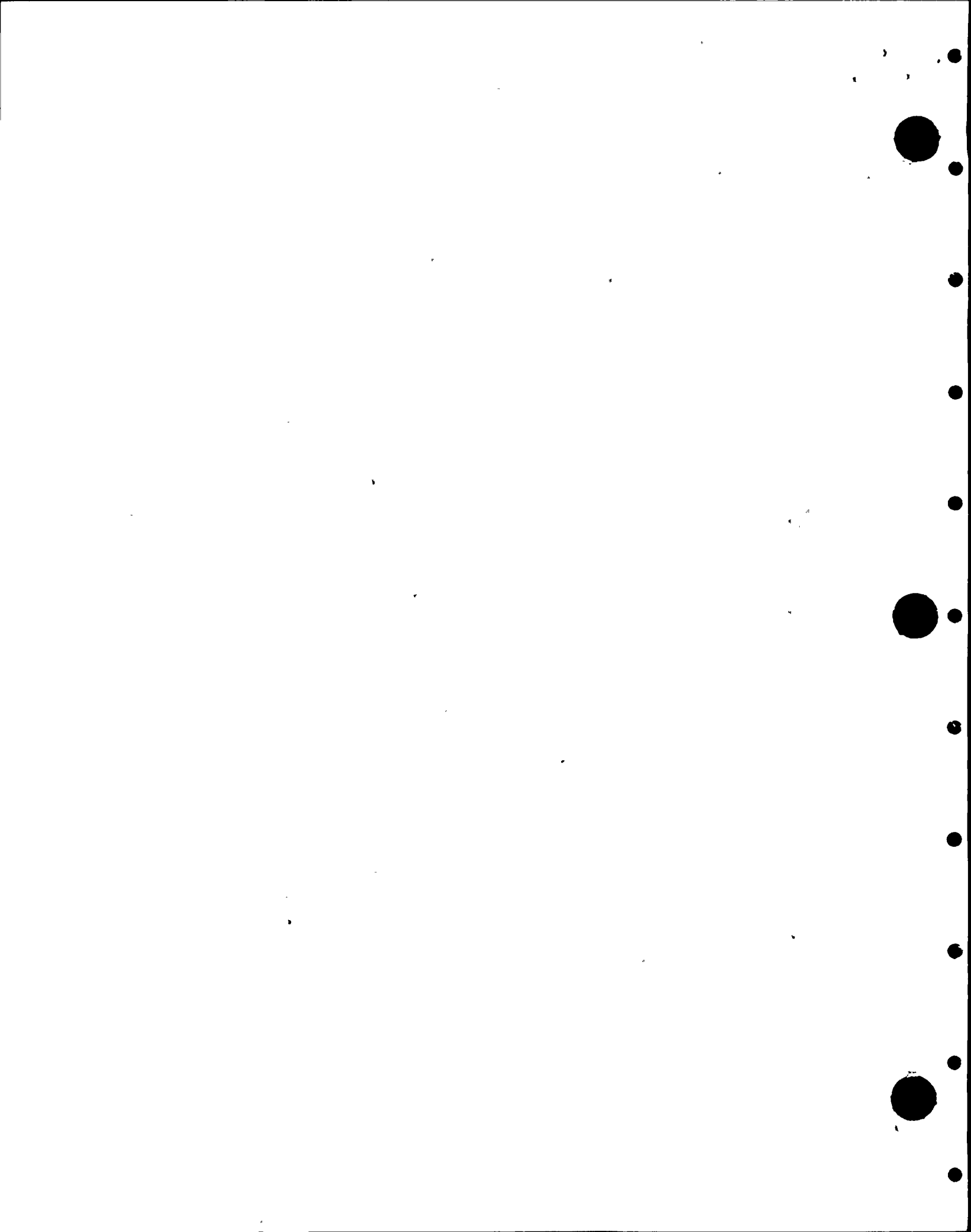


TABLE 1
 CONDENSATION OSCILLATION RIGID WALL PRESSURE
 AMPLITUDE REDUCTION FACTORS FOR
 NINE MILE POINT

Frequency Range (Hz.)	<u>Reduction Factor - 8 Downcomers Bays</u>		<u>Reduction Factor - 4 Downcomer Bays</u>	
	<u>Max. Value</u>	<u>Average Value</u>	<u>Max. Value</u>	<u>Average Value</u>
0-1	0.83	0.81	0.77	0.62
1-2	0.83	0.81	0.77	0.62
2-3	0.83	0.81	0.77	0.62
3-4	0.83	0.81	0.77	0.62
4-5	0.83	0.81	0.77	0.62
5-6	0.98	0.94	0.86	0.72
6-7	0.83	0.81	0.77	0.62
7-8	0.83	0.81	0.77	0.62
8-9	0.83	0.81	0.76	0.62
9-10	0.83	0.81	0.76	0.62
10-11	0.83	0.81	0.76	0.62
11-12	0.82	0.81	0.76	0.62
12-13	0.82	0.81	0.76	0.62
13-14	0.82	0.81	0.76	0.62
14-15	0.82	0.81	0.76	0.62
15-16	0.82	0.81	0.76	0.62
16-17	0.82	0.80	0.76	0.62
17-18	0.82	0.80	0.76	0.62
18-19	0.82	0.80	0.76	0.62
19-20	0.82	0.80	0.76	0.62
20-21	0.82	0.80	0.76	0.62
21-22	0.82	0.80	0.76	0.62
22-23	0.82	0.80	0.76	0.62
23-24	0.82	0.80	0.76	0.62
24-25	0.82	0.80	0.75	0.62
25-26	0.81	0.80	0.75	0.62
26-27	0.81	0.80	0.75	0.62
27-28	0.81	0.79	0.75	0.62
28-29	0.81	0.79	0.75	0.62
29-30	0.81	0.79	0.75	0.61
30-31	0.81	0.79	0.75	0.61
31-32	0.81	0.79	0.75	0.61
32-33	0.81	0.79	0.75	0.61
33-34	0.80	0.79	0.74	0.61
34-35	0.80	0.79	0.74	0.61
35-36	0.80	0.78	0.74	0.61
36-37	0.80	0.78	0.74	0.61
37-38	0.80	0.78	0.74	0.61
38-39	0.80	0.78	0.74	0.61
39-40	0.79	0.78	0.73	0.61
40-41	0.79	0.77	0.73	0.61
41-42	0.79	0.77	0.73	0.60

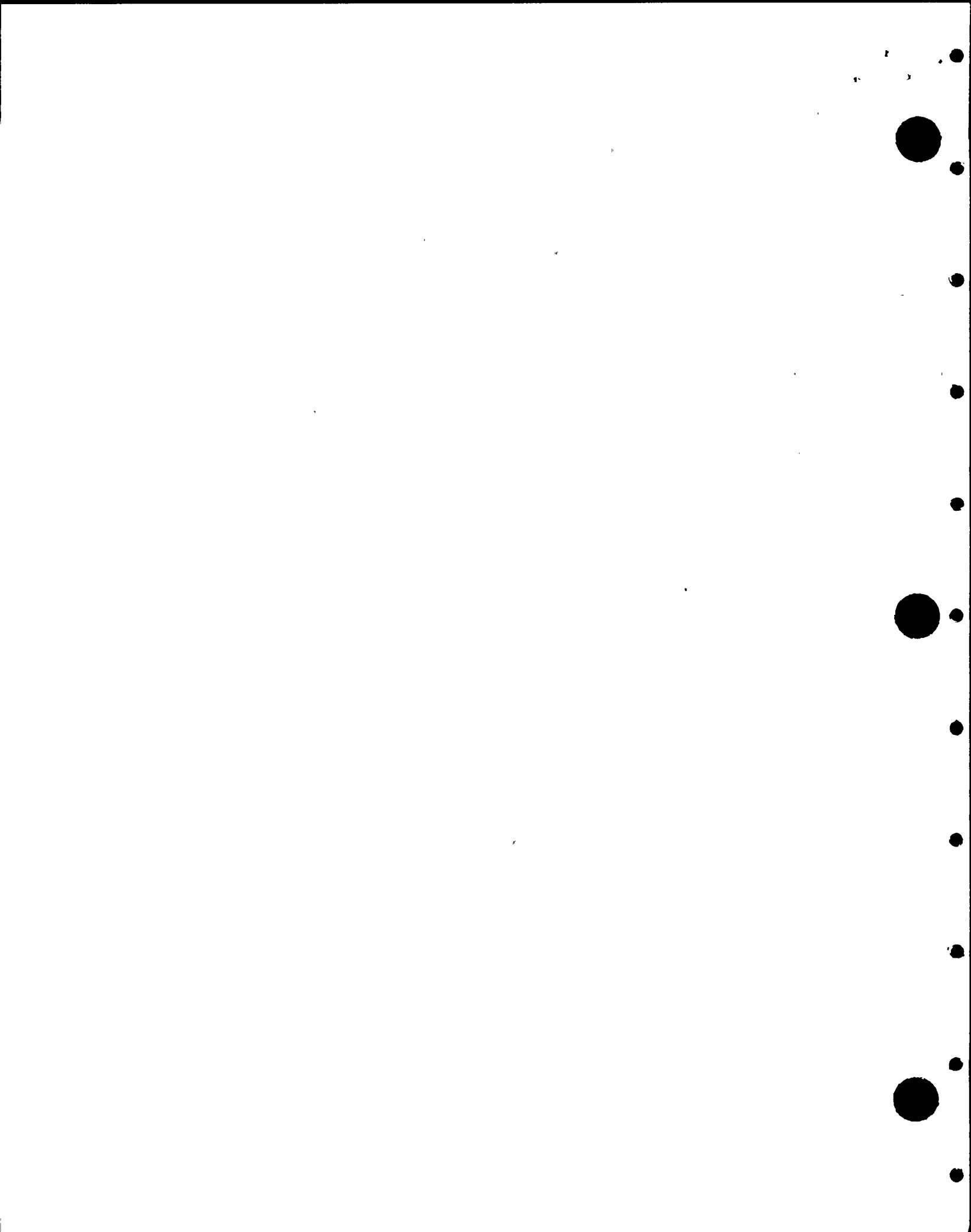
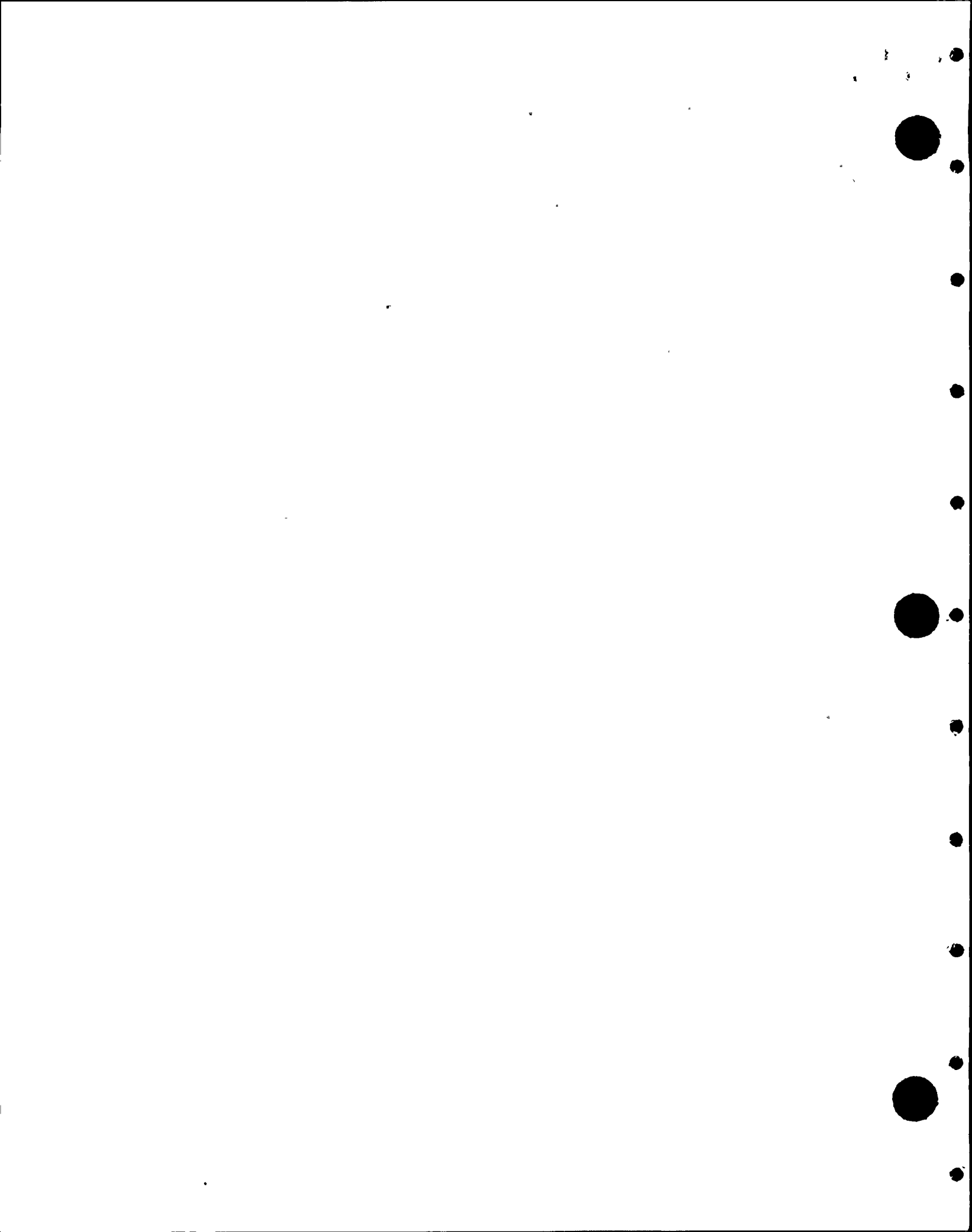


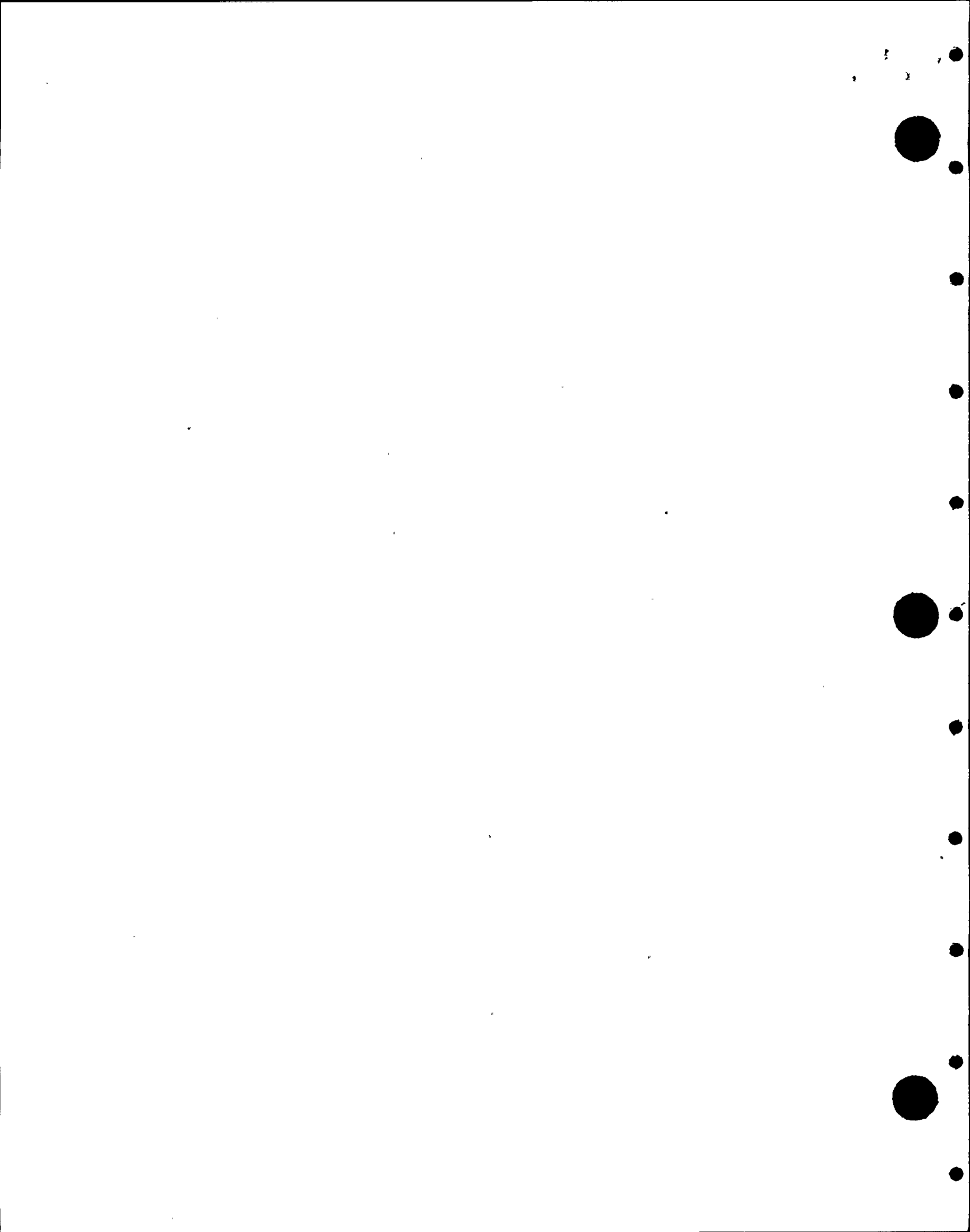
TABLE 1 (Continued)
 CONDENSATION OSCILLATION RIGID WALL PRESSURE
 AMPLITUDE REDUCTION FACTORS FOR
 NINE MILE POINT

Frequency Range (Hz.)	<u>Reduction Factor - 8 Downcomers Bays</u>		<u>Reduction Factor - 4 Downcomer Bays</u>	
	<u>Max. Value</u>	<u>Average Value</u>	<u>Max. Value</u>	<u>Average Value</u>
42-43	0.79	0.77	0.73	0.60
43-44	0.79	0.77	0.73	0.60
44-45	0.78	0.77	0.72	0.60
45-46	0.78	0.76	0.72	0.60
46-47	0.78	0.76	0.72	0.60
47-48	0.78	0.76	0.72	0.60
48-49	0.78	0.76	0.72	0.60
49-50	0.77	0.76	0.71	0.59



REFERENCES

1. Bliss, D. B. and Teske, M.E.: "FSTF Shell Condensation Oscillation Loading Correction Factors - Uncorrelated Vents," Continuum Dynamics, Inc. Report No. 79-1, Rev. 2, August 1980.
2. "Load Definition Report Mark I Condensation Loads," General Electric Company, NEDO-21888, Rev. 0.
3. Torbeck, J.E., et al.: "Mark I Containment Program, Full Scale Test Program Final Report," General Electric Company, Report No. NEDE-24539-P, March 1979.
4. Widnall, S.E., Bliss, D.D. and Zalay, A.: "Theoretical and Experimental Study of Stability of a Vortex Pair," in Aircraft Wake Turbulence and Its Detection, edited by Olsen, J., Goldberg, A. and Rogers, M. Plenum Press, New York, 1971, pp. 308-338.
5. Boyce, W.E. and DiPrima, R.C.: Elementary Differential Equations and Boundary Value Problems, John Wiley & Sons, Inc., Third Edition, New York, 1977.



APPENDIX A

ANALYSIS OF TORUS CURVATURE EFFECTS

The analysis presented in the main body of this report approximates the toroidal containment vessel by its equivalent unwrapped configuration. This appendix shows how curvature effects can be included in the framework of a more elaborate solution using a perturbation method. It is shown that the primary curvature effects are of order a/R , where a is the cross-sectional radius of the torus and R is the radius of the torus itself, measured to the cross-sectional center. Furthermore, curvature produces only a small change in the net downward and its distribution. The following development presents the problem formulation from which these important conclusions can be drawn.

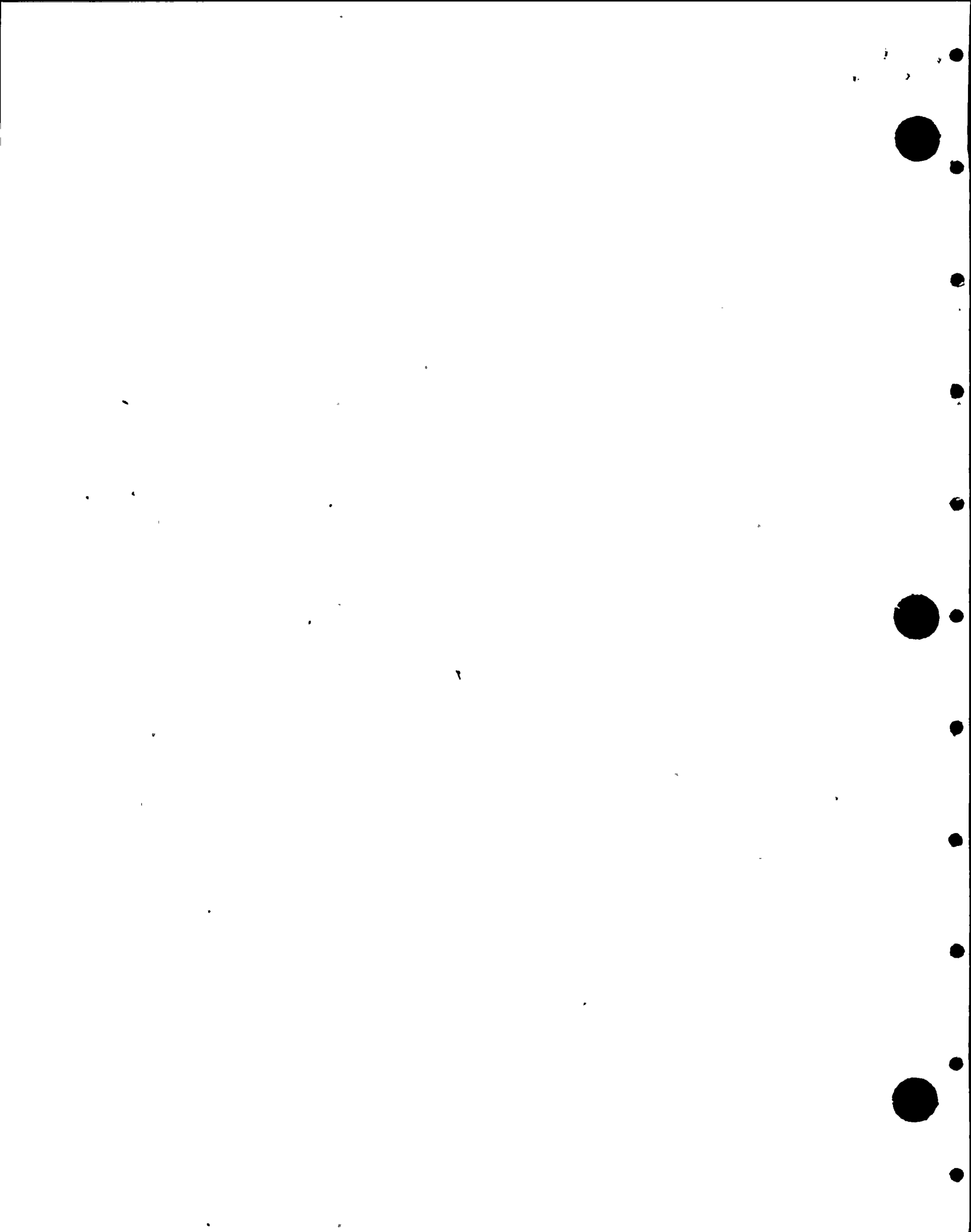
The wave equation is solved in a locally curved cylindrical coordinate system the properties of which are given in Reference 4. In these coordinates the wave equation takes the form:

$$\begin{aligned} \frac{1}{r} \frac{\partial}{\partial r} \left(r \frac{\partial p}{\partial r} \right) + \frac{\cos \theta}{R + r \cos \theta} \frac{\partial p}{\partial r} + \frac{1}{r^2} \frac{\partial^2 p}{\partial \theta^2} - \frac{\sin \theta}{r (R + r \cos \theta)} \frac{\partial p}{\partial \theta} \\ + \frac{R^2}{(R + r \cos \theta)^2} \frac{\partial^2 p}{\partial z^2} - \frac{1}{c^2} \frac{\partial^2 p}{\partial t^2} = 0 \end{aligned} \quad (A1)$$

The corresponding velocities are found by solving the momentum equation

$$-\rho_0 \frac{\partial \vec{V}}{\partial t} = \vec{\nabla} p = \frac{\partial p}{\partial r} \hat{i}_r + \frac{1}{r} \frac{\partial p}{\partial \theta} \hat{i}_\theta + \frac{R}{R + r \cos \theta} \frac{\partial p}{\partial z} \hat{i}_z \quad (A2)$$

Defining dimensionless coordinates $\bar{r} = r/a$, $\bar{z} = z/a$ and $\bar{t} = \omega t$, and defining $\epsilon = a/R$, then gives the governing equation in dimensionless variables:



$$\frac{1}{\bar{r}} \frac{\partial}{\partial \bar{r}} \left(\frac{1}{\bar{r}} \frac{\partial p}{\partial \bar{r}} \right) + \frac{\varepsilon \cos \theta}{1 + \varepsilon \bar{r} \cos \theta} \frac{\partial p}{\partial \bar{r}} + \frac{1}{\bar{r}^2} \frac{\partial^2 p}{\partial \theta^2} - \frac{\varepsilon \sin \theta}{\bar{r} (1 + \varepsilon \bar{r} \cos \theta)} \frac{\partial p}{\partial \theta} \quad (A3)$$

$$+ \frac{1}{(1 + \varepsilon \bar{r} \cos \theta)^2} \frac{\partial^2 p}{\partial \bar{z}^2} - \left(\frac{\omega a}{c} \right)^2 \frac{\partial^2 p}{\partial \bar{t}^2} = 0$$

Note that in this Appendix, an overbar denotes a nondimensional variable.

The momentum equation expressed with dimensionless space and time variables is

$$-\rho_0 c \left(\frac{\omega a}{c} \right) \frac{\partial \vec{V}}{\partial \bar{t}} = \vec{\nabla} p = \frac{\partial p}{\partial \bar{r}} \hat{i}_r + \frac{1}{\bar{r}} \frac{\partial p}{\partial \theta} \hat{i}_\theta + \frac{1}{1 + \bar{r} \cos \theta} \frac{\partial p}{\partial \bar{z}} \hat{i}_z \quad (A4)$$

The pressure is sought in terms of a power series solution in the curvature parameter ε .

$$p(r, \theta, z, t) = \left[p_0(\bar{r}, \theta, \bar{z}) + \varepsilon p_1(\bar{r}, \theta, \bar{z}) + \varepsilon^2 p_2(\bar{r}, \theta, \bar{z}) + \dots \right] e^{i\bar{t}} \quad (A5)$$

with a similar power series for the velocity vector.

$$\vec{V}(r, \theta, z, t) = \left[\vec{V}_0(\bar{r}, \theta, \bar{z}) + \varepsilon \vec{V}_1(\bar{r}, \theta, \bar{z}) + \varepsilon^2 \vec{V}_2(\bar{r}, \theta, \bar{z}) + \dots \right] e^{i\bar{t}} \quad (A6)$$

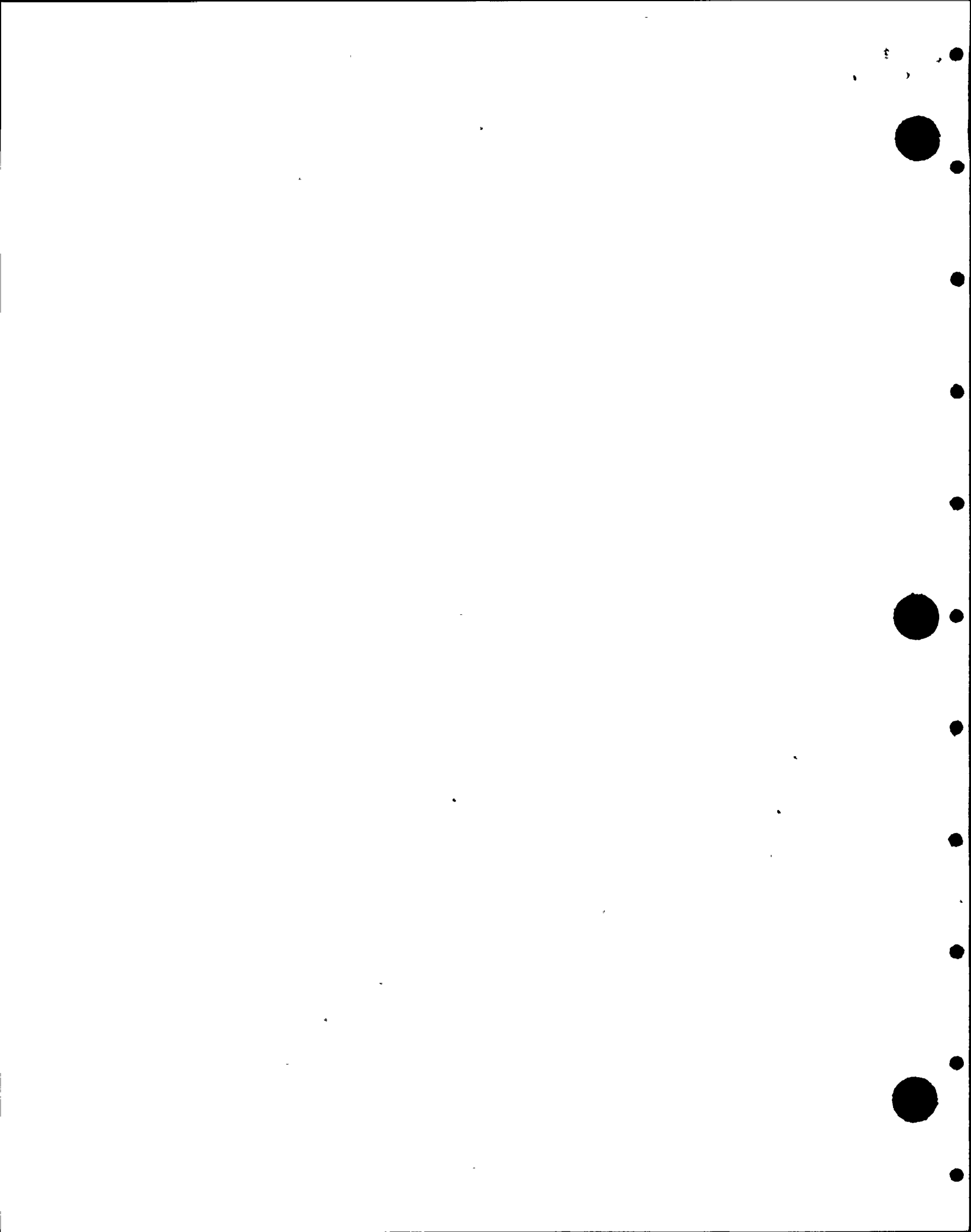
Substituting these series expansions into the nondimensional wave equation and the momentum equation, and equating like powers of ε yields equations for p_0 , p_1 , etc.

To lowest order, the wave equation becomes

$$O[1]: \quad \frac{1}{\bar{r}} \frac{\partial}{\partial \bar{r}} \left(\frac{1}{\bar{r}} \frac{\partial p_0}{\partial \bar{r}} \right) + \frac{1}{\bar{r}^2} \frac{\partial^2 p_0}{\partial \theta^2} + \frac{\partial^2 p_0}{\partial \bar{z}^2} + \left(\frac{\omega a}{c} \right)^2 p_0 = 0 \quad (A7)$$

and the corresponding momentum equation is to lowest order

$$-\rho_0 c \left(\frac{\omega a}{c} \right) \vec{V}_0 = \vec{\nabla} p_0 = \frac{\partial p_0}{\partial \bar{r}} \hat{i}_r + \frac{1}{\bar{r}} \frac{\partial p_0}{\partial \theta} \hat{i}_\theta + \frac{\partial p_0}{\partial \bar{z}} \hat{i}_z \quad (A8)$$



Note that the equation (A-7) governing p_0 corresponds to the problem of the equivalent unwrapped torus, since this equation corresponds to the case $\varepsilon \rightarrow 0$. The solution of this equation and boundary conditions was described in Reference 1, and in the main body of this report. The general solution is constructed as the sum of pressure mode solutions of the form

$$p_{0nj} = c_{nj} J_n(m_n^j \bar{r}) \sin(n\theta) \frac{\cosh[\alpha_{nj}(D-z)]}{\cosh[\alpha_{nj}D]} \quad (A9)$$

To order ε the wave equation is

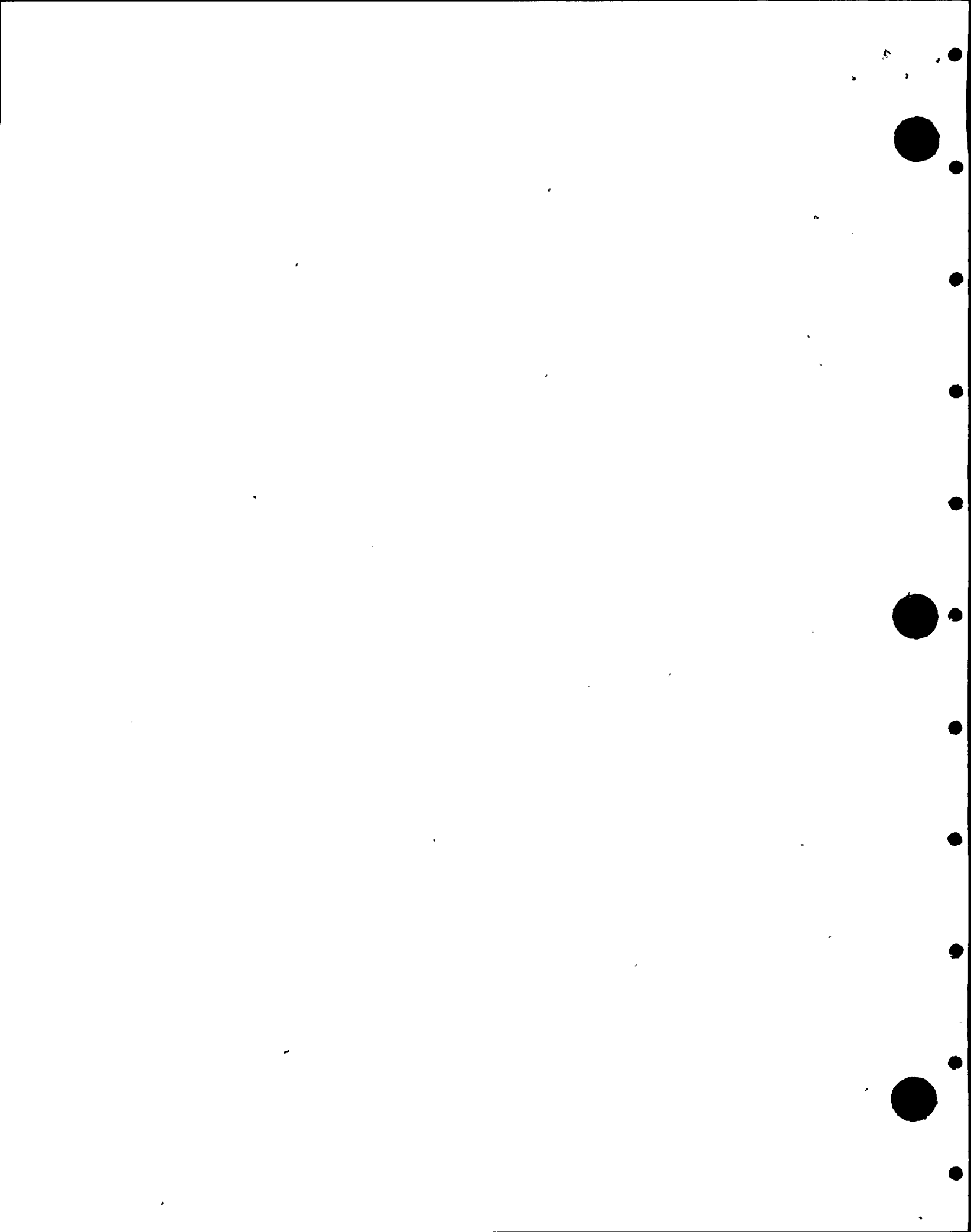
$$\begin{aligned} O[\varepsilon]: \quad & \frac{1}{\bar{r}} \frac{\partial}{\partial \bar{r}} \left(\bar{r} \frac{\partial p_1}{\partial \bar{r}} \right) + \frac{1}{\bar{r}^2} \frac{\partial^2 p_1}{\partial \theta^2} + \frac{\partial^2 p_1}{\partial \bar{z}^2} + \left(\frac{\omega a}{c} \right)^2 p_1 \\ & = -\cos\theta \frac{\partial p_0}{\partial \bar{r}} + \sin\theta \frac{1}{\bar{r}} \frac{\partial p_0}{\partial \theta} + 2\bar{r} \cos\theta \frac{\partial^2 p_0}{\partial \bar{z}^2} \end{aligned} \quad (A10)$$

and the corresponding order ε momentum equation is

$$-\rho_0 c \left(\frac{\omega a}{c} \right) \vec{V}_1 = \vec{\nabla} p_1 = \frac{\partial p_1}{\partial \bar{r}} \hat{i}_r + \frac{1}{\bar{r}} \frac{\partial p_1}{\partial \theta} \hat{i}_\theta + \left[\frac{\partial p_1}{\partial \bar{z}} - \bar{r} \cos\theta \frac{\partial p_0}{\partial \bar{z}} \right] \hat{i}_z \quad (A11)$$

Equation (A10) governing p_1 must be solved along with appropriate boundary conditions to determine the effect of curvature. It can be shown that the general solution for p_1 is constructed as the sum of pressure modes of the form:

$$\begin{aligned} p_{1nj} = & \frac{c_{nj}}{2} P_{1nj}^+(\bar{r}) \sin([n+1]\theta) \frac{\cosh[\alpha_{nj}(D-z)]}{\cosh[\alpha_{nj}D]} \\ & + \frac{c_{nj}}{2} P_{1nj}^-(\bar{r}) \sin([n-1]\theta) \frac{\cosh[\alpha_{nj}(D-z)]}{\cosh[\alpha_{nj}D]} \end{aligned} \quad (A12)$$



which are chosen to satisfy equation (A9), plus the sum of modes of the form

$$p_{0mk} = d_{mk} J_m(m_m^k \bar{r}) \sin(m\theta) \frac{\cosh[\alpha_{mk}(D-z)]}{\cosh[\alpha_{mk}D]} \quad (\text{A13})$$

which satisfy the homogeneous form of equation (A10). The primary problem is to find the functions $P_{1nj}^+(\bar{r})$ and $P_{1nj}^-(\bar{r})$ in equation (A12) that satisfy equation (A10) and the boundary condition of no flow through the rigid torus wall. Note that the functional forms of both equations (A12) and (A13) have been chosen to satisfy the reflection condition halfway around the torus ($z = D$) and the condition that the perturbation pressure vanish at the free surface ($\theta = 0$ and $\theta = \pi$). The functional form of equation (A13), which is similar to that of equation (A9), already satisfies the condition of a rigid torus wall.

Substituting equation (A12) into equation (A10) and equating like dependences of $\sin([n+1]\theta)$ and $\sin([n-1]\theta)$ gives separate nonhomogeneous Bessel equations for

$P_{1nj}^+(\bar{r})$ and $P_{1nj}^-(\bar{r})$:

$$\begin{aligned} \frac{1}{\bar{r}} \frac{\partial}{\partial \bar{r}} \left(\bar{r} \frac{\partial}{\partial \bar{r}} P_{1nj}^+(\bar{r}) \right) - \frac{(n+1)^2}{\bar{r}^2} P_{1nj}^+(\bar{r}) + (m_n^j)^2 P_{1nj}^+(\bar{r}) \\ = -\frac{\partial}{\partial \bar{r}} J_n(m_n^j \bar{r}) + \frac{n}{\bar{r}} J_n(m_n^j \bar{r}) + 2\bar{r} \alpha_{nj}^2 a^2 J_n(m_n^j \bar{r}) \equiv G_{nj}^+(\bar{r}) \end{aligned} \quad (\text{A14})$$

and

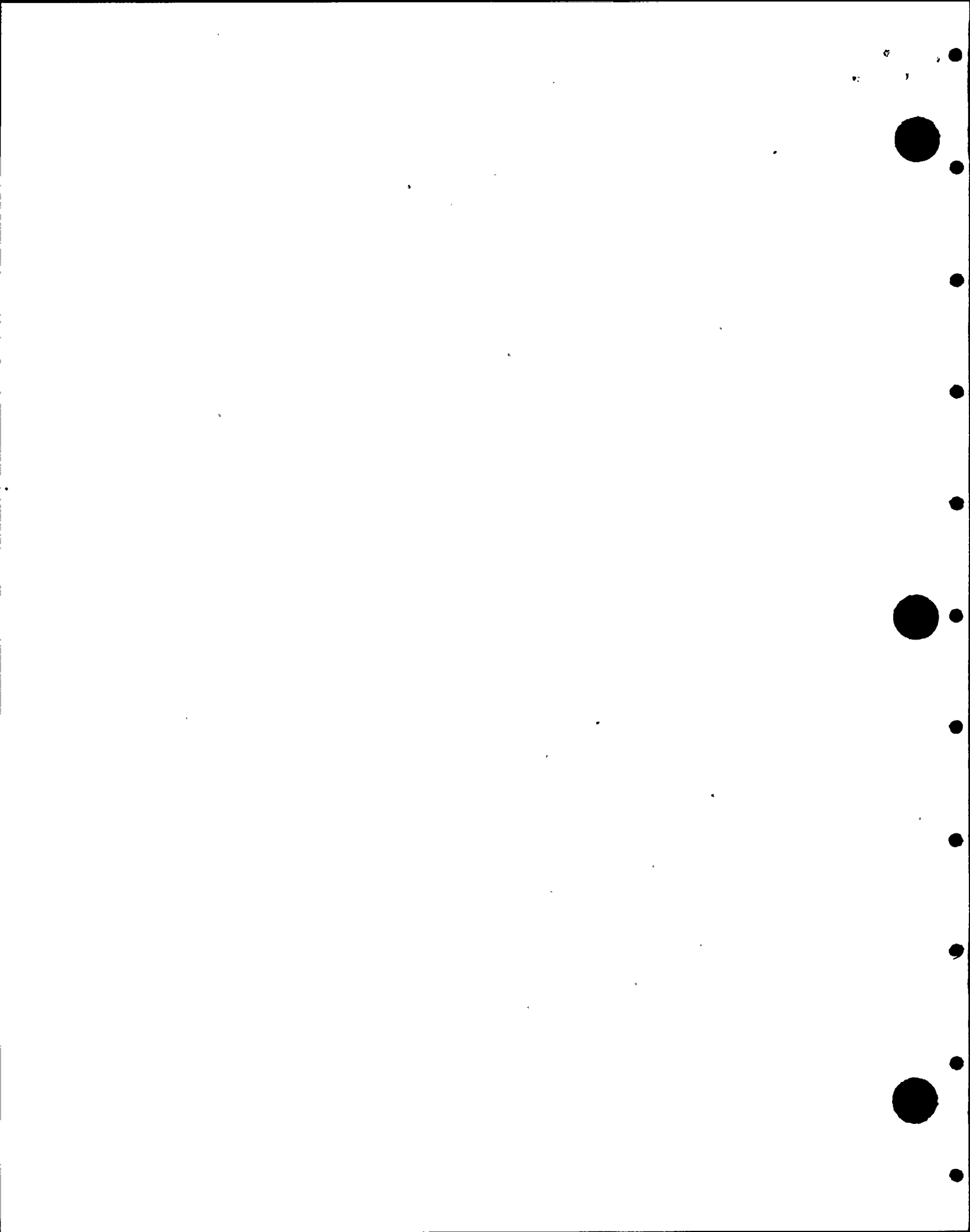
$$\begin{aligned} \frac{1}{\bar{r}} \frac{\partial}{\partial \bar{r}} \left(\bar{r} \frac{\partial}{\partial \bar{r}} P_{1nj}^-(\bar{r}) \right) - \frac{(n-1)^2}{\bar{r}^2} P_{1nj}^-(\bar{r}) + (m_n^j)^2 P_{1nj}^-(\bar{r}) \\ = -\frac{\partial}{\partial \bar{r}} J_n(m_n^j \bar{r}) - \frac{n}{\bar{r}} J_n(m_n^j \bar{r}) + 2\bar{r} \alpha_{nj}^2 a^2 J_n(m_n^j \bar{r}) \equiv G_{nj}^-(\bar{r}) \end{aligned} \quad (\text{A15})$$

These Bessel equations have homogeneous solutions of the form

$$P_{1nj}^+(\bar{r})_H = A_{nj}^+ J_{n+1}(m_n^j \bar{r}) + B_{nj}^+ Y_{n+1}(m_n^j \bar{r}) \quad (\text{A16})$$

and

$$P_{1nj}^-(\bar{r})_H = A_{nj}^- J_{n-1}(m_n^j \bar{r}) + B_{nj}^- Y_{n-1}(m_n^j \bar{r}) \quad (\text{A17})$$



The coefficients $B_{nj}^+ = B_{nj}^- = 0$ since the Bessel function Y_{n+1} and Y_{n-1} are singular at the origin. Once the homogeneous solutions are known for a second order linear ordinary differential equation, the particular solution can be constructed by the method of variation of parameters, see Reference 5. A very lengthy calculation gives the result

$$P_{1nj}^+(\bar{r}) = \frac{2}{\pi m_n^j} \left(U_{Y_{nj}^+}(1) - \frac{Y'_{n+1}(m_n^j)}{J'_{n+1}(m_n^j)} U_{J_{nj}^+}(1) \right) J_{n+1}(m_n^j \bar{r}) - \frac{2}{\pi m_n^j} \left[U_{Y_{nj}^+}(\bar{r}) J_{n+1}(m_n^j \bar{r}) + U_{J_{nj}^+}(\bar{r}) Y_{n+1}(m_n^j \bar{r}) \right] \quad (A18)$$

where

$$U_{Y_{nj}^+}(\bar{r}) = \int_0^{\bar{r}} \bar{r} Y_{n+1}(m_n^j \bar{\xi}) G_{nj}^+(\bar{\xi}) d\bar{\xi} \quad (A19)$$

and

$$U_{J_{nj}^+}(\bar{r}) = \int_0^{\bar{r}} \bar{r} J_{n+1}(m_n^j \bar{\xi}) G_{nj}^+(\bar{\xi}) d\bar{\xi} \quad (A20)$$

Likewise,

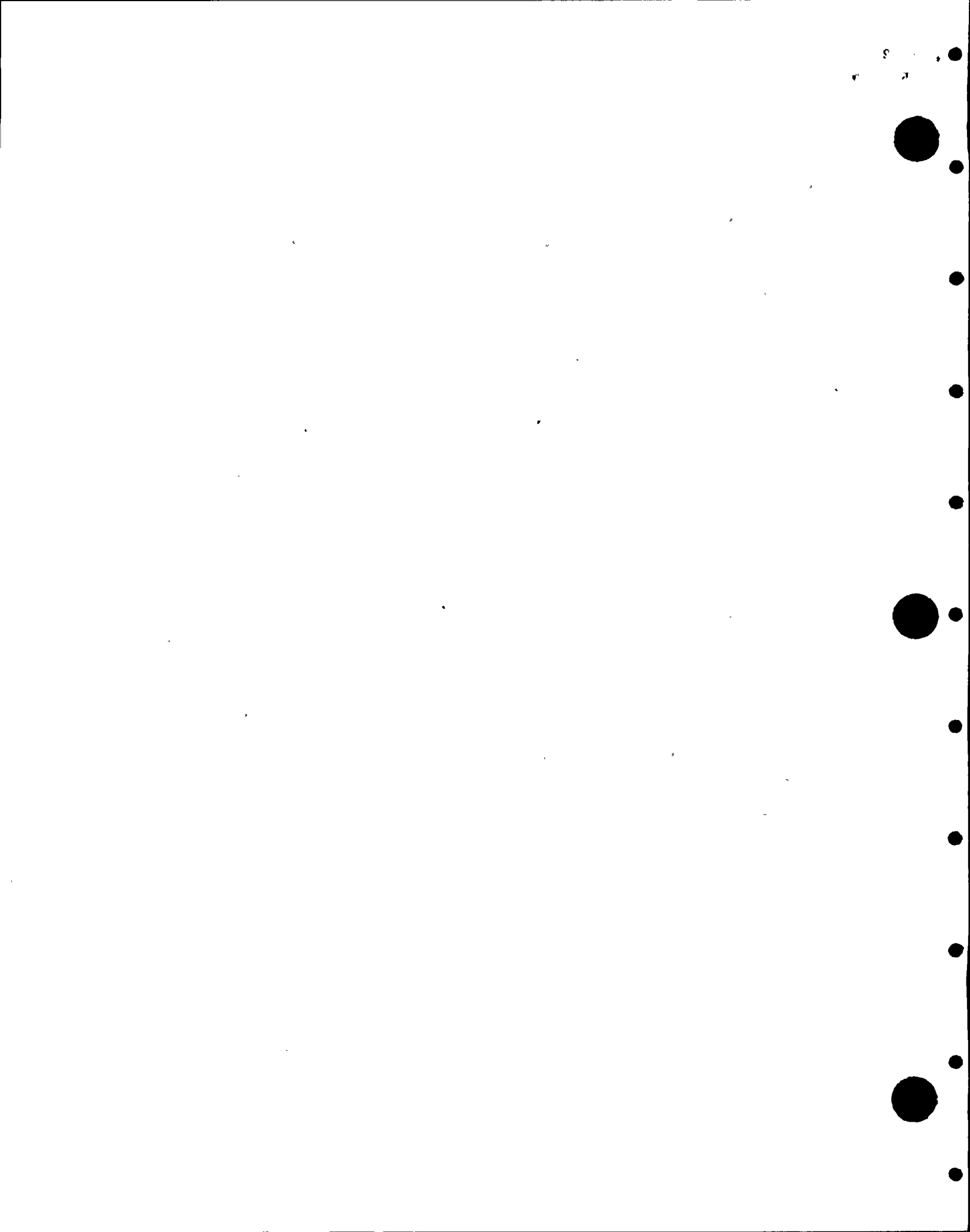
$$P_{1nj}^-(\bar{r}) = \frac{2}{\pi m_n^j} \left(U_{Y_{nj}^-}(1) - \frac{Y'_{n-1}(m_n^j)}{J'_{n-1}(m_n^j)} U_{J_{nj}^-}(1) \right) J_{n-1}(m_n^j \bar{r}) - \frac{2}{\pi m_n^j} \left[U_{Y_{nj}^-}(\bar{r}) J_{n-1}(m_n^j \bar{r}) + U_{J_{nj}^-}(\bar{r}) Y_{n-1}(m_n^j \bar{r}) \right] \quad (A21)$$

where

$$U_{J_{nj}^-}(\bar{r}) = \int_0^{\bar{r}} \bar{r} J_{n-1}(m_n^j \bar{\xi}) G_{nj}^-(\bar{\xi}) d\bar{\xi} \quad (A22)$$

and

$$U_{Y_{nj}^-}(\bar{r}) = \int_0^{\bar{r}} \bar{r} Y_{n-1}(m_n^j \bar{\xi}) G_{nj}^-(\bar{\xi}) d\bar{\xi} \quad (A23)$$



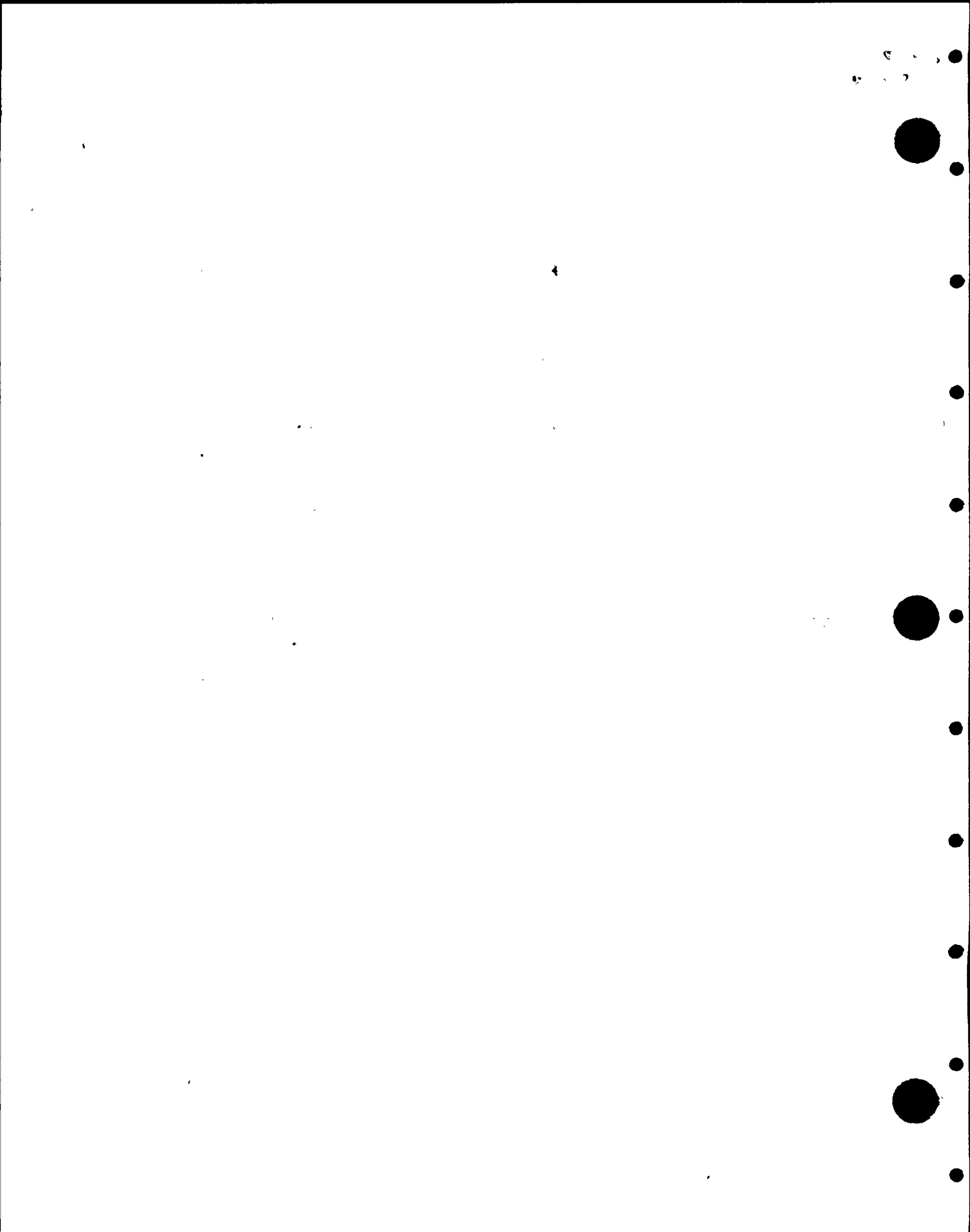
In the above solutions, equations (A19) and (A21), portions of the homogeneous solution, equations (A16) and (A17), have been added to satisfy the boundary condition that the normal velocity vanish on the rigid torus walls.

The general solution for the pressure field, which includes terms of $O[1]$ and $O[\epsilon]$, can now be assembled by summing equations (A9), (A12), and (A13) over all indices, and substituting these summations into equation (A5).

$$\begin{aligned}
 p(r, \theta, z, t) = & \sum_{j=1}^{\infty} \sum_{n=1}^{\infty} c_{nj} \left[J_n(m_n^j \bar{r}) \sin(n\theta) + \frac{\epsilon}{2} P_{1nj}^+(\bar{r}) \sin([n+1]\theta) \right. \\
 & \left. + \frac{\epsilon}{2} P_{1nj}^-(\bar{r}) \sin([n-1]\theta) \right] \frac{\cosh[\alpha_{nj}(D-z)]}{\cosh[\alpha_{nj}D]} e^{i\bar{t}} \quad (A24) \\
 & + \sum_{k=1}^{\infty} \sum_{m=1}^{\infty} \epsilon d_{mk} J_m(m_m^k \bar{r}) \sin(m\theta) \frac{\cosh[\alpha_{mk}(D-z)]}{\cosh[\alpha_{mk}D]} e^{i\bar{t}}
 \end{aligned}$$

All the terms in equation (A24) satisfy the rigid wall boundary condition on the torus sides, the free surface condition, and the end reflection condition halfway around the torus. The remaining constants c_{nj} and d_{mk} are used to satisfy the vent source velocity boundary condition in the plane $z = 0$. This is most easily done by choosing d_{mk} such that the $O[\epsilon]$ velocity component normal to this plane vanishes at $z = 0$. From the momentum equation, this condition is equivalent to requiring the z -derivative of the $O[\epsilon]$ terms in equation (A24) to vanish at $z = 0$. Then the constants d_{mk} are re-expressed in terms of the constants c_{nj} . The advantage of this approach is that the remaining constants c_{nj} then take on exactly the same values as given previously, since the $O[\epsilon]$ terms no longer contribute directly to the source boundary condition. A very lengthy calculation, utilizing the orthogonality relations for sine functions and for Bessel functions, then gives:

$$\begin{aligned}
 d_{mk} = & \frac{-2 [\alpha_{mk} \tanh(\alpha_{mk} D)]^{-1}}{\left[1 - \left(\frac{m}{m_m^k}\right)^{-1}\right] J_m^2(m_m^k)} \sum_{j=1}^{\infty} \left\{ c_{m-1,j} \int_0^1 P_{1m-1,j}^+(\bar{r}) J_m(m_m^k \bar{r}) \bar{r} d\bar{r} \right. \\
 & \left. + c_{m+1,j} \int_0^1 P_{1m+1,j}^-(\bar{r}) J_m(m_m^k \bar{r}) \bar{r} d\bar{r} \right\} \quad (A25)
 \end{aligned}$$



Finally the vent velocity boundary condition must be applied. Because of the way the solution has been structured, with $O[\epsilon]$ terms vanishing at $z = 0$, only the $O[1]$ terms participate, making the process identical to that described in Reference 1. Following similar notation, let

$$c_{nj} = \hat{c}_{mk} \frac{2i\rho\omega Q \cosh(\alpha_{nj}D)}{\pi a^2 J_n(m_n^j)} \quad (A26)$$

where \hat{c}_{mk} is still given by equation (8) in the main body of the report.

The above permits an estimate to be made as to the magnitude of load reduction to be anticipated from a curvature correction. First note that, as in the main body of the report, the net vertical load is associated with $\sin\theta$ dependence in the modes, hence in equation (A24), $n = 2$ and $m = 1$ provide the only contribution from the order ϵ terms. Second, note that the downcomers are constructed in pairs and that for each downcomer pair the portion of the order ϵ solution which leads to a net vertical load seems to cancel. Physically interpreted, one source in the pair raises the load while the other reduces the load by an equal amount, to this order correction. Therefore, to this order, there is no change in total load and it seems that the change in total load occurs at order $\epsilon^2 = a^2/R^2$. This ratio evaluated for Nine Mile Point is order of 0.04 and is judged too small in light of other uncertainties to pursue further.

